

STUDIES ON THE ROLES OF LIPIDS IN MEMBRANE STRUCTURE AND FUNCTION

BY

MARCEL B. BALLY

B.Sc., Texas A&M University, 1977

M.Sc., Texas A&M University, 1979

A THESIS SUBMITTED IN PARTIAL FULFILMENT OF
THE REQUIREMENTS FOR THE DEGREE OF
DOCTOR OF PHILOSOPHY

in

THE FACULTY OF GRADUATE STUDIES

Department of Biochemistry

We accept this thesis as conforming
to the required standard

THE UNIVERSITY OF BRITISH COLUMBIA

August 1984

©Marcel B. Bally, 1984

In presenting this thesis in partial fulfilment of the requirements for an advanced degree at the University of British Columbia, I agree that the Library shall make it freely available for reference and study. I further agree that permission for extensive copying of this thesis for scholarly purposes may be granted by the head of my department or by his or her representatives. It is understood that copying or publication of this thesis for financial gain shall not be allowed without my written permission.

Department of Biochemistry

The University of British Columbia
1956 Main Mall
Vancouver, Canada
V6T 1Y3

Date Sept 28, 1984

ABSTRACT

Lipids in membranes satisfy two basic roles. First they provide a matrix with which membrane proteins are associated and second, they provide a structural bilayer for maintaining a permeability barrier. This thesis investigates certain aspects of the structural and permeability barrier properties of lipids employing simple protein free model membrane systems.

It is demonstrated, employing ^{31}P and ^2H NMR techniques, that cholesterol engendered formation of non-bilayer structures in multilamellar vesicles (MLVs) composed of phosphatidylethanolamine (PE) and either phosphatidylserine (PS) or phosphatidylcholine (PC). Further the presence of cholesterol, in conjunction with Mg^{2+} , facilitated Ca^{2+} triggered formation of non-bilayer organizations in the PS containing systems. It is indicated that in these complex multicomponent systems where multiple structural phases (*ie.* bilayer, hexagonal, and "isotropic") coexist, that the phospholipids exhibit ideal mixing behaviour.

A basic consequence of the barrier properties of a lipid bilayer is an ability to maintain a membrane potential ($\Delta\psi$), which is required for a variety of membrane mediated transport processes. To investigate the role of lipids in maintaining $\Delta\psi$, and the direct effect of $\Delta\psi$ on transport functions, a large unilamellar vesicle (LUV) preparation free of impurities is required. This thesis describes a novel procedure for generating LUVs, by extrusion of MLVs through polycarbonate filters (pore size 100 nm). LUVs can thus be obtained from a wide variety of lipid species and mixtures in the absence of lipid solubilizing agents. Vesicles exhibiting $\Delta\psi$ in response to a Na^+/K^+ ion gradient (K^+ inside) are characterized. It is shown that such a K^+ diffusion potential can drive the uptake of a variety of biologically active molecules (*eg.* local anaesthetics, antineoplastic agents, biogenic amines (dopamine)) which have cationic and lipophilic characteristics. The transport process appears to proceed by a antiport cation/lipophilic cation exchange process that is driven by the transmembrane potential.

TABLE OF CONTENTS

ABSTRACT	i
TABLE OF CONTENTS	iii
LIST OF TABLES	vii
LIST OF FIGURES	viii
ABBREVIATIONS	x
ACKNOWLEDGEMENTS	xii

1 INTRODUCTION

1.1 Membrane Structure: A Historical Perspective	1
1.2 Rational for Investigating the Role of Lipids in Biological Membranes	4
1.3 Role of Lipids Within the Fluid Mosaic Model of Membranes	5
1.4 Model Membrane Systems	7
1.5 Chemical and Physical Properties of Phospholipids and Cholesterol	9
1.5.1 Phospholipids	10
1.5.2 Cholesterol	12
1.6 Lipid Polymorphism	14
1.6.1 Techniques for evaluating lipid polymorphism	15
1.6.2 Roles postulated for non-lamellar structures	19
1.7 The Shape Concept	21
1.8 Permeability Properties of Lipid Membranes	24
1.8.1 Passive permeability	24
1.8.2 Membrane potential	26
1.9 Summary	28

2 LIPID POLYMORPHISM: INFLUENCE OF CHOLESTEROL AND DIVALENT CATIONS ON THE STRUCTURAL PREFERENCES OF MIXED LIPID MODEL SYSTEMS

2.1 Introduction	29
2.2 Materials and Methods	
2.2.1 Preparation of soyabean lipids	30
2.2.2 Synthesis of dioleoyl phospholipids	33
2.2.3 Sample preparation	35
2.2.4 Nuclear magnetic resonance	36
2.2.5 Freeze fracture	36
2.3 Results	
2.3.1 Influence of cholesterol on soya PE/PS lipid mixtures	36
2.3.2 Influence of cholesterol and Mg^{+2} on the Ca^{2+} induced bilayer to H_{11} transition in PE-PS systems	41
2.3.3 Influence of cholesterol on the mixing properties of DOPC/DOPE systems	45
2.4 Discussion	48

3 PRODUCTION OF LARGE UNILAMELLAR VESICLES BY A RAPID EXTRUSION PROCEDURE: CHARACTERIZATION OF SIZE DISTRIBUTION, TRAPPED VOLUME AND ABILITY TO MAINTAIN A MEMBRANE POTENTIAL

3.1 Introduction	54
3.2 Materials and Methods	
3.2.1 Lipid preparation	56
3.2.2 Vesicle preparation	56
3.2.3 Determination of trapped volumes	56
3.2.4 Freeze fracture and negative staining	57
3.2.5 ^{31}P Nuclear magnetic resonance	58
3.2.6 Membrane potential and permeability studies	58
3.3 Results	
3.3.1 Characterization of LUVETs	60

3.3.2 Characterization of LUVETs with a membrane potential	68
3.4 Discussion	76
4 UPTAKE OF SAFRANINE AND OTHER LIPOPHILIC CATIONS INTO MODEL MEMBRANE SYSTEMS IN RESPONSE TO A MEMBRANE POTENTIAL	
4.1 Introduction	78
4.2 Materials and Methods	
4.2.1 Materials	79
4.2.2 Vesicle preparation	80
4.2.3 Generation of a membrane potential	80
4.2.4 Uptake of safranine	82
4.2.5 Determination of membrane potential and K ⁺ efflux	82
4.2.6 Uptake of assorted drugs	82
4.3 Results	
4.3.1 Characterization of safranine accumulation by LUVETs	83
4.3.2 Uptake of methyltriphenylphosphonium (MTPP ⁺)	92
4.3.3 Uptake of charged lipophilic drugs	94
4.4 Discussion	97
5 UPTAKE OF DOPAMINE AND OTHER BIOGENIC AMINES INTO LARGE UNILAMELLAR VESICLES IN RESPONSE TO A MEMBRANE POTENTIAL: ACTIVE TRANSPORT IN THE ABSENCE OF A CARRIER PROTEIN	
5.1 Introduction	105
5.2 Materials and Methods	
5.2.1 Materials	107
5.2.2 Preparation of vesicles	107
5.2.3 Determination of membrane potential	109
5.2.4 Uptake assays	110

5.3 Results	
5.3.1 Accumulation of dopamine in response to a transmembrane electrochemical potential	111
5.3.2 Influence of external pH on the uptake of dopamine	115
5.3.3 Influence of trapped ATP on dopamine accumulation	117
5.3.4 Uptake of other biogenic amines	120
5.4 Discussion	122
6 SUMMARIZING DISCUSSION	128
BIBLIOGRAPHY	131

LIST OF TABLES

1	Commonly occurring fatty acid moieties and phospholipid headgroups	11
2	Physical characteristics of vesicles produced by extrusion	66

LIST OF FIGURES

1	The fluid mosaic model of membrane structure	3
2	General structure of a phospholipid	11
3	Structure of cholesterol	13
4	^{31}P -NMR, ^2H -NMR, and freeze-fracture characteristics of phospholipids in various phases	17
5	Polymorphic phases and corresponding dynamic molecular shapes	22
6	^{31}P and ^2H NMR spectra of DOPE as a function of temperature	37
7	^{31}P -NMR spectra from dispersions of soya PE in the presence of varying amounts of soya PS and cholesterol	39
8	Freeze-fracture micrographs of soya PE-soya PS mixtures in the presence and absence of equimolar cholesterol	40
9	^{31}P -NMR spectra from dispersions of soya PS and soya PE in the presence of varying amounts of cholesterol and Ca^{2+}	42
10	^{31}P -NMR spectra from dispersions of soya PS and soya PE after dialysis against Mg^{2+}	43
11	^{31}P -NMR spectra from dispersions of soya PS and soya PE after dialysis against Mg^{2+} and Ca^{2+}	44
12	^{31}P -NMR spectra from soya PS and soya PE mixtures in the presence and absence of 1 M NaCl	46
13	^{31}P and ^2H NMR spectra from of DOPE/DOPC mixtures and cholesterol	47
14	Influence of cholesterol on the quadrupolar splitting observed for ^2H -DOPC	49
15	^{31}P -NMR signal intensity arising from egg PC vesicles prepared by extrusion of multilamellar vesicles	61
16	Micrographs of negatively stained egg PC vesicles	62
17	Freeze-fracture micrographs of vesicles of varying lipid composition	63
18	Size distribution of soya PC LUVETs	64
19	Trapping efficiency of LUVETs	68
20	Membrane potential in soya PC LUVETs in the absence of valinomycin	70
21	Membrane potential in soya PC LUVETs in the presence of valinomycin	72

22	Comparison between the membrane potential determined by [^3H]-MTPP $^+$ and K $^+$ distribution	73
23	Comparison between the membrane potentials obtained for various transmembrane K $^+$ chemical gradients as detected by [^3H]-MTPP $^+$ and the theoretical potentials	75
24	Structures of safranine, MTPP $^+$, chlorpromazine, dibucaine, propranolol, vinblastine, and adriamycin	81
25	Spectrophotometric response of safranine	84
26	Influence of increasing safranine concentrations on the safranine response	86
27	Levels of LUVET associated safranine as a function of transmembrane potential	87
16	Magnitude of the safranine response as a function of internal safranine concentration and membrane potential	89
29	Time course for accumulation of safranine	90
30	K $^+$ release from LUVETs on addition of safranine	91
31	Influence of lipid composition on the safranine response	93
32	Accumulation of [^3H]-MTPP $^+$ (initial exterior concentration of $20 \times 10^{-8} \text{ M}$) by LUVETs	95
33	Accumulation of MTPP $^+$ (initial exterior concentration of 2 mM) by LUVETs	96
34	Uptake of chlorpromazine and dibucaine into LUVETs	98
35	Uptake of propranolol by LUVETs	99
36	Uptake of vinblastine and adriamycin into LUVETs	100
37	Model of safranine uptake	102
38	Structures of dopamine, epinephrine, and serotonin	108
39	Accumulation of dopamine by LUVETs experiencing a K $^+$ diffusion potential	112
40	Accumulation of dopamine by LUVETs experiencing a H $^+$ diffusion potential	114
41	Influence of external pH on dopamine uptake	116
42	Comparison between the membrane potentials obtained for various pH gradients as detected by [^3H]-MTPP $^+$ and the theoretical potentials	118
43	Effect of trapped ATP on dopamine accumulation	119
44	Accumulation of epinephrine and serotonin by LUVETs	121
45	Postulated mechanism for the uptake of dopamine	124

ABBREVIATIONS USED

ΔA_{516}	Change in absorbance at 516 nm
ΔQ	Quadrupolar splitting
$\Delta\psi$	Transmembrane electrochemical potential
ATP	Adenosine triphosphate
Al_2O_3	Aluminium oxide
BLM	Black lipid membrane
CAPS	3-(cyclohexylamino) propanesulfonic acid
CSA	Chemical shift anisotropy
CCCP	Carbonyl cyanide m-chlorophenylhydrazone
DMSO	Dimethylsulfoxide
EPSP	N-(2-Hydroxyethyl)piperazine-N'-3-propanesulfonic acid
ESR	Electron spin resonance
GPC	Glyceryl phosphorylcholine
H_{11}	hexagonal
$HClO_3$	Perchloric acid
HEPES	[4-(2-Hydroxyethyl)]-piperazine ethanesulfonic acid
KGlu	Potassium glutamate
LUVs	Large unilamellar vesicles
LUVETs	Large unilamellar vesicles by extrusion techniques
MES	2-(N-Morpholino)ethanesulfonic acid
MLVs	Multilamellar vesicles
MoO_3	Molybdenum trioxide
MTPP ⁺	Methyltriphenylphosphonium
$NaHSO_4$	Sodium bisulfite
Na_2SO_4	Sodium sulfite
NMR	Nuclear magnetic resonance

Phospholipids

DOPC	1,2-dioleoyl- <i>sn</i> -glycero-3-phosphorylcholine
[C ₁₁ - ² H ₂]DOPC	1,2-(11,11-dideuteriodioleoyl)- <i>sn</i> -glycero-3-phosphorylcholine
DOPE	1,2-dioleoyl- <i>sn</i> -glycero-3-phosphorylethanolamine
[C ₁₁ - ² H ₂]DOPE	1,2-(11,11-dideuteriodioleoyl)- <i>sn</i> -glycero-3-phosphorylethanolamine
E (egg)	Lipids derived from hen egg yolk
PA	Phosphatidic acid
PC	Phosphatidylcholine
PE	Phosphatidylethanolamine
PG	Phosphatidylglycerol
PI	Phosphatidylinositol
PS	Phosphatidylserine
S (soya)	Lipids derived from soya bean extract
psi	Pounds per square inch
SUVs	Small (sonicated) unilamellar vesicles
T _c	Gel to liquid-crystalline transition temperature
TLC	Thin layer chromatography

ACKNOWLEDGEMENTS

Acknowledgement sections are sometimes treated in a lighthearted fashion and therefore maybe taken in a lighthearted manner. For this reason I want to stress the point, clearly and in a manner that will be taken seriously, that this thesis was by no means an individual effort. The ideas, concepts, and technical expertise from each member of the lab were vital to the completion of this work. Therefore I want to do more than simply acknowledge these individuals for they are all co-authors of this manuscript. These individuals are:

Pieter Cullis, Mick Hope, Colin Tilcock, Tom Madden, Lawrence Mayer, Cees van Echteld, Rajiv Nayer, Blake Farren, Helen Loughley, Tom Redelmeier, and Eric Sommerman. I would especially like to thank Pieter and Mick, who created an environment which made scientific research a pure joy. Your enthusiasm is something I will always admire. Also, thanks for not making me finish the Sendi virus project.

This work was supported financially by fellowships from the University of British Columbia, Mom and Dad, and the Forestry Department (You'll have to think about that one).

Finally, I would like to thank my brothers, Alain and Andy, for not dropping me from that second story hotel window fifteen years ago, I knew if I was given a chance I could accomplish something worthwhile.

To
be is to do
(*Socrates*)

To
do is to be
(*Jean-Paul Sartre*)
Do be do be do
(*Frank Sinatra*)

and

To
Christina and Jlonka

INTRODUCTION

1.1 Membrane Structure: A Historical Perspective

The cytoplasm of a cell is physically separated from the surrounding environment by means of a cell membrane. The fact that the cytoplasm is chemically quite different from the external milieu yet can acquire necessary metabolites from the surroundings illustrates *prima facie* the role of the membrane in providing a selectively permeable barrier. However, beyond this basic role of separation, biological membranes participate in many complex phenomena ranging from roles involving inter- and intra-cellular communication to mediating cellular immune responses.

Biological membranes are composed primarily of lipids and proteins, with a small amount of associated oligosaccharides. To date, models defining the organization of these components in membranes have been based on three basic observations derived from studies which have spanned the last 50 years. The first observation, based on the initial investigations of Gorter and Grendel (1925) and developed later by Danielli and Davson (1935), was that the lipid component of membranes was arranged in a bimolecular leaflet organization. This familiar structure is represented by the phospholipid bilayer, which accommodates the amphipathic characteristics of the lipids such that the polar headgroups are in direct contact with the aqueous environment while the fatty acid chains are buried in the hydrophobic core of the membrane.

The second observation(s) concerned the location of the protein component in relation to the lipid bilayer model postulated by Danielli and Davson. Formulation of these models relied on information derived from a number of techniques which had been developed for determining protein structure (x-ray crystallography, optical rotary dispersion, and circular dichroism) and for visualizing membranes (electron microscopy and freeze fracture technology). Robertson (1957) proposed the unit membrane model, which summarized data derived mostly

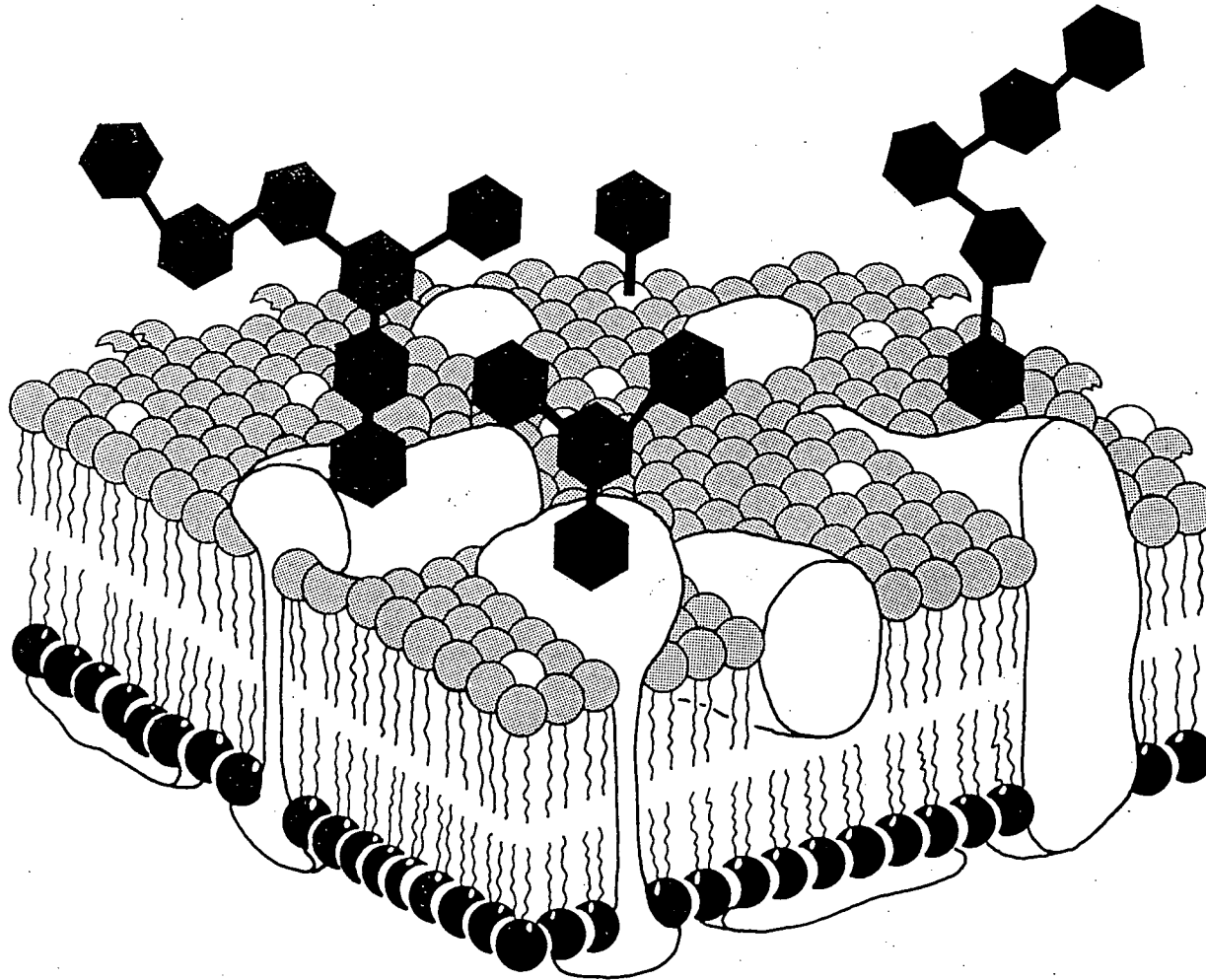
from x-ray diffraction and electron microscopic studies of the myelin sheath, that suggested that proteins, in extended β -form, were spread out as monolayers coating the lipid bilayer. It was later demonstrated that a substantial fraction of membrane associated protein was in an α -helical conformation and appeared to be maintained within the lipid bilayer as globular structures. Characterization of these integral membrane proteins (in contrast to peripheral membrane proteins which are loosely associated with the surface of membranes) resulted in the postulation of a variety of models for membrane structure suggesting hydrophobic protein-lipid interactions where protein molecules were actually intercalated within the lipid bilayer (for reviews see Vanderkooi and Green, 1970; Hendler, 1971; Stoeckenius and Engelman, 1969; Korn, 1966; Bretscher, 1973).

The third observation was that the components of a membrane existed in a fluid, mobile, state. Utilizing the technique of differential scanning calorimetry it was demonstrated as the temperature was increased through a particular value aqueous dispersions of phospholipids undergo an exothermic transition (the gel to liquid-crystalline phase transition) which corresponded to the transition of the acyl chains from a rigid, immobile, state to a fluid state. At physiological temperatures membrane lipids were found to be generally in a fluid state (Chapman, 1966; Stein *et al.*, 1969; Melchoir, 1970). In addition, the lateral movement of lipids and proteins in biological membranes had been demonstrated by a variety of techniques. This is exemplified by the classic experiment of Frye and Edidin (1970) which demonstrated, using immunospecific labeling, that the surface components of two cell types intermixed after the cells were fused. This spreading of components was shown to be dependent on the external temperature.

These observations have been successfully accommodated in the currently accepted "fluid mosaic" model for the structure of biological membranes, which was proposed by Singer and Nicolson in 1972. Briefly, the model (see Fig. 1) was derived from thermodynamic considerations concerning membranes and associated components. Hydrophobic and hydrophilic interactions were maximized so that the lowest free energy state for the functional membrane could be attained (for reviews see Singer, 1977; Tanford, 1980). This required that the

Fig. 1. The fluid mosaic model of membrane structure. In this model, developed by Singer and Nicolson (1972), membrane proteins are shown to be interspersed within regions of a predominantly fluid phospholipid bilayer, forming a mosaic pattern.

Plasma membrane



Cytosol

nonpolar components of membranes, such as the fatty acid chains of the phospholipids and the nonpolar amino acid residues of proteins, were in minimum contact with the aqueous environment while the polar groups, polar amino acids, headgroups of phospholipids, and associated carbohydrate moieties, were in maximum contact with the aqueous environment. The integral membrane proteins were depicted as being embedded in a phospholipid matrix, providing a mosaic structure in which integral proteins were interspersed within sections of membrane bilayer. Further, the model stressed that both the protein and lipid components were capable of lateral movement within the membrane.

1.2 Rationale for Investigating the Role of Lipids in Biological Membranes

Beyond the fundamental view of membrane structure as modeled by Singer and Nicolson, it is necessary to explain the great diversity in chemical composition of a biological membrane. Any particular biological membrane may contain a variety of phospholipids (having different polar head groups and hydrocarbon chains), varying amounts of sterols, and a host of differing proteins. In addition, within a given membrane these different components are arranged asymmetrically such that the inner surface of a membrane is compositionally different from the outer surface (for reviews see van Deenen, 1981; Etemadi, 1980a; Etemadi, 1980b). This compositional diversity would, at least in part, be determined by the functional requirements of the membrane. In this context, it has been firmly established that the major functional role of lipids in biological membranes involves the formation and maintenance of the bilayer structure. This has been demonstrated through observations that phospholipid preparations normally spontaneously adopt the bilayer structure on hydration (Dervichian, 1964; Bangham *et al.*; 1965) and that biological membranes contain regions of bilayer structure (Finean and Robertson, 1958). However, a single phospholipid species such as phosphatidylcholine could provide the fluid bilayer structure of membranes. Since several hundred lipid species can be present in a typical mammalian cell membrane, other functional roles for lipids must exist. This aspect of lipid diversity, as it relates to membrane structure and function, provides the major focus of this thesis. Specifically, model systems composed of

single and mixed lipid components have been utilized to identify potential roles for lipids in biological membranes.

The objectives of this introduction will be to (i) discuss the functional roles of lipids in terms of the fluid mosaic model of membranes, (ii) discuss the systems utilized to model the structural and functional features of membranes, (iii) review some of the chemical and physical properties of phospholipids and cholesterol, (iv) describe the structural preferences of lipids, introducing the concept of lipid polymorphism and defining the roles which have been postulated for non-lamellar structures, (v) discuss the roles of lipids in providing a permeability barrier, and (vi) discuss the concept that different lipids assume different molecular shapes. Throughout these discussions the scope of this thesis as it relates to each area will be emphasized.

1.3 Role of Lipids Within the Fluid Mosaic Model of Membranes

In general terms, the fluid mosaic model suggested that the lateral mobility of membrane proteins was essential for proper membrane function and was related to a variety of membrane mediated cellular phenomena, including malignant cell transformation (the original example illustrated by Singer and Nicolson; 1972), fertilization (Johnson and Edidin, 1978), cell growth (Collard *et al.*, 1977), and differentiation (Kawasaki *et al.*, 1978). One rationale for lipid diversity was therefore established on the basis that membrane function could be regulated by changes in fluidity within local regions of the membrane. Indeed, changes in lipid microviscosity had been shown to influence the functions of integral membrane proteins with specific carrier, receptor, and enzymatic functions (Warren *et al.*, 1974a; Warren *et al.*, 1974b; Jacobs and Cuatrecasas, 1977; Kimelberg, 1977; Chapman and Correll, 1977). Since it was demonstrated that the gel to liquid-crystalline phase transition of phospholipids was sensitive to acyl chain length and degree of unsaturation and the headgroup composition (Chapman, 1968), as well as the presence of cholesterol (Ladbrook *et al.*, 1968; Hubbel and McConnel, 1971) and integral membrane proteins (Cornell *et al.*, 1978; Silviu, 1982), it was proposed that *in vivo* regulation of membrane proteins could be "fine tuned" by a variety of

factors that are mediated by specific lipids such as cholesterol.

Rationalizing lipid diversity in terms of membrane fluidity presents certain difficulties when one considers that gel state lipids do not appear to be present in most eukaryotic systems. The unsaturated nature of naturally occurring lipids results in gel to liquid-crystalline phase transitions well below physiological temperatures, as shown for the lipids of the erythrocyte (van Dijck, 1976). In addition, several studies demonstrated that incorporation of integral membrane proteins usually reduces the hydrocarbon transition temperature (Papahadjopoulos *et al.*, 1975b; Houslay *et al.*, 1975) and indicated that integral membrane proteins were excluded from regions of gel state lipid (Grant and McConnel, 1974; Kleeman and McConnel, 1976). Presumably these data indicate that gel state lipids are not accessible to membrane proteins and therefore would not be able to regulate protein function even if present in the membrane.

A second rationale for lipid diversity was established from data which indicated that membrane bound enzymes required a well define lipid annulus for optimal function (for review see Devaux and Seigneuret, 1984). The evidence however does not provide a convincing argument for the presence of a defined lipid annulus. It has been demonstrated that a variety of enzymes, such as cytochrome oxidase (Vik and Capaldi, 1977), (Na⁺, K⁺)-ATPase (Hilden and Hokin, 1976), C55-isoprenoid alcohol phospholipase (Gennis and Strominger, 1976), and (Ca²⁺, Mg²⁺)-ATPase (Hesketh *et al.*, 1976), function well when reconstituted in model systems which contain any one of a variety of lipids. This point is further emphasized by experiments which demonstrated that (Na⁺, K⁺)-ATPase and sarcoplasmic reticulum ATPase could function well in a pure detergent environment (Dean and Tanford, 1977). In addition, conclusions derived from ESR (electron spin resonance) data suggesting the presence of "boundary lipid" appear to be only valid on the ESR time scale of 10⁻⁸-10⁻¹⁰ sec (ESR is not sensitive to motions requiring longer times to occur). Deuterium (²H) NMR (time scale of 10⁻⁶ sec) studies have not been able to distinguish between the boundary lipid and the bulk lipid phase suggesting that lipids in the annulus exchange with bulk lipid at a rate of 10⁻⁶-10⁻⁷ sec. These points are illustrated by studies on cytochrome oxidase and sarcoplasmic reticulum

ATPase which show a two component ESR spectra indicative of a "mobile" and "immobile" component (Hesketh *et al.*, 1976; Marsh, 1978) while ^2H -NMR studies showed the existence of only one mobile component (Oldfield *et al.*, 1978; Oldfield *et al.*, 1979).

Related to the previous discussion, several investigations suggested that specific lipid-lipid interactions may result in the formation of compositionally distinct lipid domains (for review see Oldfield and Chapman, 1972) that would be functionally significant in biological membranes. For example, investigations which demonstrated that Ca^{2+} , an agent which mediates *in vivo* fusion events, induced the phase segregation of phosphatidylserine in mixed lipid systems (Papahadjopoulos, 1978; Dluhy *et al.*, 1983) supported the concept that fusion of membranes would require phase separation of phospholipid components, providing a site for fusion to occur at the phase boundaries. Data presented in this thesis (see Chapter 2) and elsewhere (Tilcock *et al.*, 1984), however, indicate that in complex multicomponent membrane systems such as the biological membrane that individual lipid species have no tendency to segregate into functionally or structurally distinct domains.

1.4 Model Membrane Systems

To investigate the basic structural and physical characteristics of biological membranes it is useful to isolate individual components and attempt to model the more complex system by incorporating these components in simple well-defined systems. Indeed much of the current concept of membrane structure and function has been derived from investigations which utilize model membrane systems composed of naturally occurring or synthetic lipid species in the presence or absence of an isolated membrane protein. A discussion of protein reconstitution in model membrane systems is beyond the scope of this thesis, for those interested there are several reviews of this subject (see Racker, 1979; Eytan, 1982).

Hydration of a dry phospholipid film results in the spontaneous formation of structures which are composed of numerous closed concentric lipid bilayers separated by aqueous compartments (Bangham *et al.*, 1965). These multilamellar vesicles (MLVs) are perhaps the

most frequently utilized preparation for defining the properties of lipids. This is due in part to the ease of preparation, which involves quite literally addition of a buffer to a dried lipid film followed by a good shake to generate and disperse the large (radius greater than 200 nm) lipid aggregates. Many of the biophysical approaches used for determining the motional and structural properties of lipids, including the diffraction, spectroscopic, and calorimetric techniques, utilize MLVs as model systems (for example see Chapter 2).

In addition, MLVs have been used to characterize a variety of membrane associated functions, ranging from monovalent and divalent cation permeability to protein-lipid interactions. The data derived from these investigations are often ambiguous due to the size heterogeneity and the numerous aqueous compartments present, hence different model systems were developed to circumvent these problems. These included procedures for generating unilamellar vesicles (for reviews see Bangham *et al.*, 1974; Pagano and Weinstein, 1978; Szoka and Papahadjopoulos, 1980) and the black lipid membrane (BLM; for review see Fettiplace *et al.*, 1974). The latter preparation is a mechanically supported lipid bilayer produced by spreading a lipid-solvent solution across a hole in a plastic sheet which separates two aqueous compartments. This model system has been particularly useful in characterizing the permeability properties of lipids in a bilayer configuration. However, the results from experiments employing BLMs are difficult to interpret since these preparations always contain a certain amount of residual solvent which has been shown to influence the bilayer thickness (Benz *et al.*, 1975) as well as the transport properties of these membranes (Benz *et al.*, 1977).

The applicability of unilamellar vesicles in defining permeability and transport functions is obvious, however the majority of techniques which have been developed to produce these vesicles also have shortcomings (see Szoka and Papahadjopoulos, 1980). In the case of small (sonicated) unilamellar vesicles, which have a diameter less than 30 nm, artifacts resulting from the high degree of membrane curvature (the inner to outer monolayer phospholipid ratio is typically 1:2) resulting in packing restraints. Other preparations which produce large (greater than 100 nm diameter) unilamellar vesicles (LUVs) utilize organic solvents or detergents that are difficult to completely remove subsequently. For this reason a novel technique for

producing large unilamellar vesicles (LUVs) has been developed and is described in detail in Chapter 3 of this thesis. Chapter 3 provides an adequate review of pertinent literature, therefore further discussion concerning the utilization and properties of LUVs will not be provided here. It is sufficient to state that these vesicles provide an ideal model for characterizing ion permeability (see Chapter 3) and transport properties (see Chapters 4 and 5) in systems of defined lipid mixtures and, in addition, may provide a useful model vesicle system for the reconstitution of membrane proteins (Madden *et al.*, 1984).

1.5 Chemical and Physical Properties of Phospholipids and Cholesterol

The fundamental question as to why there is such a heterogeneous population of lipids in a biological membrane still remains. Clearly differences in lipid composition play fundamental roles in membrane structure as well as the regulation of membrane protein activity and membrane mediated events such as fusion. An indication of the lipid diversity and the properties of these lipids in isolation and in mixtures will be presented. The variety of lipid species present in a typical eukaryotic membrane include phospholipids and cholesterol, as well as an assortment of other species including glycolipids, neutral lipids, and free fatty acids. In addition there are variations in the headgroup composition, represented by different phospholipids and gangliosides (glycolipids), in the fatty acyl chain composition of individual lipid species, and the number of chains present (*e.g.* the lysophospholipids have a single acyl chain). Clearly it would be inappropriate to review the chemical and physical properties of all lipid species, much of which is detailed in a variety of texts (for excellent reviews see Zubay, 1983). The major lipids employed in this thesis are phospholipids and cholesterol, therefore the more general aspects of these lipids will be summarized here. The ability of different lipids to adopt other structural phases in addition to the bilayer configuration, defined as lipid polymorphism, is an important physical parameter of lipids that will be discussed separately (see section 1.6).

1.5.1 Phospholipids

In general, most lipid species exhibit amphipathic characteristics. This is represented by the most abundant lipid class, the phospholipids, which contain a strongly hydrophilic head group and one, or more commonly two, acyl chains which can be 12 to 24 carbons long with varying degrees of unsaturation. The major classes of phospholipids are shown in Fig. 2, and the more common variations in acyl chains are given in Table 1. The fatty acid chains are esterified to glycerophosphate, forming phosphatidic acid (PA), which can condense with a base to form phosphatidylcholine (PC), phosphatidylethanolamine (PE), phosphatidylserine (PS), phosphatidylinositol (PI), or phosphatidylglycerol (PG). The fatty acid chains of naturally occurring lipids commonly contain an even number of carbons, with an unsaturated chain normally confined to the *sn*2 position of the glycerol backbone and a saturated chain, often palmitic acid (16:0), in the *sn*1 position.

The physical properties of phospholipids are influenced largely by headgroup interactions and acyl chain mobility (for reviews see Chapman, 1975; Lee, 1975; Seelig, 1978; Cullis and de Kruijff, 1979; Boggs, 1980). Some of these properties have been characterized by the temperature at which the gel to liquid-crystalline phase transition occurs (T_c). For example, bilayers composed of a synthetic PC, which contain long saturated acyl chains have a higher gel to liquid-crystalline phase transition temperature compared to PC species with shorter saturated acyl chains. The presence of a double bond in the acyl chains (normally *cis*) results in a marked decrease in the T_c (Chapman, 1975). The thermotropic phase properties of phospholipids are also influenced by headgroup composition (Cameron *et al.*, 1981), where a difference of 22°C has been observed in the T_c of dioleoyl (18:1*c*/18:1*c*) PC ($T_c = -22^\circ\text{C}$) and dioleoyl PE ($T_c = 0^\circ\text{C}$). Several lipid species, including PA, PS, PG, and PI, have a negatively charged headgroup at physiological pH and the repulsive effects between these headgroups results in a decrease in the T_c (van Dijk *et al.*, 1978). Clearly the charge of a lipid is not the only factor influencing the T_c . PA, PG, and PS all bear a negative charge at neutral pH yet the T_c of PA can be as much as 25°C higher than either PG or PS.

Fig. 2. General structure of a phospholipid showing the more common headgroups.

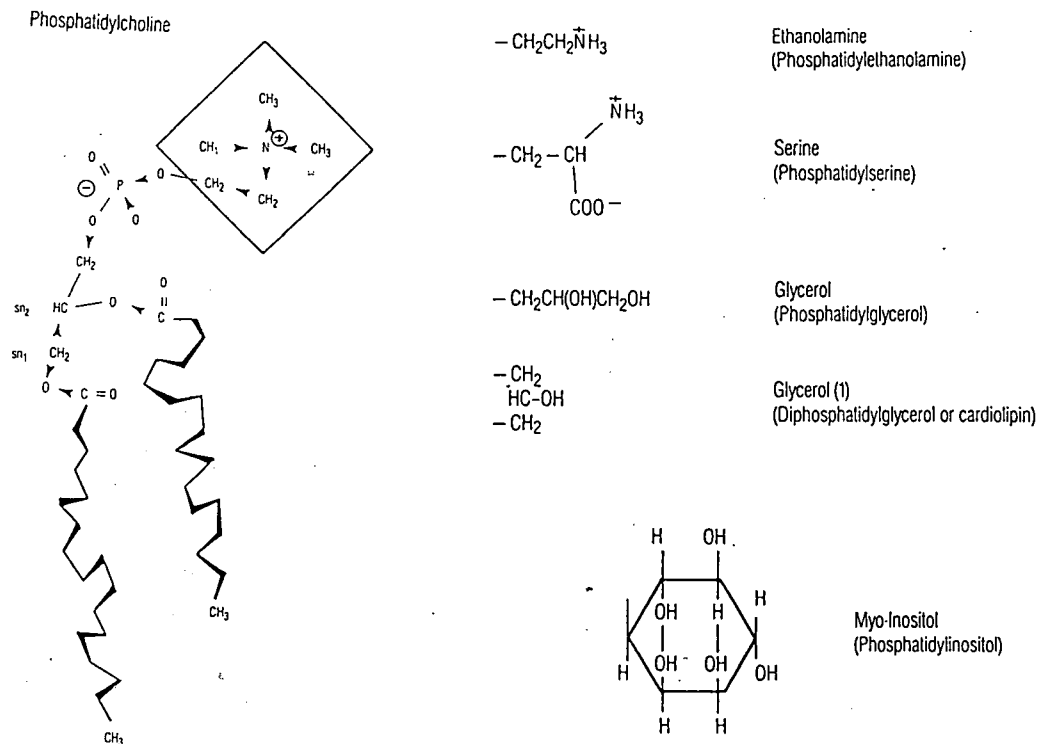


Table 1 Commonly occurring fatty acid moieties.

Structure	Common name
<i>Saturated fatty acids</i>	
$\text{CH}_3(\text{CH}_2)_{10}\text{COOH}$	Lauric
$\text{CH}_3(\text{CH}_2)_{12}\text{COOH}$	Myristic
$\text{CH}_3(\text{CH}_2)_{14}\text{COOH}$	Palmitic
$\text{CH}_3(\text{CH}_2)_{16}\text{COOH}$	Stearic
$\text{CH}_3(\text{CH}_2)_{18}\text{COOH}$	Arachidic
$\text{CH}_3(\text{CH}_2)_{22}\text{COOH}$	Lignoceric
<i>Unsaturated fatty acids</i>	
$\text{CH}_3(\text{CH}_2)_5\text{CH}=\text{CH}(\text{CH}_2)_7\text{COOH}$	Palmitoleic
$\text{CH}_3(\text{CH}_2)_7\text{CH}=\text{CH}(\text{CH}_2)_7\text{COOH}$	Oleic
$\text{CH}_3(\text{CH}_2)_4\text{CH}=\text{CHCH}_2\text{CH}=\text{CH}(\text{CH}_2)_7\text{COOH}$	Linoleic
$\text{CH}_3\text{CH}_2\text{CH}=\text{CHCH}_2\text{CH}=\text{CHCH}_2\text{CH}=\text{CH}(\text{CH}_2)_7\text{COOH}$	Linolenic
$\text{CH}_3(\text{CH}_2)_1(\text{CH}=\text{CHCH}_2)_3\text{CH}=\text{CH}(\text{CH}_2)_3\text{COOH}$	Arachidonic

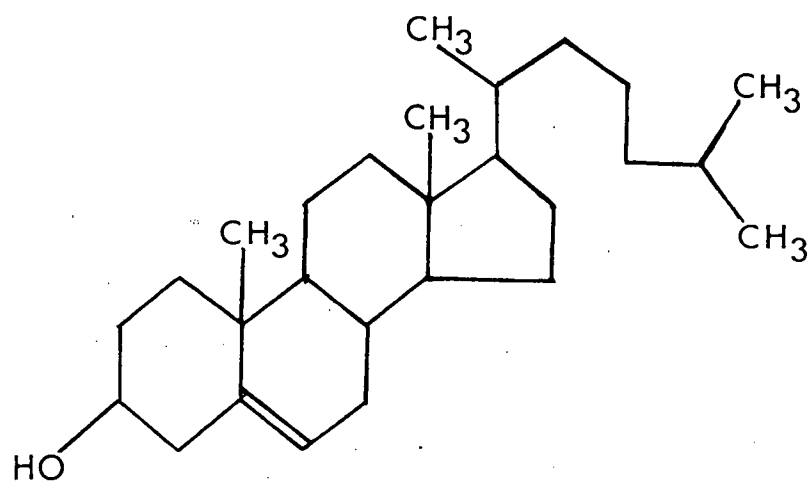
with identical acyl chain composition (van Dijck, 1978).

In addition to the effects on thermal properties of lipids, the presence of ionizable groups allows for a number of physiologically relevant factors, such as pH, ionic strength, and the presence of divalent cations, to isothermally modulate the behaviour of lipids. The ability of divalent cations such as Ca^{2+} to induce phase segregation of lipids in model membrane systems has already been discussed. Several investigators have also shown that changes in pH can exert profound effects on the structure and properties of PS containing membranes (Harlos *et al.*, 1979; Hope and Cullis, 1980; Tilcock and Cullis, 1981).

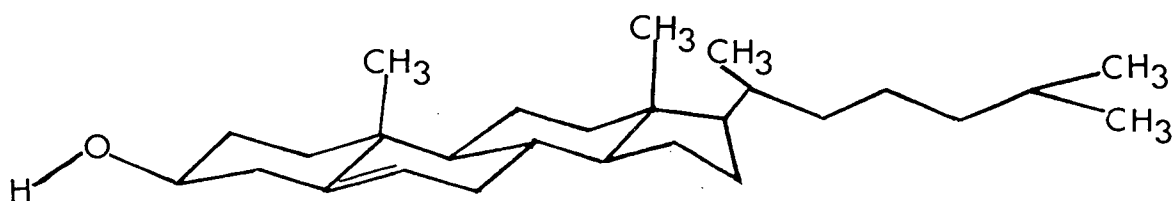
1.5.2 Cholesterol

The major neutral lipid component in the plasma membrane of eukaryotic organisms is cholesterol. The structure of cholesterol (Fig. 3) bears no resemblance to phospholipids, however this steroid ring does possess amphiphathic characteristics due to the presence of the 3 β -hydroxyl group at one end of the molecule. Cholesterol orients itself in a phospholipid bilayer such that this hydroxyl group is adjacent to the fatty acyl carbonyls of the phospholipid (Huang, 1977), while the rigid steroid nucleus is associated with the acyl chains. A consequence of this association is a reduction in the number of gauche conformations which occur in the region of the first ten carbons of the acyl chains (Kawato *et al.*, 1978; Rance *et al.*, 1982), a point illustrated by pressure-area monolayer curves which indicate that cholesterol exerts a condensing effect (represented by a decrease in the area occupied per lipid molecule) in a PC monolayer. The presence of cholesterol in PC bilayers results in a decrease in the enthalpy change associated with the transition (Ladbroke *et al.*, 1968). This effect has been attributed to the ability of cholesterol to increase lipid order above the phase transition while decreasing the order below the transition. On the basis of these data it was suggested that the major role of cholesterol in membranes was to control membrane fluidity. As stated previously, the role of fluidity in the regulation of membrane function is doubtful.

Fig. 3. Structure of cholesterol.



CHOLESTEROL



It has been well established that cholesterol is an essential structural requirement for many biological membranes and influences a variety of membrane mediated functions from the passive permeability of ions to the regulation of enzymatic activities (for reviews see Demel and de Kruijff, 1976; Block, 1981). The influence that cholesterol has on the behaviour of lipids (and proteins) in membranes is still the subject of intense investigations and forms the basis of much of this thesis. In Chapter 2 the role of cholesterol in modulating the polymorphic phase behaviour (see section 1.6) of mixed lipid systems is examined. In addition, Chapter 4 presents a preliminary study investigating the effects of cholesterol on membrane mediated transport processes.

1.6 Lipid Polymorphism

As discussed previously, many phospholipids spontaneously adopt a bilayer organization upon hydration. In addition to this configuration it has been demonstrated that a variety of lipids can adopt different structural phases, such as the hexagonal (H_{11}) phase characterized by cylinders of lipids in an "inverted" (headgroups oriented inwardly towards aqueous channels) organization (see Fig. 4). This lipid polymorphism has been recognized for more than 20 years, when Luzzatti and co-workers, using the technique of X-ray diffraction, initially documented the occurrence of non-lamellar lipid structures depending on the state of lipid hydration and temperature (Luzzatti and Husson, 1962; Luzzatti *et al.*, 1968; Luzzatti and Tardieu, 1974). However, the significance of these alternate phases in relation to membrane structure and function was not realized until it was shown that physiologically relevant factors (pH, ionic strength, acyl chain composition and the presence of divalent and/or other lipid species) could isothermally influence the structural preference of naturally occurring lipids (for reviews see Cullis and de Kruijff, 1979; Cullis *et al.*, 1983; de Kruijff *et al.*, 1984). These non-bilayer phases almost certainly play important roles in defining membrane structure and function. For this reason, the role of lipids as related to their structural preference will be a central theme for this dissertation. Chapter 2 examines some factors which regulate the formation of non-lamellar structures, while the remaining chapters examine the role of bilayer

forming lipids in regulating ion permeability and membrane mediated transport process. It would be advantageous at this stage to briefly review the experimental techniques utilized to characterize the macroscopic structures adopted by hydrated model lipid systems and to discuss the roles which have been postulated for these alternate phases.

1.6.1 Techniques for evaluating lipid polymorphism

A diverse set of techniques have been utilized to investigate the polymorphic phase behaviour of lipids, including X-ray and neutron diffraction (Luzzatti, 1968; Buldt *et al.*, 1979; Zaccai *et al.*, 1979; Blaurock, 1982), freeze-fracture electron microscopy (Verkleij, 1984), differential scanning calorimetry (Cullis and de Kruijff, 1978b), and ^2H and ^{31}P nuclear magnetic resonance (NMR) spectroscopy (Davis, 1983; Seelig, 1977; Seelig, 1978; Cullis and de Kruijff, 1979). NMR and freeze-fracture techniques were employed in studies presented in this thesis, therefore the discussion will be confined to these procedures. It should be emphasized, however, that diffraction techniques are the only procedures that provide unequivocal information on the structures adopted by hydrated lipids. As discussed by Cullis and de Kruijff (1979), the other techniques are extrapolative in nature, relying on previous X-ray diffraction data. Currently, there is a great deal of evidence which demonstrates that the structural assignments based on NMR data are in agreement with X-ray diffraction data (Marsh and Seddon, 1982; Seddon *et al.*, 1983; Tilcock *et al.*, 1984).

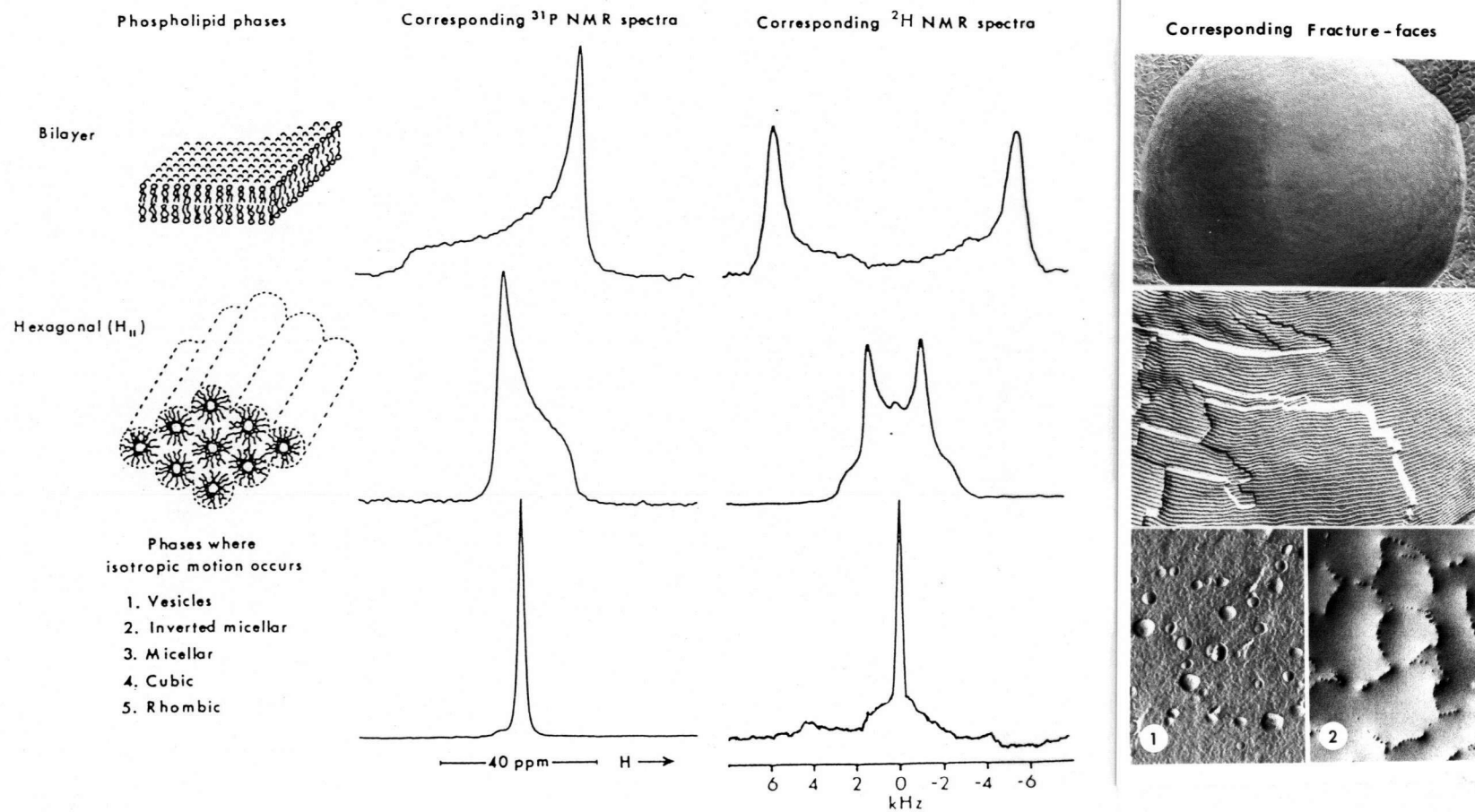
Nuclear magnetic resonance spectroscopy. Nuclei such as ^{31}P exhibit a quantum mechanical quantity known as "spin". For ^{31}P the spin quantum numbers are $+1/2$ or $-1/2$. This imparts to the nuclei characteristics of a small bar magnet when placed in a strong magnetic field. In particular, nuclei with spin $1/2$ can be considered as magnets which are oriented such that the "north" pole is oriented towards the north pole of the magnet giving rise to the strong magnetic field, whereas for nuclei with spin $-1/2$ the situation is reversed. Clearly the nuclei with spin $-1/2$ are then in a "lower energy" situation, and an energy difference then exists between the spin $-1/2$ and $1/2$ states when a strong magnetic field is

present. The NMR experiment involves exciting transitions between these two states (which requires radiofrequency irradiation) and monitoring the energy absorbed. This gives rise to a resonance at a particular frequency, which is usually characterized in terms of a parameter known as the "chemical shift". This chemical shift is calculated as the frequency separation between the resonance of interest and some standard, divided by the irradiation frequency itself. As the irradiation frequency is usually in the MHz range, this chemical shift parameter is usually multiplied by a factor of 10^6 and expressed as parts per million (ppm).

The magnetic field experienced by the ^{31}P (phosphorus) nuclei associated with the phosphodiester bond found in most phospholipids is partially shielded by the surrounding electron cloud. This shielding will differ according to the orientation of the phosphate segment in the magnetic field. As a result a ^{31}P nuclei will resonate at different frequencies according to the orientation, resulting in a large "chemical shift anisotropy" (CSA) and a characteristic broad ^{31}P -NMR spectrum for non-oriented, dried phospholipid samples. When phospholipids are hydrated, the motion available to the phospholipid in a bilayer organization influences the ^{31}P -NMR lineshape. For large (radius greater than 200 nm) liquid-crystalline bilayers (such as MLVs) this motion is restricted to rapid axial rotation of the lipid. For a non-oriented sample this gives rise to a broad lineshape with a low field shoulder and a high field peak separated by an effective CSA of -40 to -50 ppm (see Fig. 4). Most of the phospholipids examined exhibit similar values of CSA, providing essentially equivalent spectra for these lipids in a liquid-crystalline bilayer organization. This is a useful characteristic if more complex lipid mixtures (such as a biological membrane) are examined, since all the signals arising from phospholipids in a bilayer organization combine to produce a composite bilayer lineshape.

In situations where lipids can experience other forms of rapid motion, in addition to rotation about the long axis, additional narrowing of the ^{31}P NMR spectrum is observed. This is the case for small vesicles, where vesicle tumbling and rapid lateral diffusion of the lipids around the vesicle allow isotropic motional averaging over all possible orientations. The resulting ^{31}P NMR spectrum is characterized by a narrow lineshape as illustrated in Fig. 4. A variety of other phases, such as the inverted micellar configuration, cubic, or rhombic phases,

Fig. 4. ^{31}P -NMR, ^2H -NMR, and freeze-fracture characteristics of phospholipids in various phases.



allow isotropic motion (see Fig. 4), hence it is difficult to assign a lipid phase on the basis of this narrow ^{31}P NMR spectrum and conclusions must be corroborated by data from other techniques such as freeze-fracture, or X-ray diffraction. Lipids in the H_{11} phase also experience additional motional averaging in comparison to lipids in a large bilayer configuration due to diffusion of the lipids around the cylinder structures. The resulting ^{31}P NMR spectra are narrower by a factor of two, with an effective CSA of -20 ppm, and have a reversed asymmetry.

The previously mentioned advantage of ^{31}P NMR, that all ^{31}P signals combine to give rise to a composite spectra reflecting the overall organization of the phospholipids, may also be considered a disadvantage. In systems composed of two or more lipid species it would at times be useful to determine the phase properties of each individual component (for an example see Chapter 2). ^2H NMR provides an excellent technique for determining the phase properties of a specifically deuterated lipid. The ^2H nucleus has spin quantum numbers of $+1$ and -1 , which give rise to a quadrupole moment. The ^2H NMR spectra derived from a partially deuterated lipid in a large bilayer organization contains two absorption peaks (see Fig. 4). The separation of the peaks, defined as the quadrupole splitting, is related to the ^2H order parameter. Similar to the situation described for ^{31}P NMR, the ^2H NMR spectrum with its characteristic quadrupole splitting is dependent on the motional properties of the lipids. Lipids in the H_{11} phase provide a spectra with essentially a 2 fold reduction in the quadrupole splitting in comparison to lipids in the bilayer organization. When isotropic motional averaging occurs, as in the case with small vesicles, the quadrupole splitting collapses resulting in a spectrum with a single narrow line.

Freeze-fracture electron microscopy. The local morphology exhibited by lipids in model membrane systems can be observed utilizing the technique of freeze-fracture electron microscopy, and freeze-fracture data is useful in verifying the structural assignments derived from NMR experiments (see Chapter 2). The freeze-fracture technique relies on the fact that in a frozen sample which contains membrane structures a fracture plane will proceed through

the hydrophobic interface between the bilayer leaflets (Pinto da Silva and Branton, 1970). Once fractured the sample is coated with platinum and carbon, the sample itself is digested away and the resulting replica is examined using an electron microscope.

Micrographs of phospholipids in a bilayer organization show smooth sheets, as the fracture occurs in the center of the bimolecular leaflet, while H_{11} phase structures are seen as striated patterns created as the fracture plane proceeds between the hexagonally packed cylinders (see Fig. 4). In addition, freeze-fracture micrographs are sometimes useful in providing defined structural information for lipids which exhibit a narrow NMR spectra indicative of any number of phases which allow isotropic motional averaging. An elegant example of this is given by studies which defined the nature of the lipidic particle (Verkleij, 1984).

1.6.2 Roles postulated for non-lamellar structures

The number of functional roles for lipids in biological membranes is increased substantially when non-bilayer organizations are considered. As indicated earlier, a number of isolated lipids, primarily unsaturated PEs, preferentially adopt the H_{11} phase. In general, the presence of other lipids stabilize the bilayer configuration for these lipids (for example see Chapter 2). As previously discussed, a great variety of physiologically relevant factors, including specific ions, other lipids, and proteins, can induce the formation of non-lamellar alternatives in multicomponent systems. A clear example of this concerns model systems composed of cardiolipin which assume the bilayer organization until the divalent cation Ca^{2+} is added, triggering a bilayer to H_{11} phase transition (Cullis *et al.*, 1978b).

Clearly the diversity of lipids in membranes is more complex than required to merely provide a structural matrix for non-lipid components and a semi-permeable barrier. This function, discussed in greater detail in section 1.7, would be satisfied by the bilayer forming lipids such as PC and sphingomyelin. The presence of non-bilayer forming lipids (PEs) would allow for the formation of non-bilayer structures, a function that could be regulated by the presence of lipids whose phase behaviour are sensitive to external variables. Numerous roles

have been proposed for non-bilayer organizations in membranes, including membrane fusion (which most likely precedes via the formation of inverted micellar structures; see Verkleij, 1984), exocytosis (Nayar *et al.*, 1982b), transbilayer transport of lipids and ions (Cullis *et al.*, 1980; Noordam *et al.*, 1981), intermembrane communication (Cullis *et al.*, 1983), and protein insertion and transport (de Kruijff *et al.*, 1984). In addition, it has been suggested that non-bilayer lipids may define the structure of certain regions of biological membranes. For example it is thought that the tight junction results from two membranes that exist in a semi-fused state, where the inner lamelli of two cells are separated by a cylinder of H_{11} -phase lipid (Kachar and Reese, 1982). These proposals have been discussed in detail elsewhere (Cullis *et al.*, 1983; de Kruijff *et al.*, 1984).

The most convincing argument for the role of non-lamellar structures *in vivo* is in the case of membrane fusion, a process that mediates a variety of biological phenomena such as fertilization, endocytosis (uptake of extracytoplasmic material), and exocytosis (release of cellular material). Since this area is relevant to the data presented in Chapter 2, the supportive evidence will be briefly summarized. It is conceptually difficult to perceive a membrane fusion event occurring without some local disruption of the bilayer organization, hence this process is likely mediated by the formation of an alternative structure. Indeed, numerous studies have demonstrated a strong correlation between membrane fusion and the appearance of non-bilayer structures. Chemical fusogens, such as glycerolmonooleate, which are able to induce fusion of both model and biological membranes, also enhanced the formation of non-lamellar phases in these systems (Hope and Cullis, 1981). Structurally similar agents, *e.g.* glycerolmonostearate, which were not capable of inducing fusion, do not effect the bilayer organization. In addition, the divalent cation Ca^{2+} usually required for *in vivo* fusion events, provokes the formation of the H_{11} phase in mixed lipid model systems that contain PE and the acidic phospholipid PS (Tilcock and Cullis, 1981), PG (Farren and Cullis, 1980), PI (Nayar *et al.*, 1982a), or cardiolipin (de Kruijff and Cullis, 1980). Addition of Ca^{2+} to vesicles (SUVs) with these lipid compositions induced fusion, accompanied by the formation of lipidic particles (putatively an inverted micellar structure) localized primarily at the fusion juncture

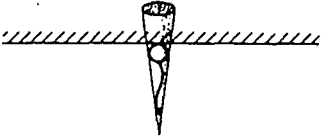
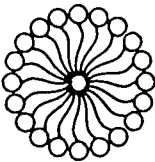
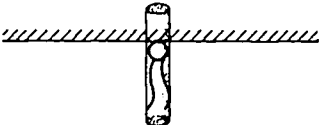
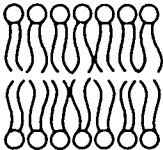
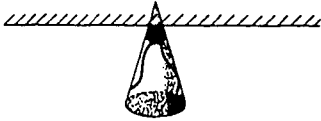
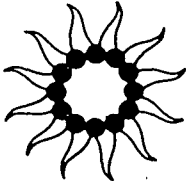
(Hope *et al.*, 1983). These data are consistent with the proposal that fusion proceeds via formation of a non-bilayer, inverted micellar, structure. Further studies designed to investigate the mechanism of exocytosis of chromaffin granule contents also suggested that formation of the inverted micelle was an necessary intermediate for the exocytosis process (Nayar *et al.*, 1982b).

1.7 The Shape Concept

A rationale for lipid diversity and the structural behaviour of lipids in membranes has been based on the proposal that the structures which lipids adopt when hydrated may be the result of their dynamic molecular shape (Israelachvili *et al.*, 1977; Cullis and de Kruijff, 1979). This proposal is consistent with the polymorphic phase properties of lipids and lipid mixtures, as well as other properties including the thermotropic behaviour of lipids, the ability of lipids to form intermolecular hydrogen bonds, and the response of lipids to physiologically relevant factors such as divalent cations

The proposed "shapes" that different lipids may assume are illustrated in Fig. 5. Lipids with a relatively small headgroup in relation to the area occupied by the acyl chains have a "cone" shape. The reverse situation, where the area occupied by the headgroup is greater than the area occupied by the acyl chains, results in an "inverted cone" shape and if the areas appropriated by the acyl chains and the headgroup are effectively equivalent, then a "cylindrical" shape is assumed. The latter example would describe the bilayer forming lipids such as PC, while the "cone" shaped lipids, *ie.* PE, would be accommodated in the H_{11} phase organization. These effects are illustrated by the properties of synthetic PEs. These lipids undergo a temperature induced bilayer to H_{11} phase transition (which occurs above the gel to liquid-crystalline phase transition) that is acutely sensitive to acyl chain composition. More specifically, this transition occurs at progressively lower temperatures in association with increases in acyl chain unsaturation (Tilcock and Cullis, 1982). The unsaturated acyl chains can be expected to assume a greater cross-sectional area with respect to the headgroup than the

Fig. 5. Polymorphic phases and corresponding dynamic molecular shapes of component lipids.

LIPIDS	SHAPE	ORGANISATION
LYSOPHOSPHOLIPIDS DETERGENTS		
	INVERTED CONE	MICEL
PHOSPHATIDYLCHOLINE SPHINGOMYELIN		
	CYLINDRICAL	BILAYER
PHOSPHATIDYLETHANOL -AMINE MONO GALACTOSYL DIGLYCERIDE CHOLESTEROL		
	CONE	HEXAGONAL PHASE

saturated chains.

In addition to the influence of the acyl chains described above, the phospholipid headgroup, and phospholipid headgroup interactions, would also have a marked effect on the molecular area occupied by a particular lipid. For instance, it has been suggested that the bulkier choline headgroup of PC prevents close packing of this lipid in comparison to lipids containing the smaller ethanolamine group (Phillips and Chapman, 1968), providing a rationale for the lower T_c observed for PC containing membranes in comparison to PE. Similarly, since the area occupied by a lipid headgroup would be affected by electrostatic repulsion, one would expect that the presence of negatively charged lipids in membranes would prevent close packing of the lipids, again providing an explanation for the higher T_c observed for these lipids in comparison to neutral lipids. The Ca^{2+} induced bilayer to H_{11} phase transition in PE/acidic phospholipid mixtures can also be explained on the basis of molecular shape and the presence of a charged lipid component. For example, formation of a cation-PS complex would be expected to decrease the ionic repulsion between headgroups thereby reducing the effective area occupied by the serine headgroup (for discussion see chapter 2). This latter point is further emphasized by data which demonstrated a pH induced bilayer (at pH of 7) to H_{11} phase (at pH of 4) transition in pure PS model systems (Hope and Cullis, 1980; the pK of the PS carboxyl group is approximately 4.0).

The shape concept has proven to be of general utility in predicting the properties of lipids under a variety of situation. Taking a building block approach one might expect that appropriate mixtures of "cone" and "inverted cone" shaped lipids would result in the formation of a bilayer structure provided ideal mixing occurs. This was shown to be the case for mixtures of PE with a variety of detergents ("inverted cone" shaped lipids), providing the rather novel concept that detergents can stabilize the bilayer organization of membranes (Madden and Cullis, 1982). In line with this reasoning, it was suggested that lipids with differing "shapes" may be required for optimal packing and sealing around irregularly shaped membrane proteins. Data from model lipid systems containing glycophorin support this notion (Van der Steen *et al.*, 1982). These proposals have been discussed in greater detail elsewhere

(Cullis *et al.*, 1983; de Kruijff *et al.*, 1984).

1.8 Permeability Properties of Lipid Membranes

As the previous discussions have indicated, there has been a great deal of effort spent on defining the roles of lipids in regulating membrane "fluidity" and the structural preferences of membranes. Ironically, the role of lipids in regulating the permeability properties of membranes is perhaps the least understood role, despite innumerable investigations that have spanned the greater part of three decades. This is due in part to the presence of a great diversity of membrane proteins that are capable of providing selective ion channels or actively generating ion gradients, the roles of which have superseded the passive (or perhaps active) role of lipids in mediating permeability functions. In addition, studies on the permeability properties of lipids have been hampered by the lack of an adequate model membrane system which is free of impurities (*ie.* solvents and/or detergents) and amenable to experimentation. Since this topic is germane to the studies presented in Chapters 3, 4 and 5, a brief summary of the permeability properties of model membrane systems will be provided with an emphasis on passive ion permeability and the role of ion gradients in generating membrane potentials. Due to the quantity of literature available it will be impossible to provide a complete review. This discussion will be limited to formulating general concepts defining the permeability properties of lipids. In addition, it is worthwhile to note that lipids play a role in regulating membrane permeability through specific and non-specific effects on membrane proteins (van Hoogevest *et al.*, 1984a; van Hoogevest *et al.*, 1984b). These effects will also not be considered here.

1.7.1 Passive permeability

The permeability properties of membranes are dramatically illustrated by the properties of MLVs, in spite of the difficulty in interpreting results from this system (see Section 1.4). MLVs respond to osmotic gradients by shrinking and swelling, behaving as ideal osmometers provided that the lipids are in a liquid-crystalline state. As a result, the permeability of these

membrane systems to water can be evaluated by measuring the shrinking and swelling rates. Such studies indicate that the permeability of water through membranes increases in association with increases in acyl chain "fluidity". Increases in acyl chain unsaturation results in an increase in water permeation while introduction of cholesterol reduces membrane permeability above the T_c and increases the rate below the T_c (Blok, 1977). Interestingly, at the point in the transition from the gel to liquid-crystalline phase where the two phases coexist one observes a peak in the rate of water permeation. This has been associated with packing defects in the membrane at the interface of the two phases. These effects of lipid composition on water permeability establish general principles. The diffusion properties of non-electrolytes such as glucose, glycerol, and erythritol, show similar characteristics to those exhibited by water. These molecules permeate more rapidly through bilayers composed of lipids that contain short or unsaturated acyl chains (Demel *et al.*, 1972; Papahadjopoulos, 1973).

The permeability of lipid membranes to a particular molecule can be defined by the permeability coefficient (P). This constant is given in units of velocity (cm/sec) and equates the flux (change in concentration with time divided by the membrane area per liter; moles/sec cm^2) to the difference in concentration (moles/ cm^3) of the molecule across the membrane. The P value for water is between 1 and 100×10^{-3} cm/sec, a value which represents a rapid equilibration of this molecule. In order to gain a greater appreciation of this parameter, it can be calculated that for a P value of 10^{-5} cm/sec, half of the entrapped material from a vesicle with a diameter of 100 nm will be released in less than 1 sec. In contrast to the rapid permeability of water through lipid membranes, the P value of ions (*e.g.* Na^+ , K^+ , Cl^- , (H^+/OH^-)) are generally in the range of 10^{-10} to 10^{-14} cm/sec irregardless of lipid composition. These P values correspond to a half-time for release of entrapped material from 100 nm vesicles of 6.4 hr to approximately 7.3 years. As one might expect the energy necessary to bring an ion across a hydrophobic (lipid) interface is substantial (40 kcal/mole; Parsegian, 1969), therefore this process represents a thermodynamically unfavorable event. Similar to the preceding examples, the permeability of a given ion appears to be related to the order or fluidity in the hydrocarbon chain, where a decrease in permeability is

observed in membrane systems containing cholesterol or long chain saturated fatty acids. In addition, ions show an increase in permeability under conditions where there is a mixture of gel and liquid-crystalline phases. The charge of a phospholipid headgroup can also strongly influence the permeability of a given ion. For instance, the presence of negatively charged lipids in a membrane will repel anions and attract cations to the lipid water interface, hence these systems are generally more permeable to cations. Under conditions where Cl^- is present on both sides of a membrane, unusually large P values (10^{-5}) are obtained for this anion. It has been suggested that this may be due to the formation of HCl and the subsequent rapid transport of this neutral molecule (Hauser *et al.*, 1973; Nicholls and Miller, 1974). This observation was consistent with data which demonstrated rapid transmembrane equilibration ($P=10^{-5}$ cm/sec) of H^+ ions in systems containing the Cl^- ion on both sides of the membrane.

1.7.2 Membrane potential

A transmembrane potential is produced when there is an ion concentration gradient across the membrane. For biological membranes these gradients occur ubiquitously across cytoplasmic membranes as well as subcellular organelles. It is becoming apparent that the membrane potential has an essential role in a variety of membrane mediated processes including amino acid and metabolite transport (Schuldiner and Kaback, 1975; Fujimura *et al.*, 1983), protein transport (Zwizinski *et al.*, 1983), protein insertion (Wickner, 1983), lipid flip-flop (McNamee and McConnell, 1973), and divalent cation transport (Saris and Akerman, 1980). Based on the far reaching implications of these processes in terms of understanding the function of membranes, it is surprising that only a few studies have examined the role of lipids in the development and maintenance of the membrane potential in vesicles. Further, the role of lipids in relation to these membrane potential dependent events has received no attention other than the rather preliminary studies presented in this thesis.

The potential generated across a membrane is the result of a number of variables, including the equilibrium distribution of ions present and the surface charge (important in defining the surface potential; for review see Ohki, 1981). In a situation where an ion gradient is present, a potential difference across the membrane will be established as the ions diffuse down their concentration gradient. The resulting diffusion potential can be calculated employing a derivation of the Nernst equation (Goldman-Hodgkin-Katz equation) that describes the relation between the electrical potential ($\Delta\psi$) and the concentrations (activities) and permeabilities of the ions present:

$$\Delta\psi = - \frac{RT}{zF} \ln \frac{P_{Na} [Na^+]'' + P_K [K^+]'' + P_{Cl} [Cl^-]' + \dots}{P_{Na} [Na^+]' + P_K [K^+]' + P_{Cl} [Cl^-]'' + \dots}$$

In descriptive terms this equation indicates that the orientation and magnitude of the diffusion potential is dependent on the mobilities (permeability coefficients, P) of the cations and anions present. In addition, the sign of the potential on the side of the membrane where the mobile species is concentrated will be the opposite sign of this species. It also indicates that the magnitude of the potential will be greater when there are large differences in cation and anion mobility.

As indicated in the previous section, most ions are relatively impermeable therefore it is sometimes necessary to increase the rate at which an ion permeates the membrane (increase the P value) in order to generate a membrane potential. This can be accomplished by the use of ionophores, a group of lipid soluble macromolecules that selectively enhance the permeability of certain ions (for reviews see Pressman and de Guzman, 1975; Ovshinnikov and Ivanov, 1977; Reed, 1979). The K^+ ionophore valinomycin is an example of a mobile carrier which acts by forming a very permeant lipid soluble complex when coupled with the ion species concerned. Other ionophores, e.g. gramicidin, create channels through the membrane allowing certain ions to permeate. It should be stressed at this point that the latter group of ionophores are relatively insensitive to the lipid environment, while the mobile ionophores are sensitive to the lipid composition and function only in membranes where the lipids are in liquid-crystalline state. Using valinomycin as an example, addition of this ionophore to vesicles

with a Na^+/K^+ ion gradient (KCl inside and NaCl outside) establishes a K^+ ion gradient (provided the P value of the Cl^- and Na^+ ions can be neglected). The more rapid movement of K^+ ions will eventually be restrained by electrostatic forces, and the resulting charge separation will result in a negative (interior) membrane potential. Additional details concerning the generation of the membrane potential and methods for evaluating the potential are discussed in Chapters 3 and 4. It must be emphasized again that these studies represent some of the first well characterized investigations of membrane potential in model LUV systems.

1.9 Summary

The preceding review has clearly shown that there is currently an excellent understanding of the chemical and physical properties of lipids (at least the major classes of eukaryotic lipids) and how at a molecular level these lipids may modulate the structure and function of membranes. The fundamental problem of lipid diversity has been reduced to the question of defining lipid functions. This thesis attempts to elucidate a few of the functional roles of lipids in model membrane systems. Specifically, in Chapter 2 the role of cholesterol in modulating the polymorphic phase behaviour of mixed lipid systems composed of naturally occurring or synthetic PEs and either PC or PS is investigated. The influence of cholesterol on the Ca^{2+} induced bilayer to H_{11} phase transition in PS containing systems is also examined. In addition, a basis for examining the role of lipids in regulating ion permeability and membrane mediated transport function is established (Chapters 3 and 4). It is further demonstrated that the transport of biologically relevant molecules can proceed in membrane systems in the absence of a carrier protein (Chapters 4 and 5), thereby defining a new and potentially exciting membrane dependent function that could be regulated by the presence of specific lipid species.

LIPID POLYMORPHISM: INFLUENCE OF CHOLESTEROL AND DIVALENT CATIONS ON THE STRUCTURAL PREFERENCES OF MIXED LIPID MODEL SYSTEMS†

2.1 Introduction

The functional roles of cholesterol in biological membranes are not well understood. As emphasized in the preceding chapter (see section 1.5.2), it is generally assumed that cholesterol plays a role in modulating the "fluidity" of the lipid environment, thereby affecting membrane function. However, as described in detail in section 1.3, there is little convincing evidence to support the proposal that fluidity plays an important role in membrane function *in vivo*. In this context, it is appropriate to examine the influence of cholesterol on physical properties of membrane phospholipids other than fluidity. In previous work (Cullis *et al.*, 1978; Cullis and de Kruijff, 1979), it was shown that cholesterol exerts a rather remarkable effect in unsaturated PC (phosphatidylcholine) - PE (phosphatidylethanolamine) systems, serving to destabilize bilayer structure and induce formation of the hexagonal (H_{11}) phase. In dioleoyl (18:1c/18:1c) PE - dioleoyl PC systems, for example, cholesterol induces apparently complete H_{11} phase structuring at equimolar proportions with respect to phospholipid (Cullis, 1978). This result was surprising in view of the ability of cholesterol to "condense" PC monolayers and reduce membrane permeability (Demel and de Kruijff, 1976) and thus in some sense stabilize bilayer structure for PC systems.

On the basis of the above, it may also be considered that cholesterol may facilitate H_{11} phase formation. In regard to this, it has been shown that the Ca^{2+} concentration needed to induce bilayer to H_{11} transitions in multilamellar (soya) PE-PS systems and to induce fusion in sonicated unilamellar vesicles are rather high (2 mM) in reference to biological systems, particularly in the cytoplasm, where the free Ca^{2+} concentrations are less than 100

† This chapter has been based on the references Bally *et al.*, (1983) and Tilcock *et al.*, (1982).

μ M. In this chapter the ability of cholesterol to act as an adjunct to the Ca^{2+} effect is examined. Further, the ability of Mg^{2+} to facilitate this process is examined. Mg^{2+} does not induce bilayer to H_{11} transitions in PE-PS systems but does induce aggregation, a step which is vital to obtaining the close apposition between bilayers apparently required before H_{11} phase formation can proceed (Cullis *et al.*, 1980). In addition, this chapter also examines in greater detail the influence of cholesterol on the preferences of DOPC-DOPE systems with the specific question of whether there is any phase segregation of either phospholipid species in systems exhibiting both bilayer and H_{11} phase structures, or whether the lipids exhibit ideal mixing behaviour.

It is demonstrated that cholesterol can induce H_{11} phase structure in previous bilayer PE-PS systems and that, in combination, the presence of (2 mM) Mg^{2+} and equimolar cholesterol can reduce the Ca^{2+} concentrations required to induce such transitions by more than an order of magnitude. It is also demonstrated that in mixed liquid-crystalline DOPC-DOPE-cholesterol systems exhibiting both bilayer and H_{11} phase characteristics, the lipids appear to be equally distributed in both phases.

2.2 Materials and Methods

2.2.1 Preparation of soyabean lipids

Soyabean PC was purified from crude (20%, w/w) soya PC purchased from Sigma (St. Louis, MO) utilizing two chromatographic procedures in series. A partially purified PC preparation was produced by chromatography on aluminium oxide (Al_2O_3 ; E. Merck, Darmstadt, Germany; for reference see Sheltawy and Dawson (1969)). Crude soya PC (75 gm) in chloroform was loaded onto a 150 X 5 cm column of Al_2O_3 (previously washed with a 1:1 (v/v) mixture of chloroform/methanol, and subsequently packed in chloroform) and eluted with a 1:20 (v/v) chloroform/methanol mixture at a flow rate of 6 ml/min. As the PC began to elute from the column the mobile phase was exchanged for a 1:1 (v/v) mixture of chloroform/methanol and the flow rate was increased to 20 ml/min. The partially purified PC

(yield of approximately 20 gm) was subsequently purified employing silica acid preparative liquid chromatography (PrepLC/System 500, Waters Associates; using PrepPak-500/silica) with chloroform/ methanol/water (60:30:4, v/v) as the mobile phase (for reference see Patel and Sparrow, 1978). The resulting lipid was shown to be greater than 99% pure as indicated by iodine vapour stained two-dimensional thin-layer chromatography (TLC; using pre-coated silica gel 60 TLC plates (0.25 mm thick; E. Merck, Darmstadt, Germany) run in the first direction in a base solvent system composed of chloroform/methanol/ammonia/water (90:54:5.7:5.4, v/v) and in the second direction with an acid solvent system composed of chloroform/methanol/glacial acetic acid/water (25:15:4:2, v/v) according to the method of Broekhuise (1969)).

Soya PE and soya PS were obtained from pure soya PC employing the headgroup exchange capacity of phospholipase D (Comfurius and Zwaal, 1977). Briefly, PC in ether (5 gm/ 100 ml) was incubated, with vigorous shaking at 40°C with 100 ml of a saturated solution of L-serine (46%, w/v, in 0.1 M acetate buffer (pH 5.6) containing 0.1 M CaCl₂) or a 15% ethanolamine solution (w/v, in the acetate/ CaCl₂ buffer after neutralization of the ethanolamine with concentrated HCl) in the presence of a crude phospholipase D preparation (see below). The progress of the reaction was followed on small TLC plates (2 X 7 cm plates cut from the large pre-coated plates used for two-dimensional TLC) which were run in the base solvent mixture and subsequently sprayed with a phosphorus staining reagent (a mixture of 2 vol water, 1 vol molybdenum trioxide reagent (40.1 gm MoO₃ in 1 L of concentrated H₂SO₄), and 1 vol molybdate reagent (1.78 gm Na molybdate in 500 ml water)), which stains phosphorus containing compounds blue upon heating, followed by charring (appearance of black spots) of the lipids and organic compounds due to the presence of H₂SO₄. Generally, after 30 min the reaction was stopped by cooling the reaction mixture, followed by low speed centrifugation (500g) for 10 min to facilitate separation of the aqueous and ether phases. The ether phase was collected, then dried using rotary evaporation. The resulting lipid, a crude mixture of unreacted PC, PS or PE, and PA, was washed to remove aqueous contaminants by suspending the lipid in 25 ml of chloroform/methanol (2:1) followed

by addition of 6 ml of water to generate a two phase system. Subsequently the organic phase was isolated and dried down. The reaction generally resulted in a 25–50% conversion for PS and a 50–75% conversion for PE.

The PS was purified using conventional low pressure column chromatography using carboxymethylcellulose as a stationary phase (Comifurius and Zwaal, 1977). Briefly, 2–4 gm of crude PS in chloroform was loaded onto a 5 X 72 cm CM-52 carboxymethylcellulose (Whatman, England; material was pre-washed in methanol) column packed in chloroform. The lipid was eluted using a continuous (0 to 50%) chloroform–methanol gradient. PS containing fractions (which eluted at approximately 25% methanol) were identified on TLC plates (run in acid solvent) using a ninhydrin spray reagent (0.2%, w/v, ninhydrin in water saturated butanol), which reacts with free amino groups forming purple–mauve spots on the plate after heating, followed by the phosphorus spray reagent described previously. The chromatographically pure PS fractions were pooled, dried, and subsequently the lipid was converted to the sodium salt as described by Hope and Cullis (1980). This procedure involved dissolving the dry lipid in a Bligh and Dyer monophasic (chloroform/methanol/water in the ratio 1:2.1:1, v/v) where the aqueous component contained 0.4 M HCl and subsequently titrating the mixture to pH = 8.0 with a Bligh and Dyer monophasic where the aqueous phase contained 0.5 M NaCl and 0.5 M NaOH. This was followed by addition of 0.4 vol of both water and chloroform to create a two-phase system. The organic phase containing the sodium salt of PS was dried and stored in chloroform under nitrogen at -20°C .

The crude soya PE was purified employing silica acid preparative liquid chromatography using a mobile phase composed of chloroform/methanol/water/25% ammonium hydroxide in a ratio of 60:30:1:1 (v/v). The pure PE fractions were identified on TLC plates using a similar procedure described for PS. Pure soya PE was stored in chloroform under nitrogen at -20°C . Both lipids were shown to be greater than 99% pure as indicated by iodine vapour stained two-dimensional TLC chromatography.

The phospholipase D used for the transphosphatidylation reactions was partially purified from the inner leaves of savoy cabbage employing the procedure of Kates and Sastry (1969). Briefly, 4–6 kg of the inner yellowish–green leaves of savoy cabbages were homogenized in 3 L of ice–cold water. The resulting homogenate was filtered through cheesecloth and centrifuged at 2,000g for 30 min to remove bulk fiber. The supernatant was adjusted to pH 5.5 with 4*N* HCl and fractions were heated rapidly (within 2 min) to 55°C in a boiling water bath to precipitate contaminating proteins. The fractions were immediately cooled to 0°C, and subsequently centrifuged at 13,000g for 30 min. The supernatant was collected and the remaining proteins, including phospholipase D, were then precipitated by addition of ice cold acetone (1 vol supernatant: 2 vol acetone) with continuous stirring for 15 min. The precipitate settled out of solution within 2 hr at 4°C and was isolated by centrifugation (1000g for 10 min) after the bulk of the unprecipitated material was removed by aspiration. The precipitate was lyophilized to remove residual acetone and stored at –70°C until used. For the conversion reactions, 200–500 mg of the preparation was suspended in 20 ml of 0.2 *M* sodium acetate buffer pH 5.6 containing 40 mM calcium chloride. The suspension was mixed at 0°C for 30 min and, subsequently centrifuged at 17,000g for 10 min to remove insoluble material. The resulting supernatant was utilized for the base–exchange reactions described above.

2.2.2 Synthesis of dioleoyl phospholipids

Dioleoylphosphatidylcholine was synthesized by the procedure of Warner and Benson (1977), which involved reacylating glyceryl phosphorylcholine (GPC), derived from egg PC, with the specified fatty acid imidazole. Egg PC was prepared from hen egg yolks by preparative liquid chromatography (as described for soya PC) of a chloroform/methanol (1:1, v/v) extract of acetone precipitated lipids (30 egg yolks were mixed with 1.2 L of acetone and the resulting precipitate was isolated by filtration, washed 5 additional times with 1 L acetone and subsequently extracted 3X with 500 ml of the chloroform/methanol mixture). GPC was derived from the pure egg PC by the procedure of Brockerhoff and Yarkowski (1965), which

involved the slow addition of 10 ml tetrabutylammonium hydroxide (25% in methanol, Eastman-Kodak, Rochester, NY) to 10 gm of egg PC dissolved in diethyl ether. After a 1 hr incubation at 20°C the precipitated GPC was isolated by centrifugation at 500g for 10 min. The GPC was dissolved in methanol and reprecipitated with ether to remove any contaminating acyl chains or PC. This procedure was repeated 3X and resulted in chromatographically pure GPC which was dissolved in methanol and stored at -20°C until used.

GPC (5 mmoles), dried and left under high vacuum overnight, was dissolved (aided by sonication in a bath sonicator) in 120 ml of dimethyl sulfoxide (DMSO). Subsequently, this was added to a 20 ml solution of DMSO containing 20 mmoles of oleic acid imidazole, which was prepared by adding 22 mmoles 1,1'-carbonyldiimidazole (Sigma, St. Louis, MO) to 20 ml of tetrahydrofuran (Aldrich Chemical Co., Milwaukee, WI) containing chromatographically pure oleic acid (Sigma) followed by evaporation of the tetrahydrofuran after the reaction was completed (as the reaction occurs CO₂ gas is released as the fatty acid imidazole is produced, indicating the progress of the reaction which was normally complete at 45 min). The acylation reaction was initiated by addition of 72 ml sodium DMSO (prepared by slowly adding 1 gm of sodium metal to 75 ml of DMSO followed by stirring overnight in a flask equipped with a drying tube) and was allowed to proceed with vigorous stirring. The reaction progress was followed using small TLC plates run in the base solvent system and was usually complete within 10 to 15 min. The reaction was stopped by cooling the reaction mixture and adjusting the pH to less than 2 with 4N HCl. Immediately following this, 200 ml of water was added and the mixture was extracted 3X with a half vol of chloroform/methanol (2:1, v/v). The combined chloroform extracts were washed 5X with a half vol of methanol/water (1:1, v/v) in order to remove the bulk of the DMSO. The washed extract was dried (forming a brownish oil) and the excess DMSO and unreactive fatty acyl imidazole were removed by preparative liquid chromatography on silica using chloroform/methanol/water (60:30:3, v/v) as the mobile phase. In general this was followed by additional purification on carboxymethylcellulose using a step gradient of 1% methanol in chloroform followed by 10%

methanol to elute the DOPC. The resulting lipid was greater than 99% pure as determined by two-dimensional TLC.

DOPE was prepared from DOPC utilizing the headgroup exchange capacity of phospholipase D as described previously. Deuterated DOPC and DOPE were synthesized as described above using 11,11-dideuteriooleic acid which was synthesized by a modification of the procedure of Tucker *et al.* (1971), based on a Wittig condensation of nonanol-2-d₂ with methyl 9-iodononanoate (Farren *et al.*, 1984) and was kindly provided by Dr. S.B. Farren.

2.2.3 Sample preparation

Samples for NMR studies were prepared from an appropriate mixture of the lipids (purified as described above, with cholesterol purchased from Sigma) in chloroform in a 10-mm NMR tube. Chloroform was evaporated under nitrogen and the sample was then kept under high vacuum for approximately 2 hr. The dry lipid mixtures were hydrated with 0.7 ml of buffer (100 mM NaCl, 10% (v/v) deuterated water, and 10 mM HEPES (pH 7.4)) by vortex mixing in the presence of a glass agitator to facilitate lipid dispersal (for PE-PS-cholesterol mixtures the samples were hydrated at 4°C). In the case of the ³H-labeled lipids the samples were prepared in deuterium-depleted water (obviously no deuterated water was used in the buffer).

Soya PE and PS samples were titrated with calcium by adding aliquots of 100 mM stock solution of the chloride salt. To ensure equilibration of the divalent cation with the lipid, the samples were subjected to three freeze-thaw cycles employing liquid nitrogen. Samples requiring dialysis were sealed in 0.6 cm diameter dialysis tubing (Spectrapor membrane tubing, 12,000–14,000 MW cutoff; Spectrum Medical Ind., Los Angeles, CA) following hydration and equilibrated against the required Ca²⁺ and/or Mg²⁺ concentration at 4°C for 6 hr. Control experiments employing ⁴⁵Ca revealed maximal binding of Ca²⁺ to soya PS occurred within 4 hr. A 10-fold molar excess of the divalent cation in the dialysate over PS was utilized in all dialysis experiments. Lipid degradation following the 6 hr of dialysis was found to be less than 1%, as determined by TLC.

2.2.4 Nuclear magnetic resonance

^2H NMR and ^{31}P NMR spectra were obtained by using a Bruker WP200 spectrometer. For ^{31}P NMR, free induction decays were accumulated from up to 1000 transients by employing a 15- μs 90° radio-frequency pulse, 20-kHz sweep width, and 0.8-s interpulse delay, in the presence of broad-band proton decoupling. An exponential multiplication corresponding to 50-Hz line broadening was applied to the free induction decay prior to Fourier transformation. For ^2H NMR, free induction decays were accumulated for up to 20,000 transients by employing a 15- μs 90° radio-frequency pulse, 30-kHz sweep width, and 0.04-s interpulse delay. An exponential multiplication corresponding to a 100-Hz line broadening was applied prior to Fourier transformation. Unless specified, all spectra were recorded at a temperature of 30°C .

2.2.5 Freeze fracture

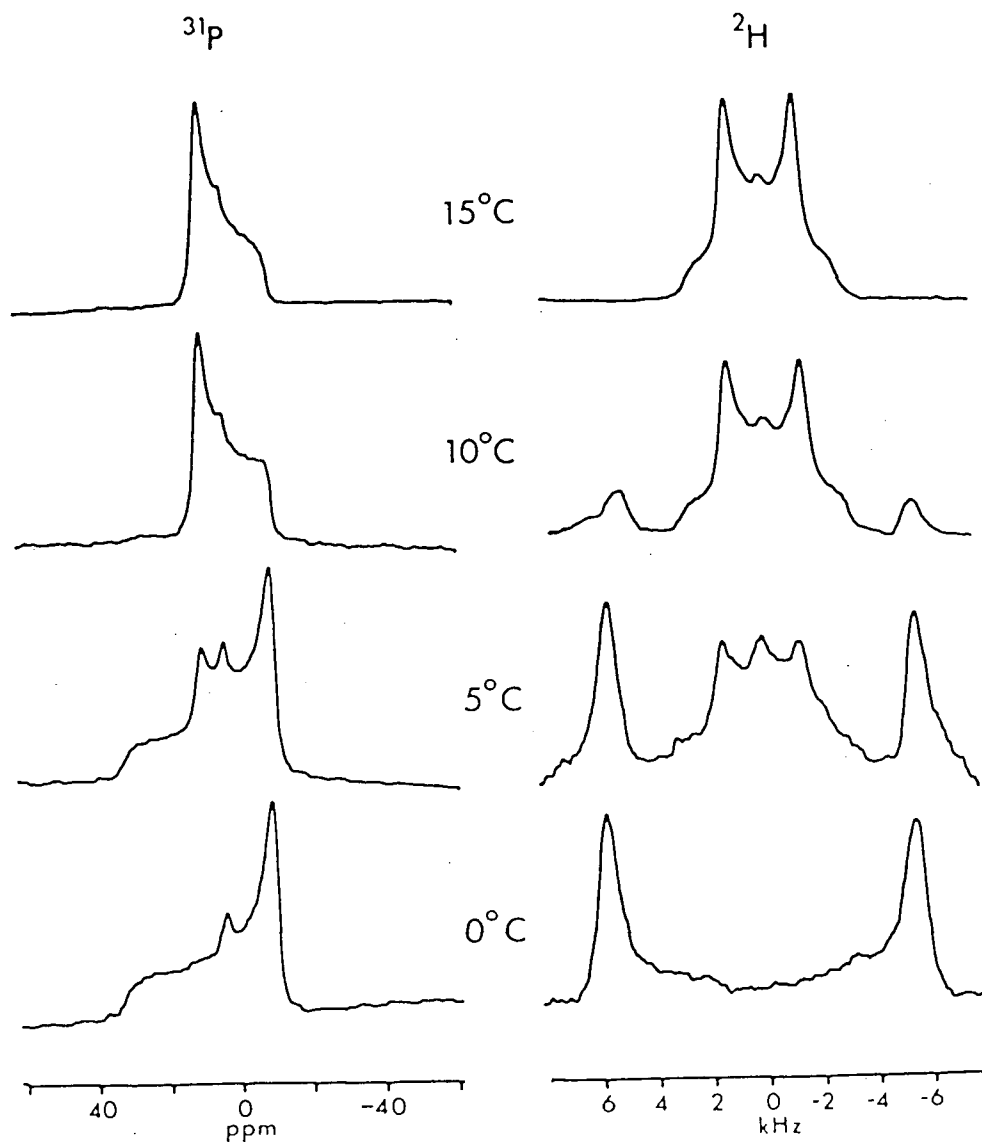
Freeze-fracture was performed on appropriate samples (described in section 2.2.3) containing 25% (v/v) glycerol as a cryoprotectant. The samples were frozen in a liquid freon slush. Freeze-fracture studies were performed on a Balzers BAF 301 apparatus, and replicas were viewed employing a Phillips 400 electron microscope. All freeze-fracture studies were kindly provided by Dr. M.J. Hope.

2.3 Results

2.3.1 Influence of cholesterol on soya PE/PS lipid mixtures

The use of NMR techniques to assign phase structures of lipid mixtures is described in section 1.6.1 and is illustrated by the data in Fig. 6 which shows ^{31}P and ^2H NMR spectra of DOPE as a function of temperature. The ^{31}P NMR spectra illustrate a bilayer to hexagonal (H_{11}) transition occurring as the temperature is raised through 10°C as indicated by the change in line shape from one with a low-field shoulder and high-field peak separated

Fig. 6. ^{31}P and ^2H NMR spectra as a function of temperature of fully hydrated dioleoylphosphatidylethanolamine (DOPE) which is ^2H labeled at the C_{11} position of the acyl chains ($[\text{C}_{11}-^2\text{H}_2]\text{DOPE}$). The ^{31}P NMR spectra were obtained at 81.0 MHz in the presence of proton decoupling, whereas the ^2H NMR spectra were obtained at 30.7 MHz. For details see section 2.2.



by approximately 50 ppm (a bilayer spectrum) to a spectrum with reversed asymmetry which is a factor of 2 narrower (H_{11} spectrum). This transition is reflected in the corresponding 1H NMR spectra by the appearance of a narrower spectrum arising from H_{11} phase [C_{11} - 1H_2] DOPE as the temperature is raised, compared to the bilayer spectrum observed at temperatures below 5°C.

The influence of cholesterol on the polymorphic phase preferences of various soya PE-soya PS mixtures is illustrated in Fig. 7. The results presented there clearly illustrate an ability of cholesterol to destabilize a bilayer organization of such systems, particularly at PS contents below 50 mol%. Thus for the 30 mol% PS - 70 mol% PE sample a bilayer line shape is obtained in the absence of cholesterol. Increasing cholesterol contents lead first to a structure allowing isotropic motional averaging and subsequently to the ^{31}P -NMR line shape characteristic of the H_{11} -phase. This ability of cholesterol to engender H_{11} -phase formation in PE-PS systems is also illustrated by the freeze-fracture micrographs of Fig. 8. Large fracture planes characteristic of bilayer structures are observed for the 30 mol% PS- 70 mol% PE system in the absence of cholesterol (Fig. 8A), whereas the striated pattern characteristic of H_{11} -phase structures is observed in the presence of equimolar cholesterol (Fig. 8B). As indicated earlier (see section 1.6), the narrow ^{31}P -NMR resonance may arise from small lamellar structures or nonlamellar structures such as inverted micelles (de Kruijff *et al.*, 1979) which can play intermediary roles in bilayer- H_{11} transitions (Verkleij *et al.*, 1980). Freeze-fracture studies revealed the presence of small (diameter less than 100 nm) vesicles in these systems which appear to form spontaneously on hydration. This would be consistent with the behaviour of the systems containing 50 mol% PS, where intermediate (cholesterol/phospholipid ratio between 0.1 and 0.5) cholesterol contents appear to generate formation of somewhat smaller lamellar structures, but do not induce H_{11} -phase organization even for cholesterol to phospholipid ratios of 1.0.

Fig. 7. ^{31}P -NMR spectra (81.0 MHz) obtained at 30°C from aqueous dispersions of soya PE in the presence of varying amounts of soya PS and cholesterol. C/PL refers to the molar ratio of cholesterol to phospholipid. The 0-ppm position corresponds to the chemical shift of sonicated PC vesicles. For other details see section 2.2.

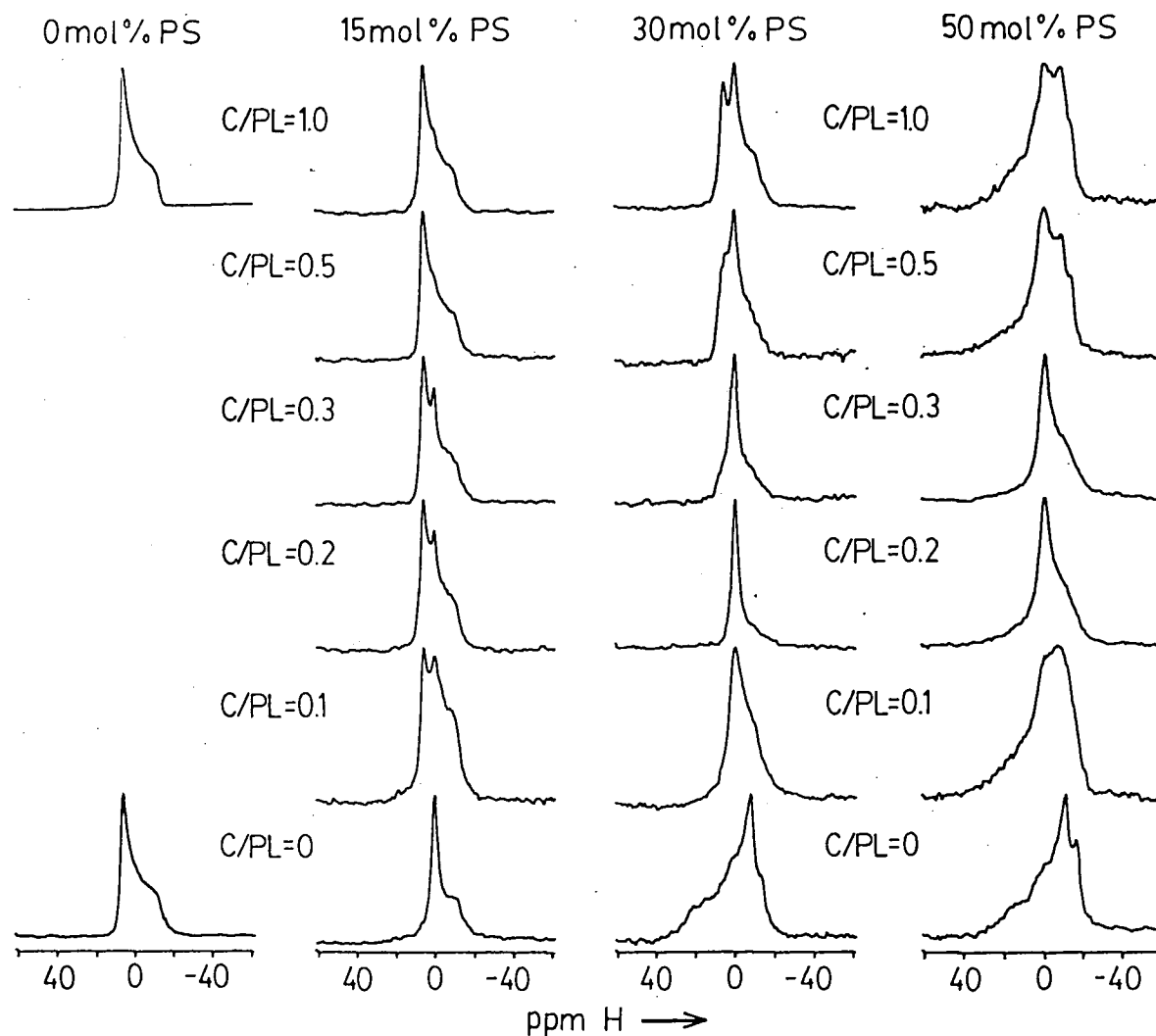
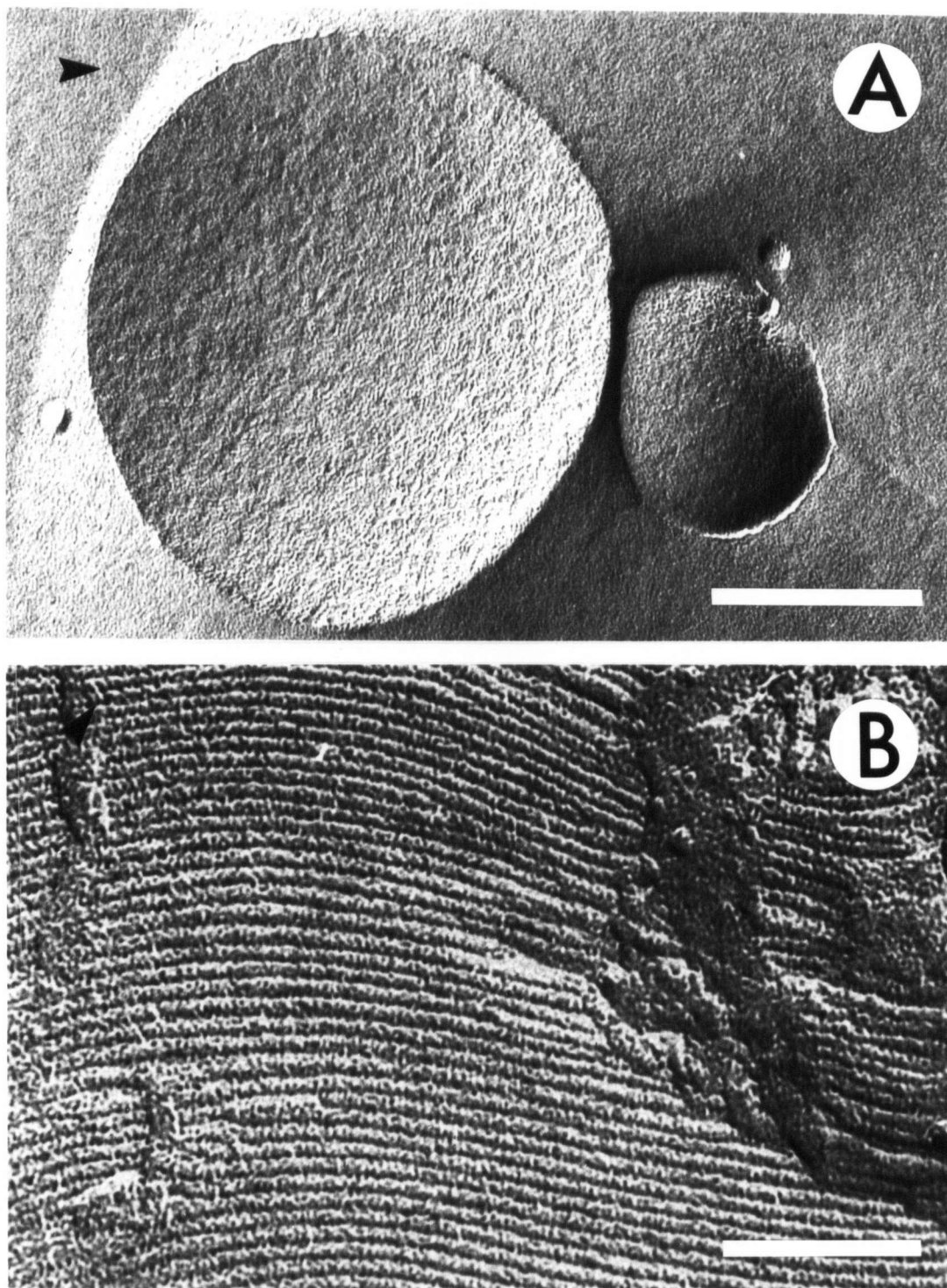


Fig. 8. Freeze-fracture micrographs of soya PE - soya PS mixtures (30 mol% PS) in the presence (B) and absence (A) of equimolar cholesterol. The white bars represent 200 (A) and 100 nm (B). The direction of shadowing is indicated by the arrowhead in each micrograph. Data was collected and reproduced with permission from M. J. Hope.



2.3.2 Influence of cholesterol and Mg^{2+} on the Ca^{2+} induced bilayer to H_{11} transition in PE-PS systems.

As indicated in sections 1.6 and 2.1, bilayer to H_{11} transitions can be triggered in PE-PS systems by the addition of Ca^{2+} (for a reference see Tilcock and Cullis, 1981). Given the ability of cholesterol to encourage H_{11} -phase formation, it may be expected that lower Ca^{2+} levels are required to trigger such transitions if cholesterol is present. Results showing this to be the case are illustrated in Fig. 9 for equimolar mixtures of soya PS-soya PE in the presence of varying amounts of cholesterol. Whereas Ca^{2+} /PS ratios R of 0.5 and higher are required to induce appreciable H_{11} -phase formation in the absence of cholesterol, similar effects are observable in samples containing 25 and 50 mol% cholesterol at Ca^{2+} levels as low as $R = 0.125$.

It has been shown previously (Tilcock and Cullis, 1981) that in contrast to Ca^{2+} , Mg^{2+} is unable to trigger bilayer- H_{11} transitions in equimolar soya PS-soya PE dispersions even at Mg^{2+} /PS ratios as high as 10.0. However, the presence of equimolar cholesterol enables Mg^{2+} -induced bilayer- H_{11} transitions to occur as illustrated in Fig. 10 for 8 mM Mg^{2+} concentrations. This leads to the possibility that lower levels of Mg^{2+} can act synergistically with Ca^{2+} to produce Ca^{2+} -induced phase transitions at lower net Ca^{2+} concentrations. Results supporting this possibility are illustrated in Fig. 11 for equimolar soya PS-soya PE systems, which were dispersed in the presence of 2 mM Mg^{2+} and subsequently dialyzed against a buffer containing 2 mM Mg^{2+} and various concentrations of Ca^{2+} (see section 2.2 for details). The addition of Ca^{2+} had little effect on the structural preference of systems containing no cholesterol. Even at 8 mM Ca^{2+} levels such systems evidenced largely lamellar ^{31}P -NMR lineshapes with a small (10%) H_{11} -phase component superimposed (see Fig. 11). However, some H_{11} -phase formation is visible for Ca^{2+} concentrations as low as 0.25 mM when equimolar (with respect to phospholipid) cholesterol is present. Thus Mg^{2+} and cholesterol in combination can act as important adjuncts for Ca^{2+} -induced phase changes in PS-PE systems.

Fig. 9. ^{31}P -NMR spectra (81.0 MHz) obtained at 30°C from aqueous dispersions of equimolar mixtures of soya PS and soya PE in the presence of varying amounts of cholesterol and Ca^{2+} . The ratio C/PL refers to the molar ratios of cholesterol to phospholipid, whereas the R refers to the molar ratio of Ca^{2+} to PS. For details of sample preparation see section 2.2. The Ca^{2+} was added to the (0.7 ml) aqueous lipid dispersions as aliquots from a 100 mM stock solution of CaCl_2 .

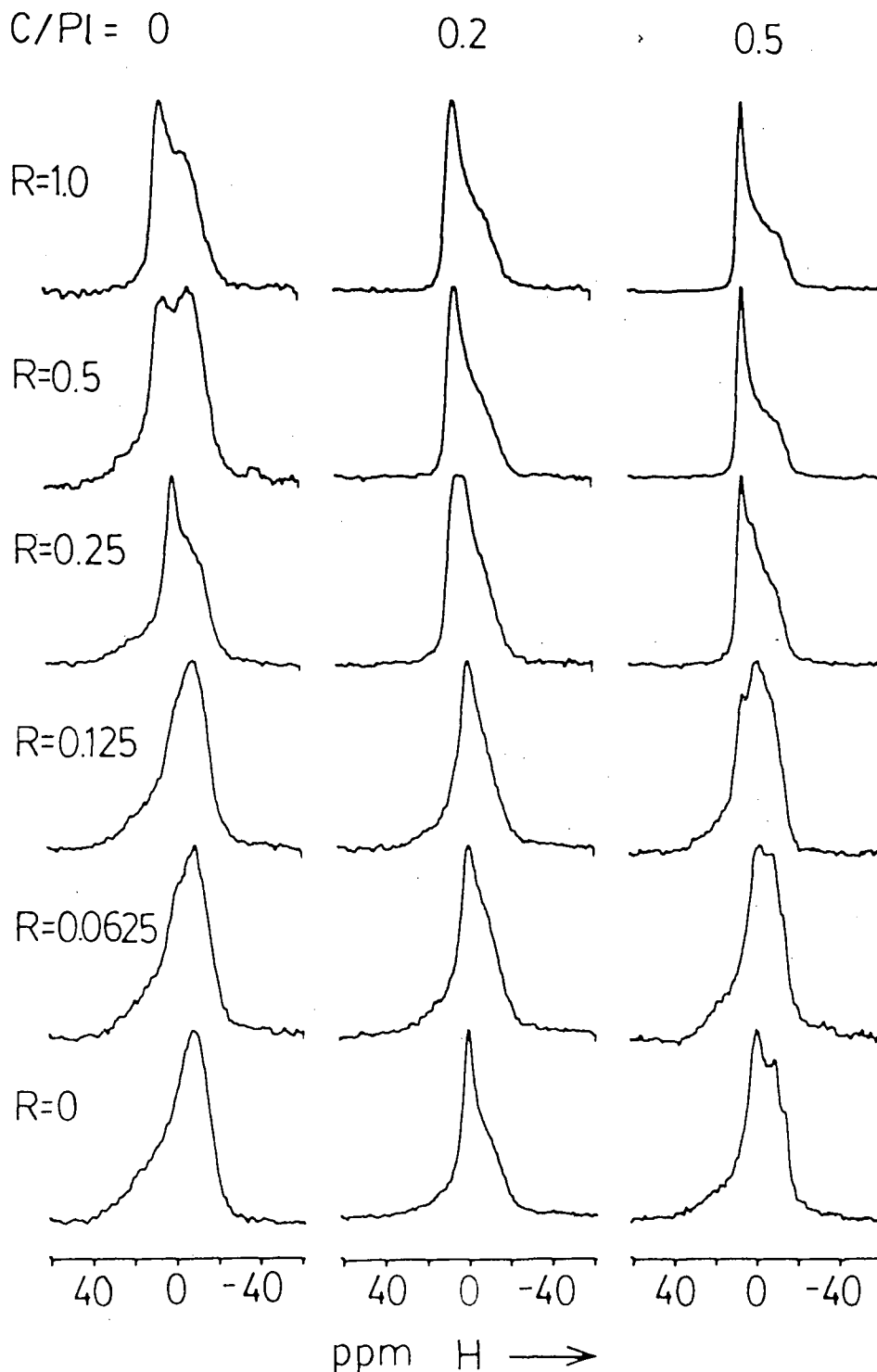


Fig. 10. ^{31}P -NMR spectra (81.0 MHz) obtained at 30°C from aqueous dispersions of equimolar mixtures of soya PS and soya PE after dialysis against the indicated concentrations of Mg^{2+} . The ratio C/PL refers to the molar ratio of cholesterol to phospholipid. For details of sample preparation see section 2.2.

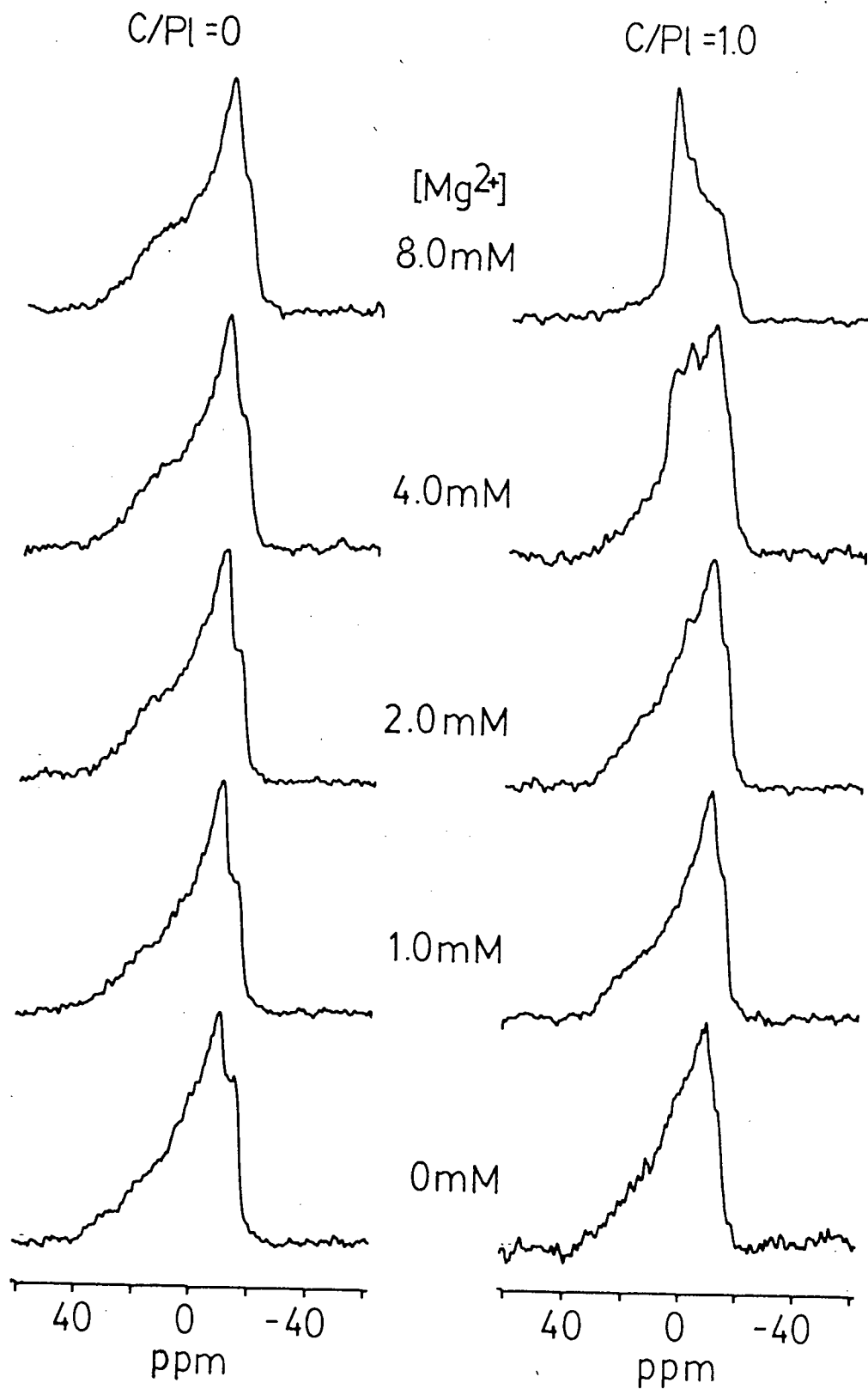
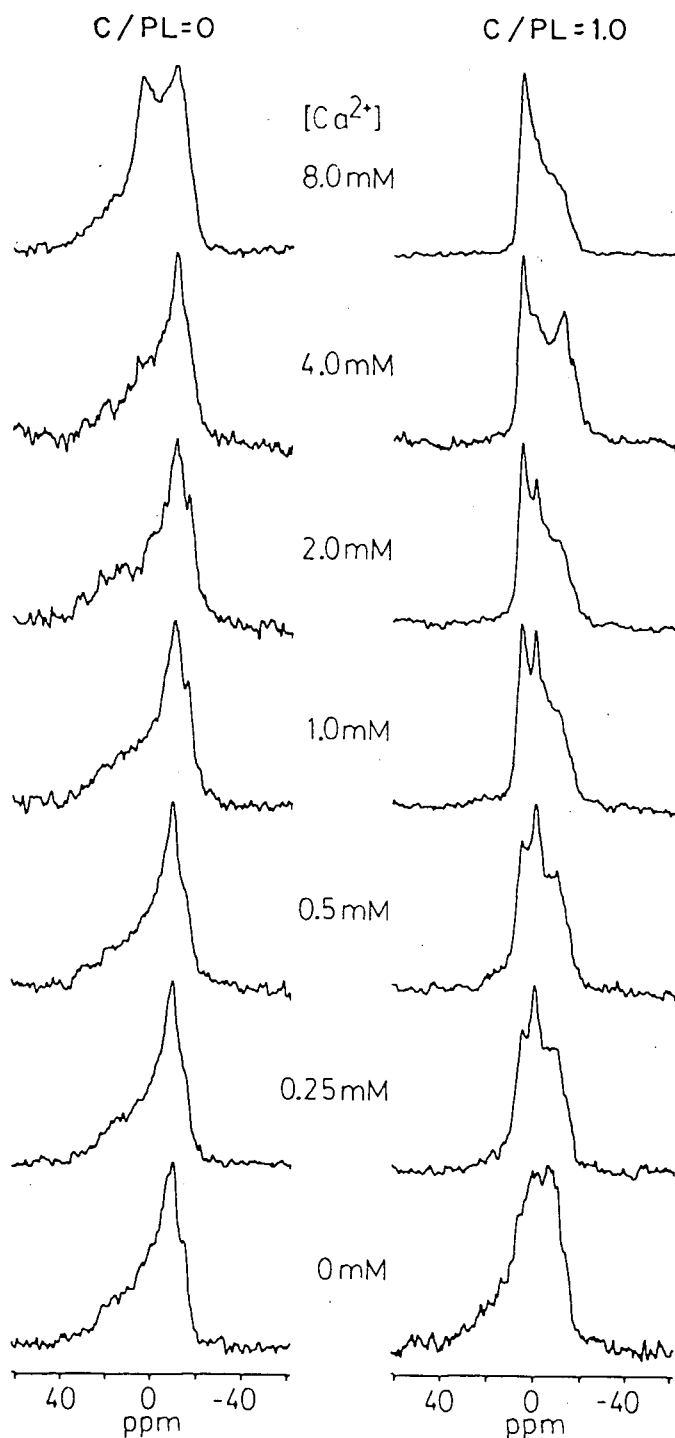


Fig. 11. ^{31}P -NMR spectra (81.0 MHz) obtained at 30°C from aqueous dispersions of equimolar mixtures of soya PS and soya PE after dispersion in the presence of 2 mM Mg^{2+} and subsequent dialysis against a buffer containing 2 mM Mg^{2+} and the indicated concentration of Ca^{2+} . The ratio C/PL refers to the molar ratio of cholesterol to phospholipid. For other details see section 2.2.



The ability of Mg^{2+} to induce polymorphic bilayer- H_{11} transitions when cholesterol is present and its inability to segregate PS in PE-PS systems in the absence of cholesterol suggests either of two possibilities. First, it may be that cholesterol facilitates PS segregation. Alternatively Mg^{2+} may act to decrease the local charge density at the membrane surface, thereby facilitating H_{11} phase formation (see section 2.4). If the latter possibility is correct, high salt concentrations should also be able to exert similar effects. This is indeed the case as indicated in Fig. 12, where it is shown that 1 M NaCl concentrations cause a large proportion of the PE-PS-cholesterol (1:1:2) dispersions to adopt the H_{11} configuration, behaviour which does not occur for the systems not containing cholesterol.

2.3.3 Influence of cholesterol on the mixing properties of DOPC/DOPE systems

The mechanism whereby cholesterol promotes H_{11} phase formation in mixed PE-PC systems is not understood. One possibility would be that it associates preferentially with the bilayer-stabilizing PC species (van Dijk *et al.*, 1976) and that the resulting PC-cholesterol complex is more readily incorporated into the H_{11} phase matrix. Alternatively, it is conceivable that cholesterol induces a lateral segregation of PC, allowing the PE to adopt the H_{11} phase it prefers in isolation. In order to investigate these possibilities, the 3H -labeled (C_{11} - 3H_2)DOPE and (C_{11} - 3H_2)DOPC lipids were employed. The ^{31}P and 2H NMR results obtained from (C_{11} - 3H_2)DOPE-DOPC (4:1) and DOPE-(C_{11} - 3H_2)DOPC (4:1) (at 40°C) in the presence of varying amounts of cholesterol are shown in Fig. 13. There are several features of interest. First, the ^{31}P NMR spectra for mixtures containing 2H -labeled DOPC or DOPE are virtually identical, both with each other and with the corresponding mixtures containing unlabeled lipids. Second, the 2H NMR spectra arising from (C_{11} - 3H_2)DOPE or (C_{11} - 3H_2)DOPC in mixtures containing the same proportions of PE, PC, and cholesterol are also very nearly identical. Thus, DOPC and DOPE appear to partition with equal probability between the various phases (bilayer, H_{11} , or isotropic) present in the sample. This result demonstrating miscibility of (liquid-crystalline) DOPE and DOPC even when different phase structures are present is rather surprising as it may have been expected that DOPC would be present at higher levels

Fig. 12. ^{31}P -NMR spectra (81.0 MHz) obtained at 30°C from equimolar mixtures of soya PS and soya PE in the presence and absence of 1 *M* NaCl. The ratio C/PL refers to the molar ratio of cholesterol to phospholipid.

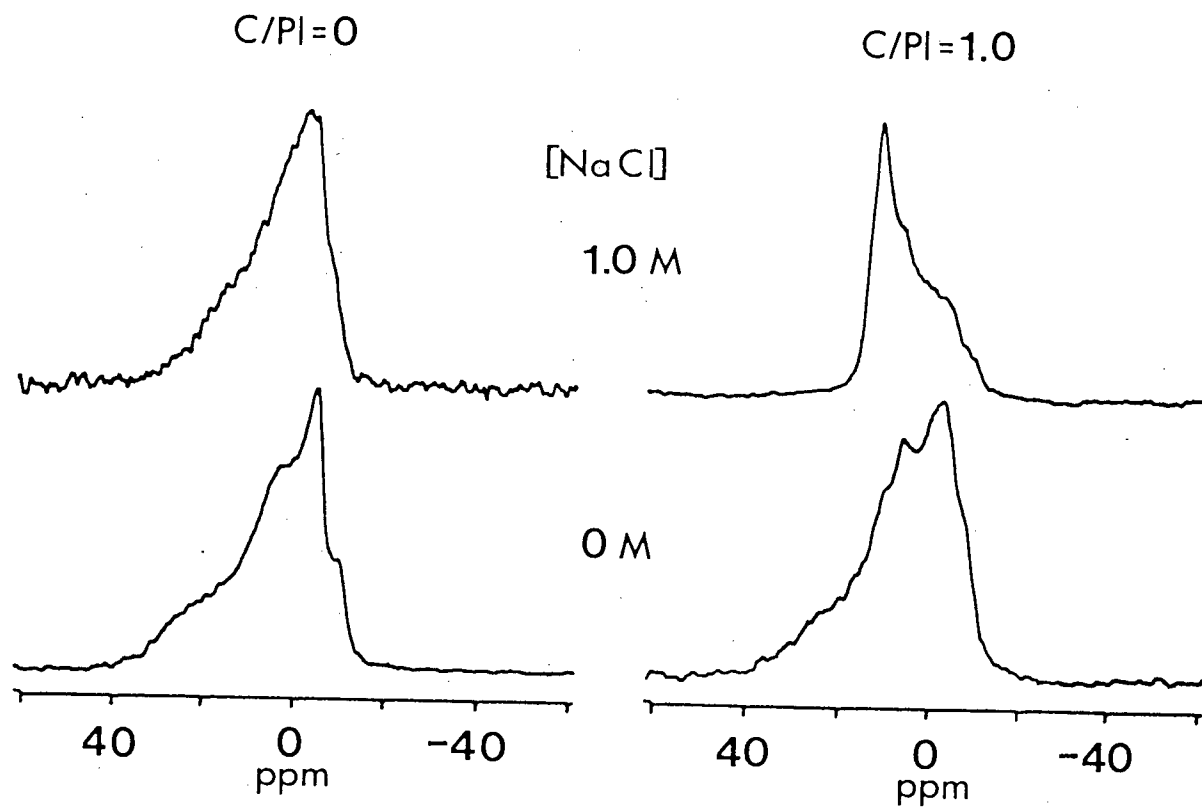
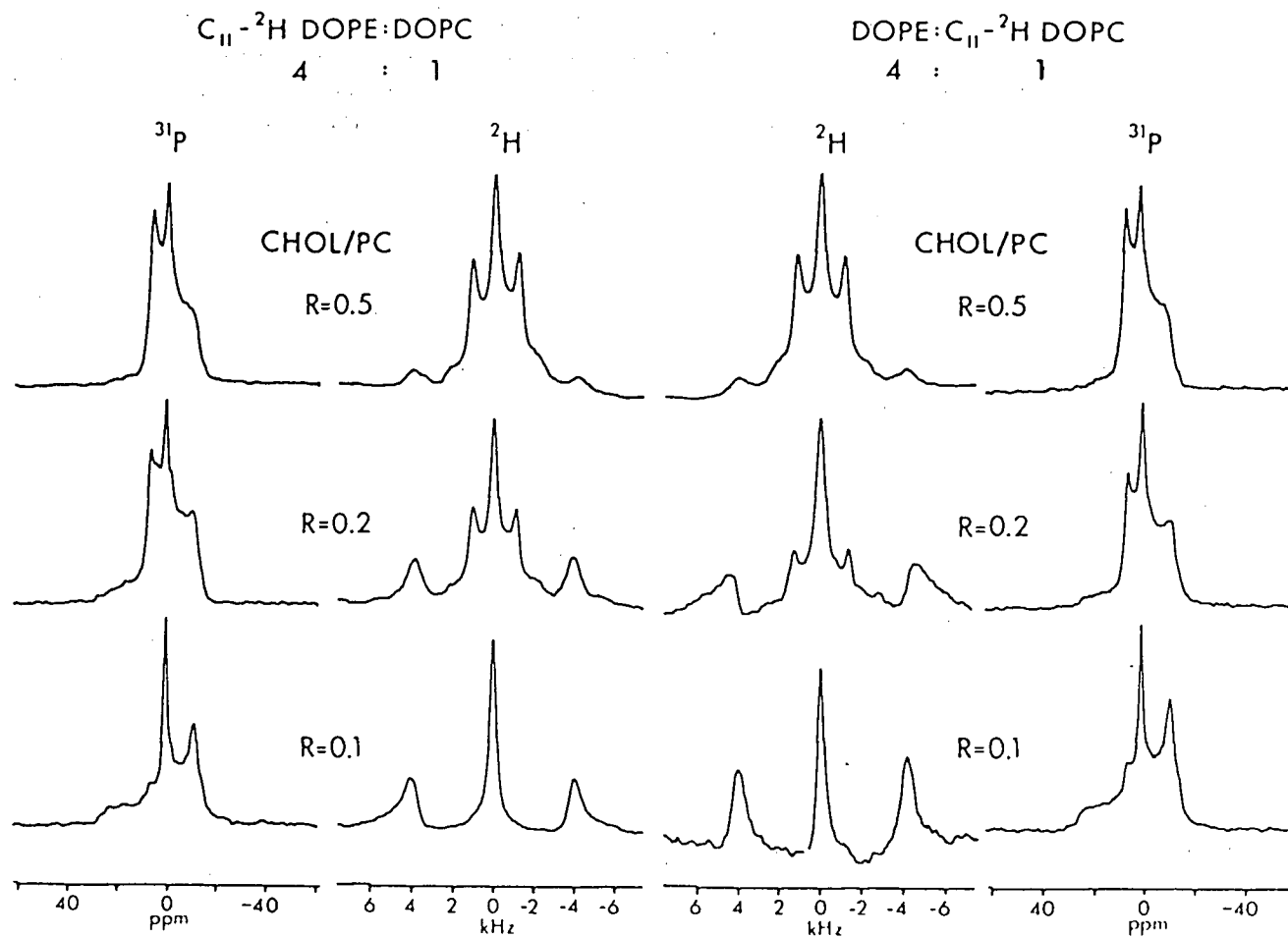


Fig. 13. 81.0 MHz ^{31}P NMR and 30.7 MHz ^2H NMR spectra at 40°C arising from aqueous dispersions of mixtures of dioleoylphosphatidylethanolamine (DOPE) and dioleoylphosphatidylcholine (DOPC) and cholesterol (CHOL) at a DOPE:DOPC molar ratio of 4:1 where either the DOPE is ^2H labeled at the C_{11} position ($[\text{C}_{11}\text{-}^2\text{H}_2]$ DOPE) or the DOPC is ^2H labeled at the C_{11} position ($[\text{C}_{11}\text{-}^2\text{H}_2]$ DOPC). The ratio R refers to the molar ratio of cholesterol to DOPC. For details of sample preparation and data manipulation see section 2.2.



in the bilayer phase component, and DOPE in the H_{11} phase component.

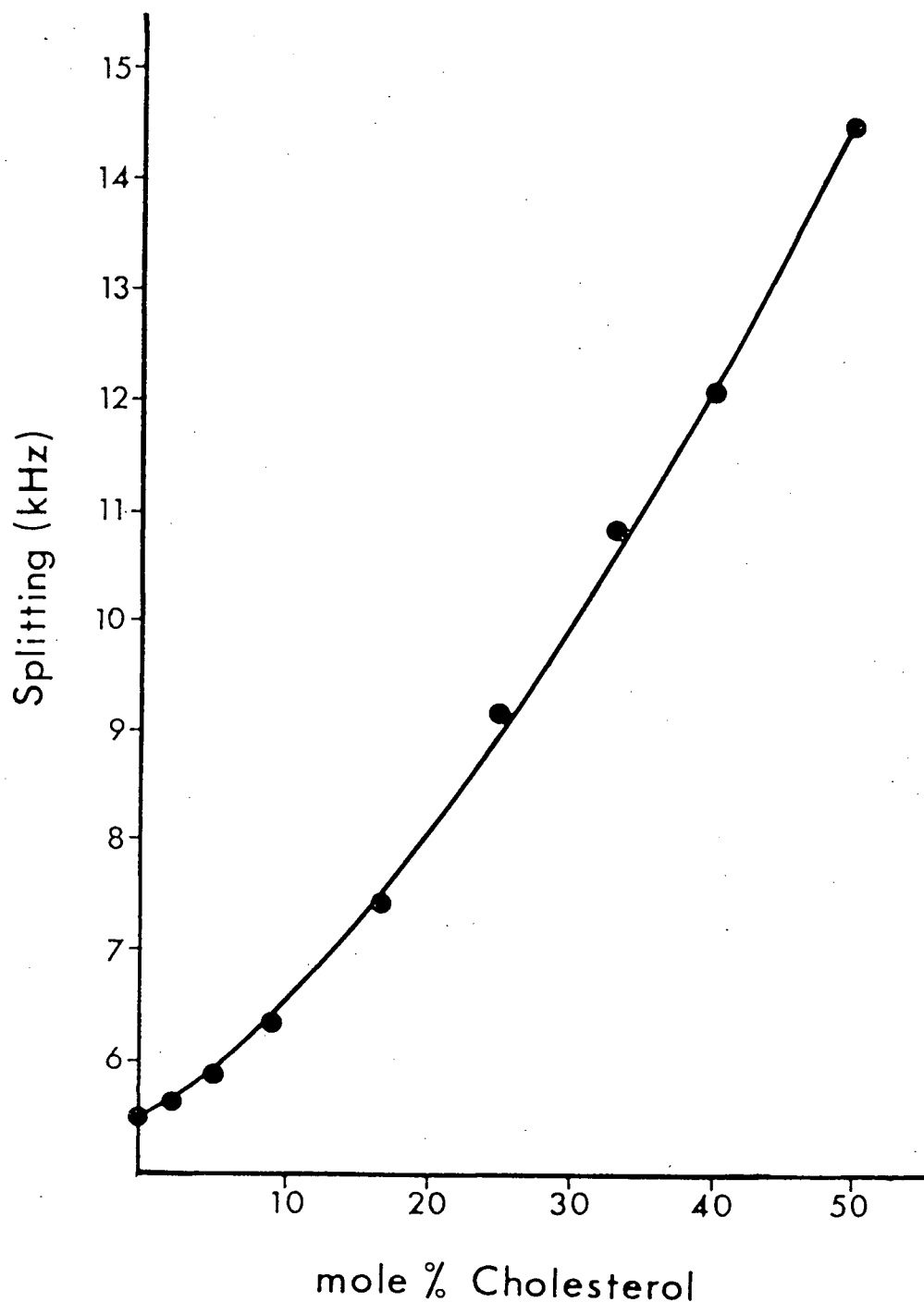
A point of interest regarding the ^2H NMR spectra of Fig. 13 concerns the values of quadrupolar splitting observed. First, the quadrupolar splittings (ΔQ) of the $(\text{C}_{11}-^2\text{H}_2)\text{DOPE}$ and $(\text{C}_{11}-^2\text{H}_2)\text{DOPC}$ are equivalent in both the bilayer and H_{11} organization. It may be noted that for the cholesterol contents corresponding to $R=0.1$, the maximum ΔQ expected for the $(\text{C}_{11}-^2\text{H}_2)\text{DOPC}$ (if all the cholesterol was associated with the DOPC) would be 6.3 kHz (Fig. 14). The value of 8.1 kHz observed both for the labeled DOPC and for DOPE indicates that bilayer phase DOPE has a more ordered hydrocarbon region than DOPC and that this increased order is also experienced by the acyl chains of the DOPC. This is again consistent with a well-mixed system. Second, even in the presence of the highest cholesterol levels used ($R=0.25$), the ΔQ of the bilayer component of the labeled DOPC sample remains at 8.3 kHz. If the cholesterol present was preferentially associated with the PC, the results of Fig. 14 suggest that the ΔQ should be increased by almost 3 kHz. Thus the results of Fig. 13 give no support for the notion of preferential association of cholesterol with PC over PE.

2.4 Discussion

The data presented here shows clearly that the presence of cholesterol in (unsaturated) PE-PS or PE-PC systems promotes formation of H_{11} -phase structure. This is expressed either as a direct result of the presence of cholesterol, or as an increased sensitivity of the structural preferences of PE-PS systems to the presence of divalent cations or increased ionic strength. The mechanism whereby cholesterol causes such effects will be discussed first and subsequently the potential biological ramifications of these effects will be considered.

The ability of cholesterol to destabilize bilayer structure in PS-PE systems is consistent with an ability to exert similar effects in (unsaturated) PC-PE systems (Cullis and de Kruijff, 1978; Cullis *et al.*, 1978, see also Fig. 13). In these systems, it was suggested that cholesterol has a net cone shape (for discussion of the shape concept see section 1.7) which in combination with PC results in a complex more compatible with H_{11} -phase structure. Such a rationale may also apply to the effects of cholesterol on the PS-PE systems, where the

Fig. 14. Influence of cholesterol on the quadrupolar splitting ΔQ observed for dioleoylphosphatidylcholine (DOPC) ^2H labeled at the C_{11} position of the acyl chains ($[\text{C}_{11}-^2\text{H}_2]\text{DOPC}$). The ^2H NMR spectra from which these data were obtained at 30.7 MHz and at a temperature of 40°C . For details of sample preparation and NMR data manipulation see section 2.2.



cholesterol has been suggested to associate preferentially with the PS component (Demel *et al.*, 1977). There are other factors which must be taken into account, however. First, cholesterol may be expected to exert a spacing effect in the mixed systems, thus reducing the electrostatic repulsion between the negatively charged serine head groups and thereby reducing the effective size of the head group. Second, although the hydration state of cholesterol in a phospholipid matrix is not known, it may be expected to be relatively poorly hydrated in comparison to phospholipids. Cholesterol in water, for example, adopts a (crystalline) monohydrate form. Given that lipids which readily adopt the H_{11} phase hydrate poorly in comparison with "bilayer" phospholipids, the reduction in bound water per unit of membrane surface due to the presence of cholesterol could also play a role in promoting H_{11} -phase structure.

The ability of cholesterol to lower the amount of Ca^{2+} required to trigger bilayer- H_{11} transition in PS-PE dispersions poses interesting problems with regard to mechanism. Tilcock and Cullis (1981) showed that in the absence of cholesterol Ca^{2+} appears to trigger H_{11} -phase formation in these systems by segregating PS into "cochleate" (Papahadjopoulos *et al.*, 1975a) domains, leaving the phosphatidylethanolamine free to adopt the H_{11} phase it prefers in isolation. Such Ca^{2+} induced segregation may occur to some extent in the presence of cholesterol, but the results obtained when Mg^{2+} is present suggest an alternative possibility. In particular, high levels (50 mM) of Mg^{2+} are ineffective for inducing lateral segregation of PS in mixed PS-PC systems (Ohnishi and Ito, 1974) and cannot trigger bilayer- H_{11} transition in mixed PS-PE systems (Tilcock and Cullis, 1981 and Fig. 10). Thus the ability of 4.0 mM and higher Mg^{2+} concentrations to induce H_{11} -phase structure when cholesterol is present either suggests that cholesterol facilitates the lateral segregation of PS or that it promotes Mg^{2+} -dependent incorporation of the PS into the H_{11} phase. The latter possibility appears the most likely as there is no evidence for a Mg^{2+} -induced segregation of PS. In particular, it may be estimated that more than 80% of the phospholipid in the soya PS-soya PE (1:1) systems containing equimolar cholesterol adopt the H_{11} configuration in the presence of 8 mM Mg^{2+} (Fig. 10). As soya PS in the presence of Mg^{2+} maintains the bilayer organization (as

does equimolar PS-cholesterol in the presence of Mg^{2+} ; M.J. Hope unpublished observation), Mg^{2+} -induced lateral segregation of PS in the sample of Fig. 10 should leave 50% of the lipid in lamellar organization, contrary to experiment. It is suggested that the presence of Mg^{2+} acts to decrease the charge density at the lipid-water interface. This may be considered to reduce the electrostatic repulsion between serine head groups, thus reducing the effective size of the serine head group and producing a net molecular "shape" more compatible with the H_{11} phase. This would allow the H_{11} -phase preferences of the PE to predominate and would correspond to the situation for Ca^{2+} -triggered H_{11} phase formation in phosphatidylglycerol-PE systems (Farren and Cullis, 1980).

The Ca^{2+} -induced triggering of H_{11} -phase formation in the soya PS-PE-cholesterol (1:1:2 on a mole basis) systems may have a similar basis as the Mg^{2+} -induced transition. The situation where 2 mM Mg^{2+} acts as an adjunct to the Ca^{2+} effect, lowering the Ca^{2+} concentrations required to 0.25 mM, would be particularly likely to proceed via this charge neutralization mechanism. This is because such concentrations of Ca^{2+} are well below those required to induce lateral segregation of PS in mixtures with PE and even below those required to trigger formation of "cochleate" crystalline PS- Ca^{2+} (2:1) complexes in pure PS systems (Tilcock and Cullis, 1981). The ability of high salt concentrations to induce H_{11} -phase structure in PS-PE-cholesterol (1:1:2) systems also corresponds to charge neutralizations effects, and it therefore appears possible that the cation-dependent macroscopic structural alterations of these systems can proceed by a common mechanism which does not necessarily involve lateral segregation of individual components.

This proposal would be supported by the investigations examining the mixing properties of DOPE/DOPC systems where cholesterol influences the polymorphic phase properties of the lipids (see Fig. 13). The results presented here suggest that cholesterol is not preferentially associated with the PC component in these systems, arguing against the possibility that cholesterol is associated with PC to form a "cone"-shaped (see Cullis and de Kruijff (1979)) complex more compatible with the H_{11} phase. Similarly, the observation that in mixed DOPE-DOPC-cholesterol systems which exhibit regions of bilayer and H_{11} phase organization

(as well as structures allowing isotropic motional averaging) the DOPC and DOPE appear to partition into these structures with equal probability argues against explanations involving segregation of different lipid species into different phase structures. More recent experiments (Tilcock *et al.*, 1984) have demonstrated, by employing ^2H NMR (and x-ray diffraction techniques) in a similar fashion to that illustrated in Fig. 13, that DOPS can adopt the H_{11} organization when Ca^{2+} is added to mixed systems composed of DOPE/DOPS containing cholesterol. This result provides more direct evidence for the conclusions derived here from the soya PE-soya PS mixed systems.

The resulting conclusion that these lipids remain ideally mixed even when such diverse structural alternatives are available to them suggests that they will also behave in a miscible fashion in less extreme situations. In particular, it has been argued that local clusters with differing lipid compositions from the surrounding bulk lipid may exist in biological membranes and that these microenvironments may modulate local function (see section 1.3). The results presented here would argue against such a hypothesis, suggesting that such clusters would not exist for times longer than the NMR time scale (10^{-5} sec).

The results presented here also have important implications for Ca^{2+} -induced fusion processes, as well as the compositions and properties of the inner monolayer of the erythrocyte membrane. These areas will be discussed in turn. First, the observation that cholesterol and cytosol levels of Mg^{2+} can reduce the Ca^{2+} concentrations required to induce nonbilayer structures in appropriate systems to 250 μM or less supports the contention that membrane fusion processes *in vivo* proceed by intermediate formation of inverted micelle and (or) inverted cylinder lipid configurations (section 1.6.2 and Cullis and Hope, 1978; Verkleij, 1984; Hope *et al.*, 1981). Previously, the high (nonphysiological) Ca^{2+} levels of 2 mM or more required to induce nonbilayer structures in and induce fusion between mixed PE-PS vesicle systems posed major problems for extrapolating to *in vivo* situations. It should be noted that other factors may act to reduce the Ca^{2+} levels required even further. These include proteins such as synexin (Creutz *et al.*, 1978; Hang *et al.*, 1981), which appear to increase the effective Ca^{2+} concentration for fusion between model systems.

The second point concerns the composition and structural preferences of the inner monolayer of the erythrocyte membrane. First, it is clear that the sensitivity of the polymorphic preferences of this lipid composition to the presence of divalent cations will be markedly enhanced by the presence of cholesterol. This is in agreement with observations that Ca^{2+} cannot trigger H_{11} -phase formation in model systems mimicking the inner monolayer composition in the absence of cholesterol (M.J. Hope, unpublished observations). Although the transbilayer distribution of cholesterol in the erythrocyte membrane has not been established, it is likely that cholesterol is present at levels approaching equimolar (with respect to phospholipid) proportions, given the ability of cholesterol to redistribute rapidly across bilayer membranes (Kirby and Green, 1977). Thus the structural preferences of the inner monolayer may be dictated by relatively low cytosol levels of Ca^{2+} or even by the local cholesterol content.

PRODUCTION OF LARGE UNILAMELLAR VESICLES BY A RAPID EXTRUSION

PROCEDURE: CHARACTERIZATION OF SIZE DISTRIBUTION,

TRAPPED VOLUME, AND ABILITY TO MAINTAIN A

MEMBRANE POTENTIAL†

3.1 Introduction

As described in section 1.4, model membrane systems are in one form or another aqueous dispersions of phospholipids that are designed to mimic some of the properties of biological membranes. Obviously MLVs (multilamellar vesicles) have little relation to biological membranes, yet they have been useful in determining the physical characteristics of a variety of lipid species. For example, the previous chapter utilized MLV model membrane systems to show that different lipid species may assume different polymorphic phases such as the bilayer and/or H_{11} configurations depending on the presence of such factors as cholesterol and/or divalent cations. In respect to understanding the role of lipids in regulating the permeability properties of membranes, however, the MLV model membrane system is of limited value (see section 1.4) and other systems must be employed. These model membrane systems must satisfy several stringent criteria, with the basic requirements that such model vesicles be closed and unilamellar and that the vesicle be reasonably large to enclose an appreciable trapped volume and to avoid problems associated with very small, highly curved systems (Schuh *et al.*, 1982).

These demands have either proved difficult to fulfill (see section 1.4 or for review see Szoka and Papahadjopoulos, 1980) or have not yet been attempted. A major problem involves the use of lipid solubilizing agents (organic solvents or detergents). These techniques often require lengthy dialysis procedures which can never completely remove the solvent or detergent employed. Further, a variety of protocols are required depending on the lipid species. For example, the limited solubility of certain lipids (*eg.*, cholesterol, phosphatidylethanolamine (PE))

†This chapter has been based on the references Hope *et al.* (1984) and Bally *et al.* (1984).

in ether or ethanol requires modification of techniques employing these solvents. Alternatively, detergent dialysis procedures employing non-ionic detergents such as octylglucoside are tedious to apply as they can involve several days of dialysis.

Before studies can be designed to analyze the permeability functions of lipids in membranes a general and straightforward protocol for production of LUVs is required. Preferably, such a technique would avoid the use of solubilizing agents, would produce vesicles of a relatively homogeneous size and would be relatively rapid. In this work a procedure which satisfies most of these criteria is presented. Further, these LUVs have been utilized to model a basic feature of biological membrane systems - namely the presence of a transbilayer membrane potential ($\Delta\psi$). The procedure for generating LUVs involves an extension of the work of Olson *et al.* (1979) who describe a technique whereby the trapped volume of large multilamellar vesicles can be increased by extrusion under relatively low pressures (less than 80 psi) through polycarbonate filters of 0.2 μm pore size. These vesicles are multilamellar with a reasonably homogeneous size distribution centred about the pore size of the membrane. It was reasoned that extrusion through smaller pores may result in vesicles sufficiently small that the presence of inner lamellae is unlikely. It is demonstrated that repeated extrusion under moderate pressures (less than 500 psi) of multilamellar vesicles through polycarbonate filters of 0.1 μm pore size results in a relatively homogenous population of unilamellar vesicles. These LUVETs (large unilamellar vesicles by extrusion techniques) can be produced rapidly (less than 15 min) in a manner which is relatively independent of lipid composition. Further, LUVETs can be generated at high lipid concentrations (up to 300 $\mu\text{mol/ml}$) and can exhibit relatively high trapping efficiencies (up to 30%). These vesicles are employed to obtain a model system exhibiting a membrane potential. In addition, certain aspects of the influence of phospholipid composition on the maintenance of the and regulation of ion permeability are investigated.

3.2 Materials and Methods

3.2.1 Lipid preparation

Egg PC and soya PC were prepared as described in sections 2.2.1 and 2.2.2 and the corresponding PE and PS derivatives were prepared from the respective PC using the base exchange capacity of phospholipase D (see section 2.2.1). PE and PS were purified and the PS's were converted to the sodium salt as described previously. Cholesterol (Sigma, St. Louis, MO) was used without further purification. All lipids were greater than 99% pure as determined by TLC.

3.2.2 Vesicle preparation

Multilamellar vesicles (MLVs) were prepared by vortexing dry lipid in the presence of the appropriate aqueous buffer. The resulting MLV dispersion was then transferred into a device (produced by Sciema Technical Services Ltd., Richmond, B.C.) which allowed the extrusion of the MLVs through standard 25 mm polycarbonate filters with 0.1 μm pore size (Nucleopore Corp., Pleasanton, CA). Briefly, MLVs (in 2–5 ml) were injected into a central chamber above the polycarbonate filters, and nitrogen pressure applied via a standard gas cylinder fitted with a high pressure (0–4000 psi) regulator. The vesicles were extruded through the filter employing pressures of 100–500 psi resulting in flow rates of 20–60 ml/min, and were collected and re-injected. Unless stated differently, the LUVET preparations were passed through two (stacked) filters 10 times. When the freeze-thaw procedure was utilized, the vesicles were sized as above, freeze-thawed (employing liquid nitrogen) and then sized again through new filters. A total of two freeze-thaw cycles were usually employed.

3.2.3 Determination of trapped volumes

To determine trapped volumes, the multilamellar vesicles were prepared in the presence of 1 μCi of ^{22}Na or ^{14}C -inulin (NEN, Canada) and the LUVETs made as indicated above.

An aliquot (100 μ l) was then loaded onto a Sephadex G-50 column packed in a 1 ml disposable syringe, and vesicles eluted by centrifugation of the column at 500g for 3 min. In the case of ^{22}Na this was sufficient to remove all the untrapped material. To remove all the untrapped inulin, however, this procedure was repeated twice or the untrapped inulin was removed using a 2 ml Ultragel (AcA 34, LKB, France) column. Aliquots of the eluted material were assayed for lipid phosphorus (Bottcher *et al.*, 1961, see following paragraph), trapped ^{22}Na was determined employing a Beckman 8000 gamma counter and trapped ^{14}C inulin was estimated using a Phillips PW-4700 liquid scintillation counter. Trapped volumes calculated are expressed as μ l of trapped volume per μ mol of phospholipid.

For the phosphate assay, samples (containing between 0.05 and 0.2 μ mole phospholipid) were digested in 0.6 ml of 70% HClO_4 at 190°C for 1 to 2 hr. Subsequently, 7 ml of ammonium molybdate reagent (0.22%, w/v, ammonium molybdate in 2% H_2SO_4 , v/v) and 0.6 ml of Fiske-Subbarrow reagent (30 gms NaHSO_4 , 1 gm Na_2SO_4 and 0.5 gms 1-amino-2-naphthol-4-sulphonic acid in 200 ml water at 40°C to aid solubilization. The reaction mixture was incubated at 100°C for 15 min, subsequently the sample was cooled to room temperature and the absorbance at 815 nm was determined.

3.2.4 Freeze-fracture and negative staining

For freeze-fracture, vesicle preparations were mixed with glycerol (25% by volume) and frozen in a freon slush. Samples were fractured and replicated employing a Balzers BAF 400D apparatus, and micrographs of replicas were obtained using a Phillips 400 electron microscope. Vesicle size distributions were determined by measuring the diameter of fractured vesicles that were 50% shadowed according to the procedure of van Venetie *et al.*

Negative staining was performed on samples placed on Formvar coated, bacitracin treated grids, using 2.5% ammonium molybdate. Micrographs were obtained using a Zeiss EM-10 electron microscope.

3.2.5 ^{31}P Nuclear magnetic resonance

^{31}P NMR was employed to provide an indication of the extent to which the vesicle preparations were unilamellar. Briefly, Mn^{2+} was added to the vesicle dispersion (3 ml, 30 μmol phospholipid per ml in a 15 mm diameter NMR tube) at levels (5 mM) sufficient to broaden beyond detection the ^{31}P NMR signal from those phospholipids facing the external medium. If the vesicles are large and unilamellar then 50% of the signal should remain following the addition of Mn^{2+} . The impermeability of the vesicles to Mn^{2+} was straightforward to demonstrate by following the timecourse of the signal intensity, which for the PC systems investigated here was stable over a period of days. Spectra were obtained employing a Bruker WP 200 NMR spectrometer operating at 81.0 MHz as described in section 2.2.4. Signal intensities were measured by cutting out and weighing spectra with triphenylphosphite (in a small central capillary in the NMR tube) as a reference.

3.2.6 Membrane potential and permeability studies

In order to produce the $\text{Na}^+ - \text{K}^+$ chemical gradients required to establish a membrane potential, LUVETs (20 μmol phospholipid per ml) were made in a KCl buffer (155 mM KCl, 20 mM HEPES, pH 7.4). Subsequently, the untrapped buffer was exchanged for a NaCl buffer (150 mM NaCl, 20 mM HEPES, pH 7.4) by passage through a Sephadex G-50 column which was pre-equilibrated with the NaCl solution. Where employed, valinomycin (Sigma, St. Louis, MO) was added in ethanol to a concentration of 1 $\mu\text{g}/\mu\text{mol}$ phospholipid. The membrane potential generated was measured by determining the distribution of the lipophilic cation ^3H -methyltriphenylphosphonium iodide (^3H -MTPP $^+$, obtained from NEN, Canada). Routinely, 1 μCi of ^3H -MTPP $^+$ in 1 μl ethanol was added to 1-2 ml of a LUVET dispersion which was then incubated at 20°C. At various times an aliquot was withdrawn and the untrapped ^3H -MTPP $^+$ removed by passage through the 1 ml Sephadex G-50 columns described above. The trapped ^3H -MTPP $^+$ was determined by liquid scintillation counting and the phospholipid determined by phosphate assay. A potential difficulty with this

procedure concerns the possibility that trapped $^3\text{H-MTPP}^+$ leaks out while on the column. However, similar results were obtained employing both the ultrafiltration technique detailed below for ^{42}K in the presence of valinomycin and an equilibrium dialysis technique. Knowledge of the trapped volume (see above) allows the concentrations of MTPP inside ($(\text{MTPP}^+)_i$) and outside ($(\text{MTPP}^+)_o$) the vesicles to be calculated, from which the membrane potential may be calculated employing the Nernst equation:

$$\Delta\psi \text{ (mV)} = -59 \log [\text{MTPP}^+]_i / [\text{MTPP}^+]_o$$

The flux of Na^+ , K^+ and Cl^- across the LUVET membranes subsequent to establishing the Na^+/K^+ distributions (K^+ inside) were determined employing the radioisotopes $^{22}\text{Na}^+$, $^{42}\text{K}^+$, and $^{36}\text{Cl}^-$ (NEN, Canada) in the absence and presence of valinomycin. Briefly, influx of Na^+ was determined by addition of $^{22}\text{Na}^+$ ($2 \mu\text{Ci/ml}$) to the external medium. Aliquots ($100 \mu\text{l}$) were then removed at various time intervals, the untrapped Na^+ removed by passage over the 1 ml Sephadex columns, and the ^{22}Na influx determined by gamma counting. Efflux of K^+ in the absence of valinomycin was determined by a similar procedure where ^{42}K was initially trapped inside the vesicles. However, when valinomycin was added the column technique could not be employed due to efflux of K^+ while on the column, necessitating an alternative technique. In this case a 10 ml ultrafiltration unit (Amicon Corp.) operated at 5 psi and fitted with a YM 10 Diaflo (Amicon Corp.) membrane was employed to separate the LUVETs from the external medium. Vesicles ($40 \mu\text{mol}$ phospholipid per ml, 20 ml total volume) were made in the presence of $^{42}\text{K}^+$ and the outside medium exchanged for the NaCl buffer. Valinomycin was added and for each time point 1 ml of the vesicle dispersion was removed and placed in the ultrafiltration unit. Aliquots ($100 \mu\text{l}$) of the (untrapped) buffer were removed (within 30 sec) and the ^{42}K content determined. Knowledge of the initial ^{42}K levels, the lipid concentration and trapped volume then allowed the distribution of K^+ to be calculated.

The Cl^- flux in and out of the LUVET systems was determined by similar procedures as the K^+ and Na^+ flux in the absence of valinomycin. In addition H^+ flux was estimated using the procedure of Nicolls and Deamer (1980), where the outside pH was measured as a function of time, which was subsequently converted to H^+ (or OH^-) flux (see section 1.8).

3.3 Results

3.3.1 Characterizations of LUVETs

The influence of repeated passages of (initially) large multilamellar EPC vesicles (MLVs) through polycarbonate filters of 0.2 μm and 0.1 μm pore size on the amount of EPC sequestered away from externally added Mn^{2+} is illustrated in Fig. 15. In the case of vesicles passed through the 0.2 μm filter the signal intensity drops to approximately 65% after five passes then remains relatively constant. This suggests an appreciable population of multilamellar vesicles, a conclusion supported by freeze fracture results (see Fig. 17(d) and related discussion). Extrusion of MLVs through the 0.1 μm filter, on the other hand, results in reduction in signal intensity to 50% after five or more passes, suggesting the presence of primarily unilamellar vesicles. This is illustrated in the negative stain micrographs of EPC LUVETs (Fig. 16) which indicate that after a single pass (Fig. 16(b)), a substantial number of multilamellar vesicles are still present in comparison to samples passed ten times through the filters (Fig. 16(c)). This conclusion is also supported by freeze-fracture studies for LUVETs formed from a variety of phospholipids as indicated in the micrograph of Fig. 17. Vesicles formed from SPC, SPC-SPS (1:1), and SPE-SPS (1:1) (Fig. 17 (a), (b), and (c) respectively) do not exhibit a significant number of cross-fractures (less than 0.1%) indicating the absence of inner lamellae. This contrasts with the SPC vesicle system formed employing a 0.2 μm filter (Figure 17(d)) where such cross-fractures are readily observable.

The size distribution of SPC LUVETs was determined from freeze-fracture micrographs according to the procedure of van Venetie *et al.* (1980) and is illustrated in Fig. 18. The half-tone columns represent SPC LUVETs prepared by passing MLVs through two (stacked) 0.1 μm pore size filters ten times. Assuming an area per phospholipid molecule of 0.6 nm^2

Fig. 15. ^{31}P NMR signal intensity arising from egg PC multilamellar vesicles (in the presence of 5 mM MnCl_2) as a function of the number of extrusions through polycarbonate filters with 100 nm (●) and 200 nm (■) pore sizes. The error bars represent standard deviations ($n = 6$ for the point at 10 extrusions through the 100 nm filter; $n = 3$ for the point at 30 extrusions). All other experimental points represent the average obtained from two separate experiments. The lipid concentration was 50 mg/ml. For other details see section 3.2.

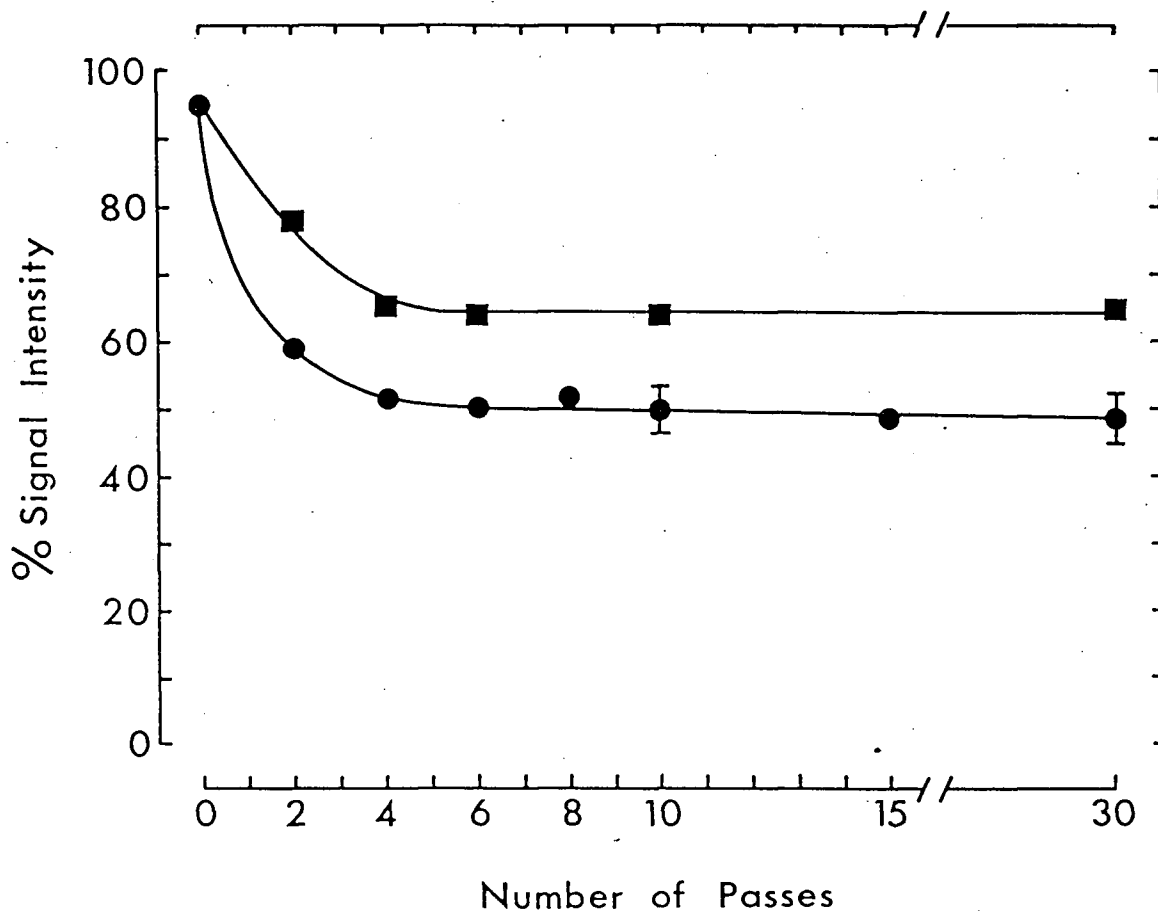


Fig. 16. Micrographs of negatively stained (2.5% (w/v) ammonium molybdate) egg PC vesicles prepared by extrusion of multilamellar vesicles (A) through 100 nm polycarbonate filters twice (B) or ten times (C) on lipid systems containing 100 mg/ml phospholipid. Sonicated (small) unilamellar vesicles (D) are included for size comparison.

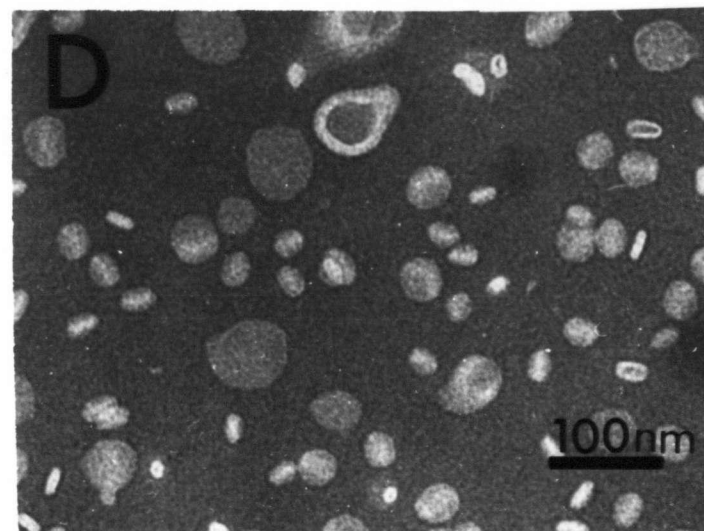
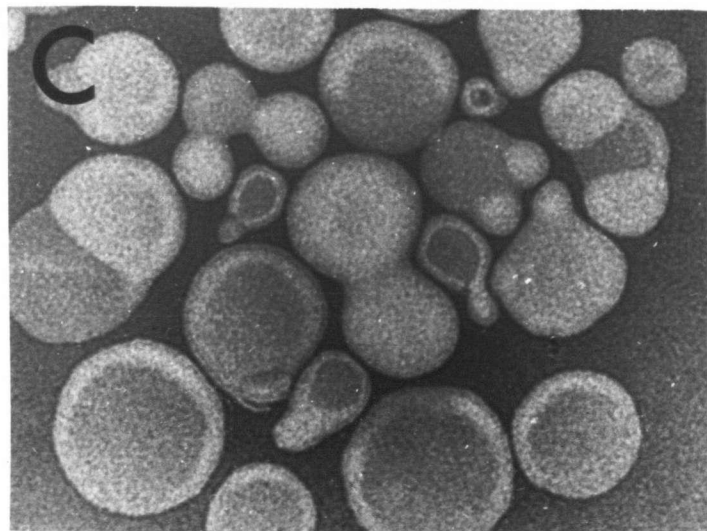
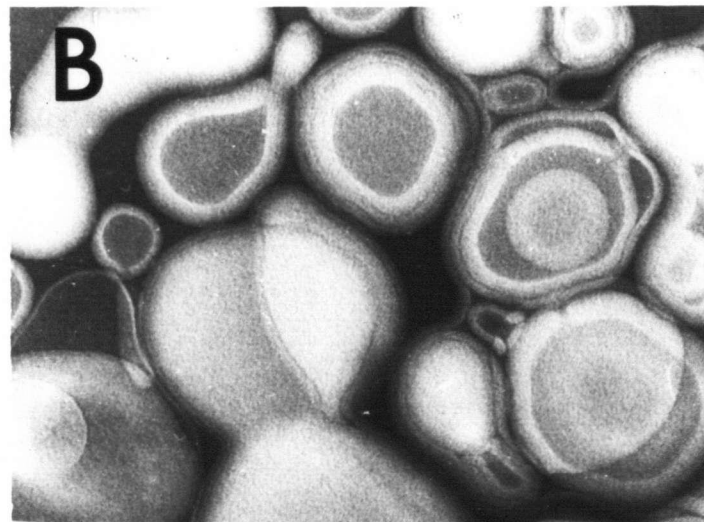
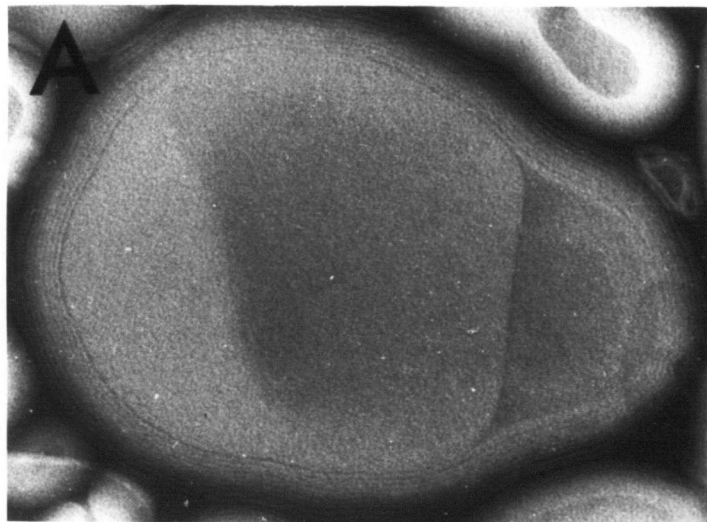


Fig. 17. Freeze-fracture micrographs of vesicles prepared by repeated extrusion of multilamellar vesicles of varying lipid composition through polycarbonate filters: (a) soya PC MLVs extruded through a 100 nm filter; (b) soya PC-soya PS (1:1) MLVs extruded through a 100 nm filter; (c) soya PE-soya PS (1:1) MLVs extruded through a 100 nm filter; (d) soya PC MLVs extruded through a filter with 200 nm pore size. The arrow in part (d) indicates a cross fracture revealing inner lamellae. All micrographs have the same magnification and the direction of shadowing is indicated by the arrowhead in the bottom right corner of each section. The extrusion procedure was repeated 10 times on lipid systems containing 50 mg/ml phospholipid. Data collected and reproduced with permission from M. J. Hope.

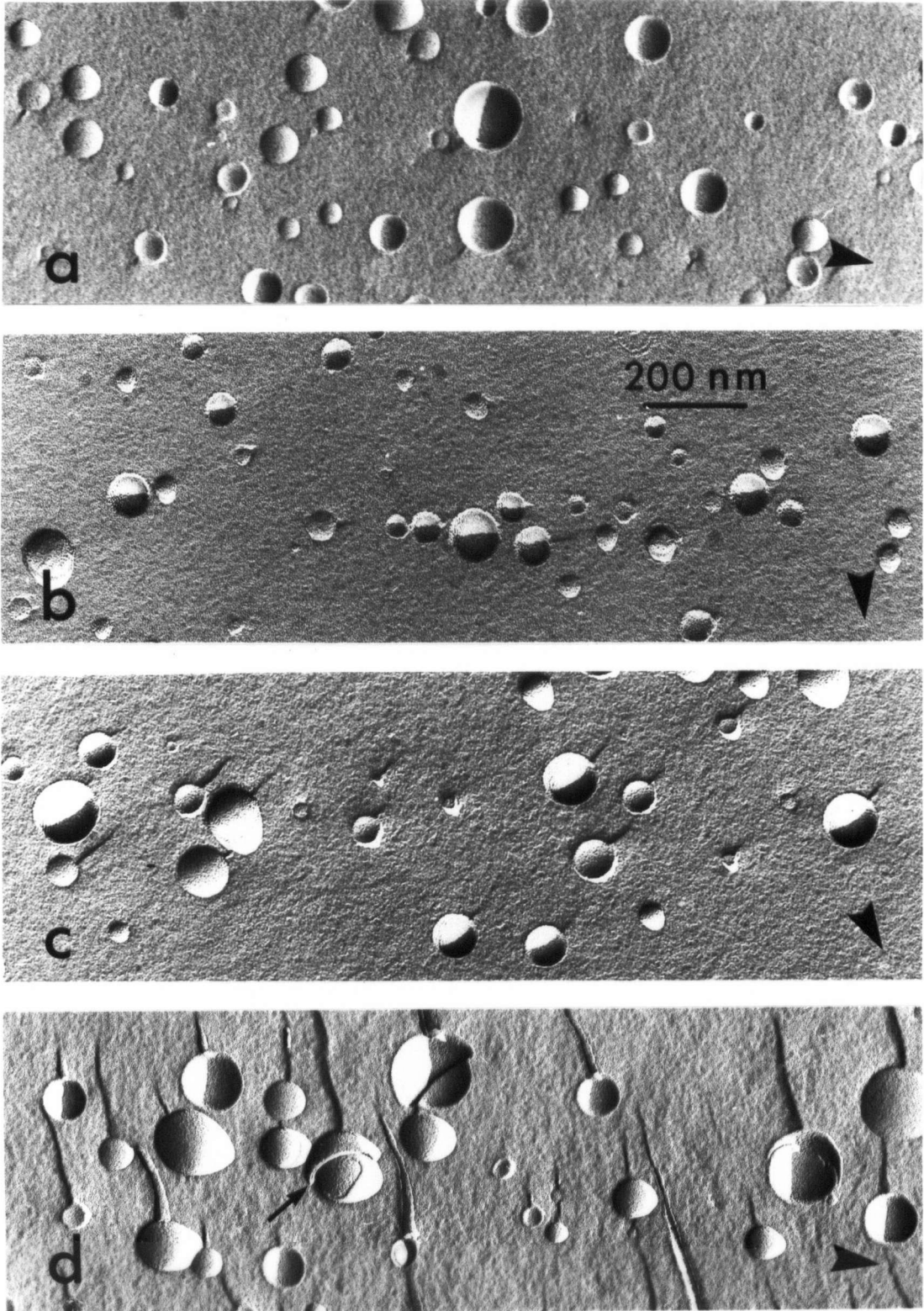
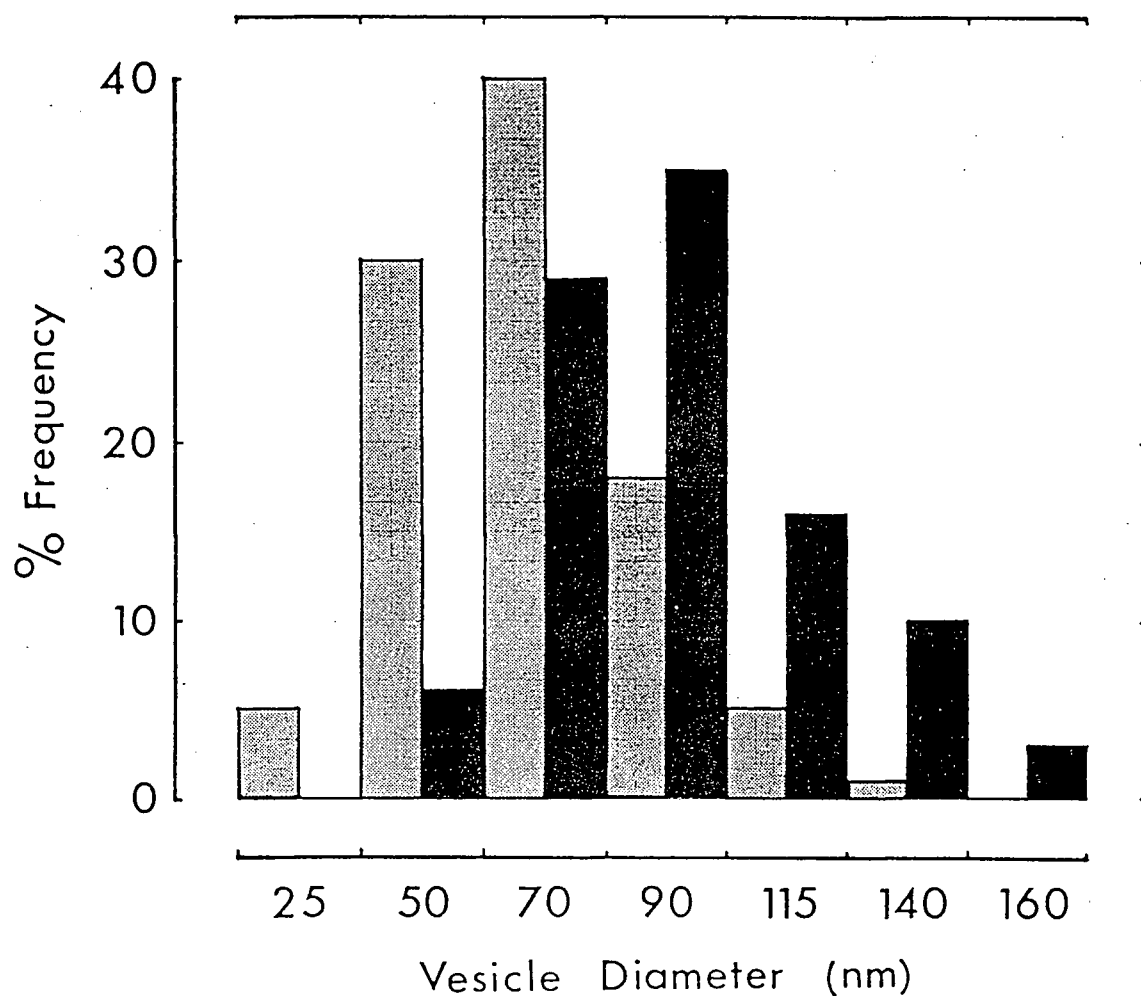


Fig. 18. Size distribution of soya PC vesicles obtained after 10 extrusions through a polycarbonate filter with 100 nm pore size. The vesicle diameters were measured from freeze-fracture micrographs employing the technique of van Venetiè *et al.* (1980). The half-tone columns represent vesicles that did not undergo a freeze-thaw cycle, the black columns represent vesicles subjected to the freeze-thaw protocol outline in section 3.2.2.



(Schieren *et al.*, 1978) and a bilayer thickness of 4 nm (Blaurock, 1982) and that the vesicles are unilamellar, the trapped volume and amount of inner monolayer phospholipid can be calculated for such a distribution. These estimates can be compared with the experimentally observed trapped volumes and amount of inner monolayer phospholipid to determine the proportion of unilamellar vesicles present. For the vesicle size distribution presented in Fig. 18 (half tone), it can be calculated that such a vesicle population (if unilamellar) would have an "inner monolayer" signal intensity (after the addition of Mn^{2+}) of approximately 43% of the original intensity and that the trapped volume would be approximately $1.6 \mu l/\mu mole$. This may be compared with the measured values of sequestered phospholipid (48%) and trapped volume ($1.2 \pm 0.2 \mu l/\mu mole$). The agreement between measured and calculated results is perhaps reasonable given the number of assumptions, in particular the area per phospholipid molecule which can greatly affect the trapped volume expressed as μl trapped per $\mu mole$ of phospholipid. However, as shown in Table 2, LUVETs composed of SPC and EPC consistently exhibit trapped volumes smaller than those expected from a unilamellar vesicle of the same diameter assuming an area/molecule of $0.6 nm^2$ and a bilayer thickness of 4 nm. If a charged phospholipid species such as phosphatidylserine is present, the theoretical trapped volume is achieved. Two possible reasons for the low trapped volumes observed for EPC and SPC LUVETs are that there are a significant number of multilamellar vesicles present in the population, or that there are a greater proportion of small vesicles present than estimated from the freeze-fracture micrographs.

It has been noted (Pick, 1981) that sonicated vesicles increase in size, but remained unilamellar, following a freeze-thaw cycle. For this reason SPC and EPC LUVETs were subjected to a freeze-thaw cycle followed by re-sizing through $0.1 \mu m$ pore size filters in an attempt to reduce the proportion of smaller vesicles in the preparation. The resulting size distribution for freeze-thawed SPC LUVETs is given in Fig. 18 (black columns). The mean diameter of the population increased by approximately 20 nm. The calculated trapped volume for this vesicle distribution is $2.3 \mu l/\mu mole$ which is in excellent agreement with the measured values for SPC LUVETs following a freeze-thaw cycle which fall within the range

Table 2 Physical characteristics of vesicles produced by extrusion of a variety of lipid mixtures through filters with a pore size of 100 nm.

Lipid	% Intensity [†]	Mean Diameter ± S.D. (nm)	Mean Trap Volume ^{††} ± S.D. (μl/ μmole)
EPC	48	71 ± 24	1.1 ± 0.1 (64)
SPC	48	70 ± 23	1.2 ± 0.2 (13)
EPC/EPS (2:1)	46	73 ± 25	1.5 (2)
SPC/SPS (2:1)	ND	73 ± 20	2.4 (2)
SPE/SPS (2:1)	ND	79 ± 36	2.0 (2)
SPS	ND	ND	2.3 (2)
EPS	ND	ND	2.2 (2)
EPC (Freeze-thaw)	51	77 ± 16	2.2 ± 0.5 (17)
SPC (Freeze-thaw)	48	94 ± 26	2.2 ± 0.1 (12)
EPC (Octylglucoside)	49	ND	1.2 ± 0.1 (3)
EPC (REV)	50	ND	1.2 (2)

[†] Intensity of ³¹P-NMR signal remaining in the presence of 5 mM Mn²⁺.

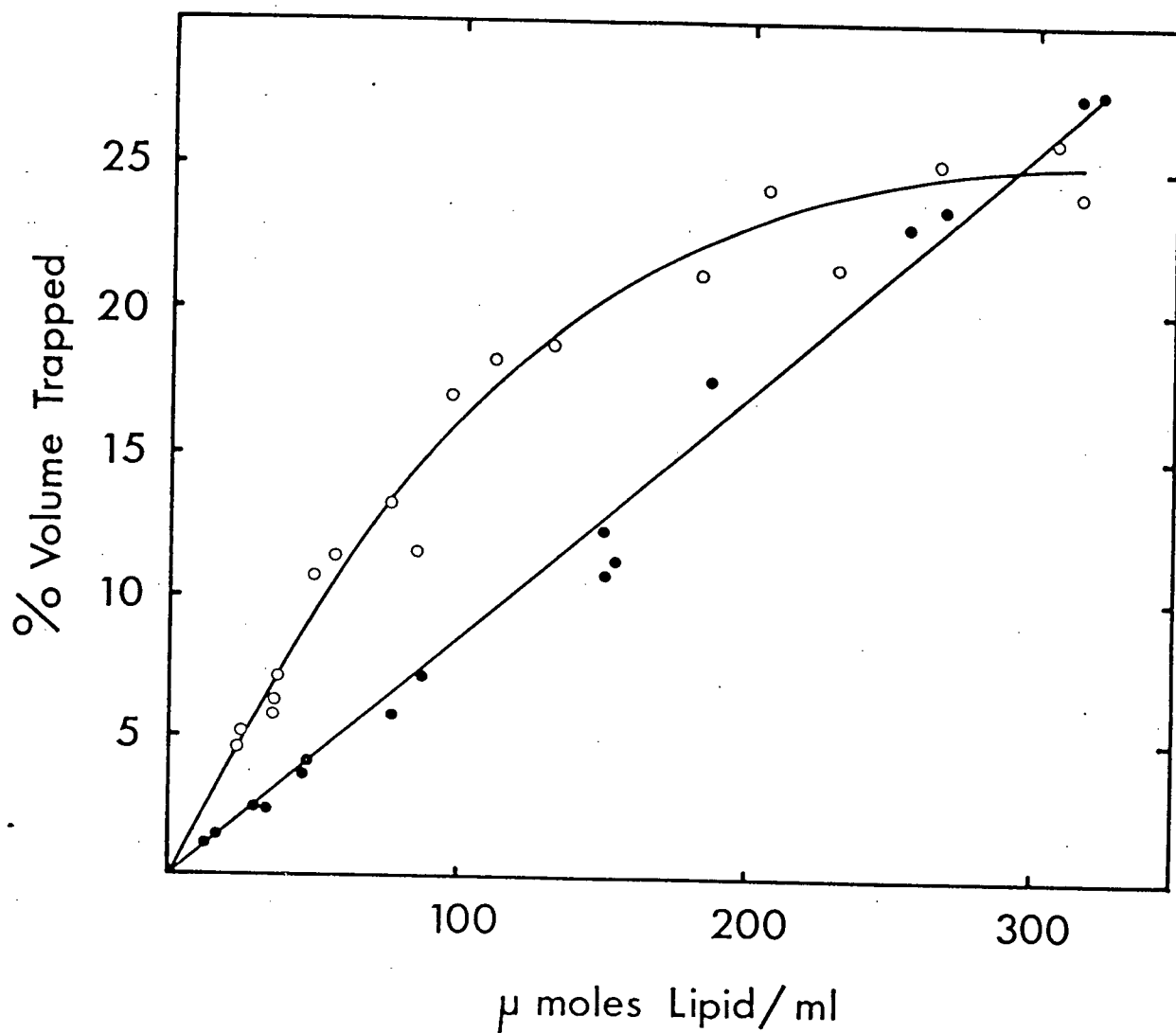
^{††} μl/μmole phospholipid (number of experiments in parenthesis).

of 2.0–2.5 μ l/ μ mole (Table 2).

These observations lead to the conclusion that the large majority of vesicles produced by repeated extrusion of PC MLVs through a filter with 0.1 μ m pore size in the absence of a freeze–thaw step are unilamellar, even though the trapped volume is smaller than expected. In order to reinforce this conclusion, EPC LUVs were prepared by two procedures which are widely accepted to produce unilamellar vesicles and subjected them to the same sizing procedure employed here. As indicated in Table 2, the trapped volumes measured for EPC LUVs produced by the octylglucoside detergent dialysis procedure (Mimms *et al.*, 1981) and the reverse phase evaporation procedure (Szoka and Papahadjopoulos, 1980), which were subsequently extruded (10 times) through the filter with 0.1 μ m pore size, are comparable to the trapped volumes obtained for the EPC LUVETs. It is pertinent to note that when the octylglucoside procedure was employed to make vesicles consisting of EPC/cholesterol (1:0.25), multilamellar vesicles were formed.

An important parameter of LUV preparations is their trapping efficiency, *ie.* the total volume of trapped buffer expressed as a percentage of the initial buffer volume used to hydrate the dried lipid film, is particularly important when the agents to be trapped are either expensive, as is the case for many drugs, or have low solubilities. The LUVET preparations described above have a trapped volume of 1–3 μ l/ μ mole phospholipid. Other preparations described in the literature have higher trapped volumes (Szoka and Papahadjopoulos, 1980) and therefore might be expected to allow better trapping efficiency. However, an advantage of the LUVET protocol is that very high lipid concentrations can be employed. This is demonstrated in Fig. 19 where the percentage of aqueous volume trapped inside the LUVETs is plotted against lipid concentration. Preparation of LUVETs at lipid concentrations of up to 300 μ moles/ml is quite possible, giving rise to a 30% trapping efficiency even though the trapped volume of the vesicles are only 1 μ l/ μ mole lipid. It is interesting to note that the freeze–thaw cycle only gives rise to significant increases in trapped volume per μ mol of lipid at lipid concentrations below 150 mg/ml. Similar types of observations have been reported elsewhere (Pick, 1981). It should be noted that the

Fig. 19. The trapping efficiency of LUVETs prepared without (●) and with (○) freeze-thawing. ^{14}C -inulin was used as a trap marker and LUVETs were prepared at various concentrations of EPC as described in section 3.2.



unilamellar nature (as determined by NMR and freeze-fracture techniques) of vesicles prepared at lipid concentrations greater than 50 $\mu\text{moles/ml}$ has not been well characterized.

3.3.2 Characterization of LUVETs with a membrane potential

The LUVET system as characterized above would appear to have a wide range of application due to the absence of contaminants (detergents, organic solvents), the ease of preparation and the generality and reproducibility of the technique. As an illustration of this utility, a simple model membrane system exhibiting a transmembrane potential $\Delta\psi$ has been developed and characterized. Reasons for such a choice include the demonstrated biological importance of $\Delta\psi$ in a variety of processes (see section 1.8) and the present lack of a well characterized unilamellar model system exhibiting a membrane potential, which would serve as an initial step in modelling the more complicated biological situation. For example, the potentials exhibited by biological membranes correspond to very large electric field gradients (a typical value of 100 mV corresponds to a transbilayer electric field of 250 kV/cm), which may be expected to influence the transmembrane distributions of charged lipid and protein components. A simple model system incorporating a membrane potential would provide an appropriate system for studying these interesting possibilities as is illustrated in the two subsequent chapters.

The particular model system characterized is a SPC LUVET preparation where Na^+/K^+ transmembrane chemical gradients (K^+ interior) are established by preparing the vesicles in a KCl buffer and then exchanging the untrapped KCl for a NaCl buffer by gel filtration. Questions addressed concern whether such systems exhibit a membrane potential in the absence of agents (valinomycin) to enhance K^+ permeability (see section 1.8), what the influence of valinomycin is, how the magnitude of $\Delta\psi$ is related to transmembrane Na^+/K^+ distributions and how the stability of the potential may be influenced by lipid composition. In order to quantify $\Delta\psi$ the radiolabelled lipophilic cation $[^3\text{H}]\text{-MTPP}^+$ was employed. This agent has been used extensively to obtain measures of $\Delta\psi$ in energized biological systems (Schuldiner and Kaback, 1975; Lichtshtein *et al.*, 1979; Young *et al.*, 1983).

As illustrated in Fig. 20, the LUVET preparations experiencing a transmembrane Na^+/K^+ chemical gradient (K^+ interior) do exhibit a membrane potential as detected by determination of outside and inside concentrations of $[^3\text{H}]\text{-MTPP}^+$. A $\Delta\psi$ of -20 mV (interior negative) is apparent at the first time interval (30 min). This $\Delta\psi$ gradually decreases to -30 mV over eight hours. It may be noted that the equilibrium distribution of MTPP^+ across the vesicle membranes was achieved within 10 min. As also indicated in Fig. 20, the Na^+/K^+ chemical gradients remain constant within the limits of experimental detection over the incubation period. This reflects the low permeability of these ions across the vesicle membrane (P value less than 10^{-10} cm/sec) and is consistent with previous observations (see section 1.8). The Na^+ influx into the SPC LUVETs remained below detection limits even after a 24 hr incubation at 20°C . These results indicate that a membrane potential is established in the SPC LUVET system in the presence of a transmembrane concentration gradient of Na^+/K^+ . This potential presumably arises from a difference in the permeability (P values) of SPC LUVETs to Na^+ and K^+ , which can create a diffusion potential if K^+ leaks out faster than Na^+ leaks in (see section 1.8 for details). This is consistent with the larger permeability coefficients observed for K^+ than for Na^+ in a variety of membrane systems (Jain and Wagner, 1980; Papahajopoulos and Bangham, 1966).

When the K^+ ionophore valinomycin is added to the SPC LUVET system with Na^+/K^+ chemical gradients, much different behaviour is observed as illustrated in Fig. 21. The (absolute) values of $|\Delta\psi|$ as reported by $[^3\text{H}]\text{-MTPP}^+$ are much larger (120 mV after 30 min incubation in the presence of valinomycin at 20°C), and $\Delta\psi$ decays fairly rapidly for longer incubation periods. In addition, this decay is accompanied by significant Na^+ influx and K^+ efflux. These results indicate that, as expected, valinomycin enhances the K^+ permeability and thus gives rise to larger (absolute) values of $|\Delta\psi|$ but also that valinomycin enhances the Na^+ permeability which results in dissipation of the K^+ electrochemical gradient as Na^+ leaks in.

In order to demonstrate that the values of $\Delta\psi$ reported by MTPP^+ reflect the K^+ diffusion potential generated, the potentials calculated from the measured interior and exterior

Fig. 20. Time course at 20°C of the membrane potential (\blacktriangle) and inside K^+ (\bullet) and Na^+ (\blacksquare) concentrations in soya PC LUVETs (20 μ mole lipid/ml) on application of a Na^+/K^+ chemical gradient (KCl interior; NaCl exterior). The gradient was established by preparing LUVETs in 150 mM KCl (pH = 7.0) and subsequent passage through a Sephadex G-50 desalting column equilibrated with 150 mM NaCl (pH = 7.0). The membrane potential was determined by measuring the transmembrane distribution of [3H]-MTPP (see section 3.2.6) whereas the interior Na^+ and K^+ concentrations were determined employing ^{22}Na and ^{42}K radioisotopes. Non-specific binding of the probe to LUVETs was measured in control experiments where K^+ was present inside and outside the vesicles, the experimental points were corrected accordingly.

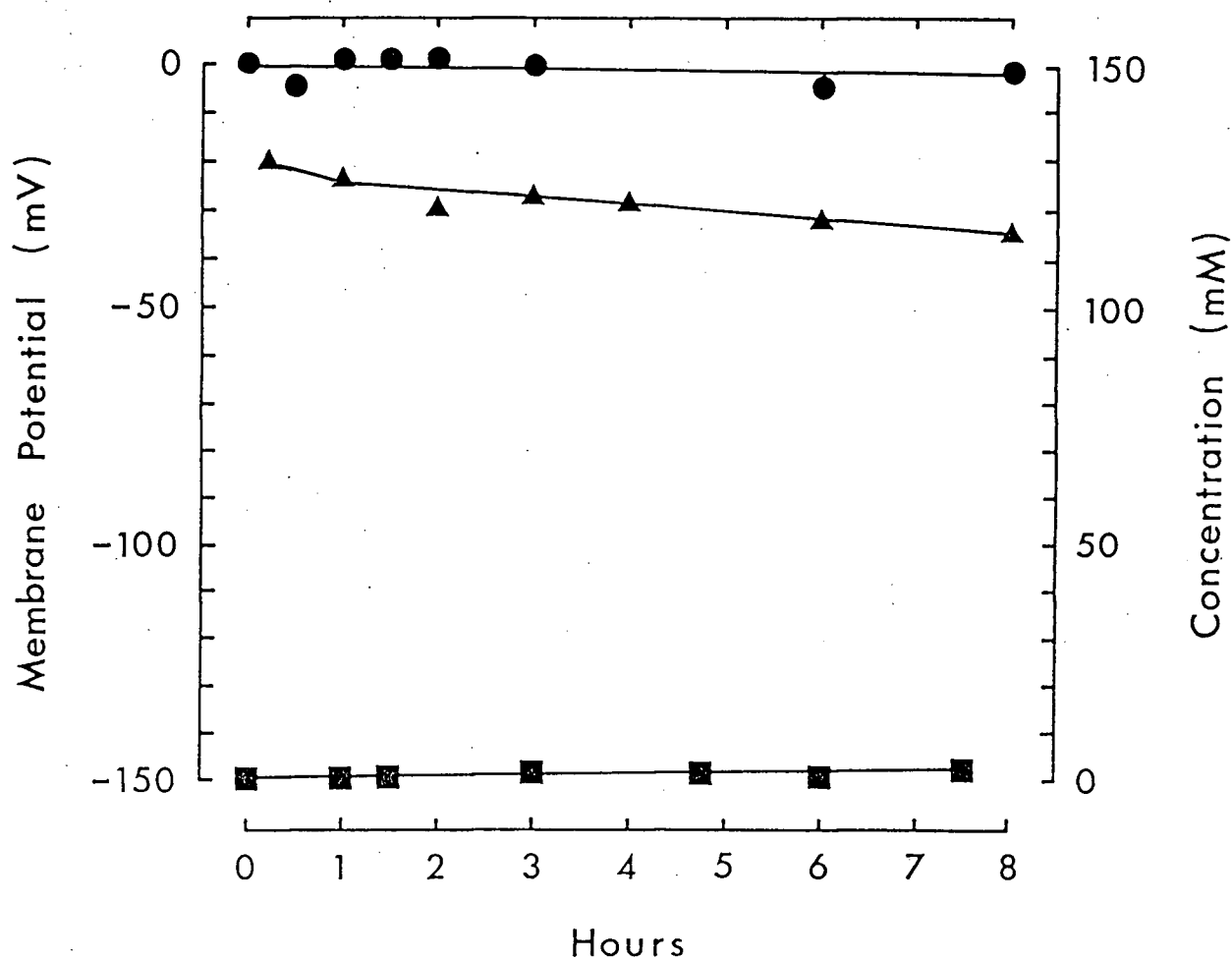
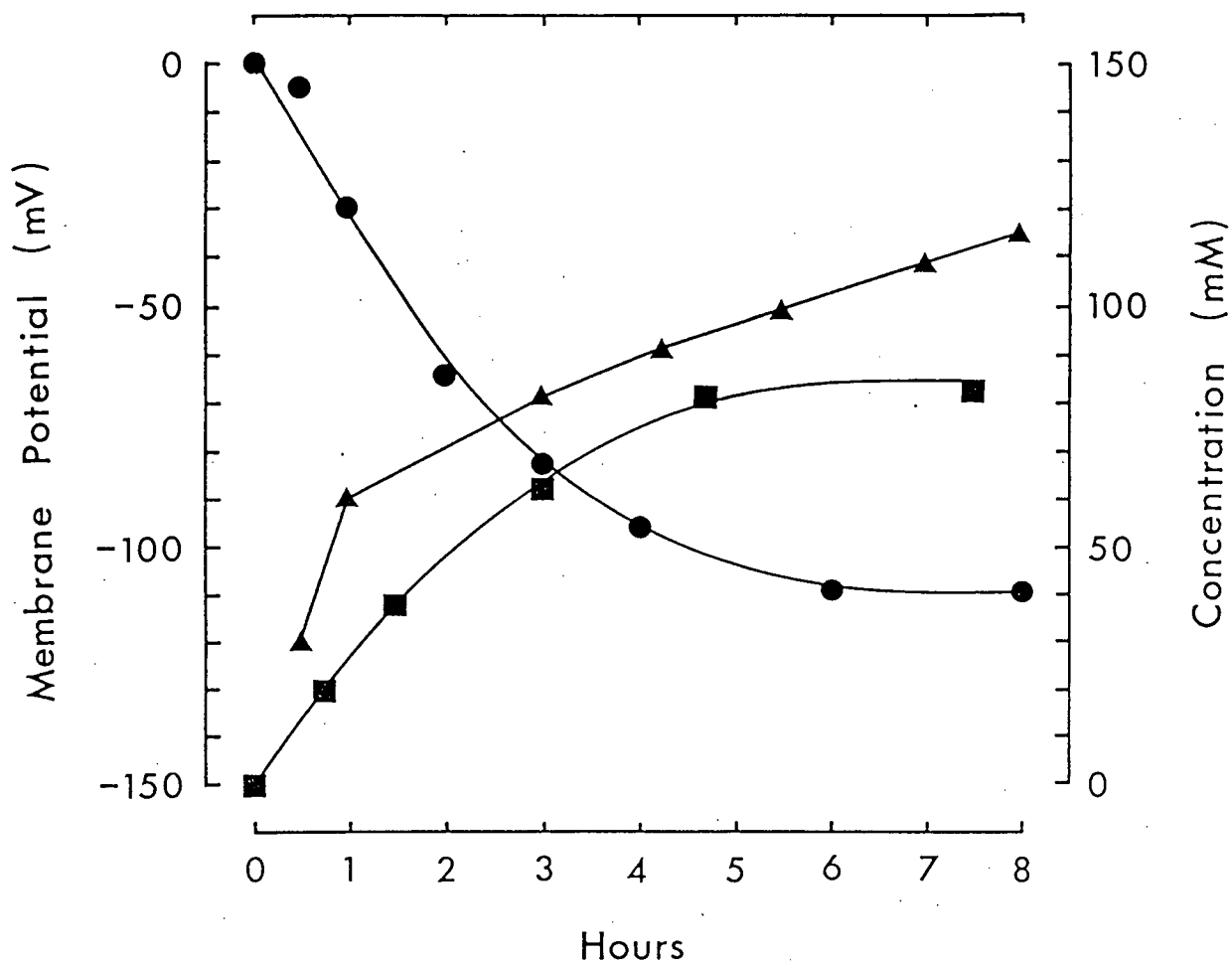


Fig. 21. Time course at 20°C of the membrane potential (▲), interior K⁺ (●) and Na⁺ (■) concentrations in soya PC LUVETs (20 μmole lipid/ml) on application of a Na⁺/K⁺ chemical gradient (KCl interior, NaCl exterior) and in the presence of valinomycin (1 μg/μmol phospholipid). For details see Fig. 20 legend.



concentrations of K^+ ($[K]_i$ and $[K]_o$) were determined employing ^{42}K as indicated in the section 3.2.6. As illustrated in Fig. 22, the values of $\Delta\psi$ obtained from both procedures are in good agreement and exhibit similar time dependent behaviour. This point is further emphasized by data illustrated in Fig. 23. Using $[^3H]$ -MTPP $^+$ to determine the valinomycin induced membrane potential exhibited by EPC LUVET systems (regular and freeze-thawed), one observes a reasonably close agreement between the value of $\Delta\psi$ calculated on the basis of known transmembrane K^+ distributions and the transmembrane distribution of $[^3H]$ -MTPP $^+$. There is some error observed at the high absolute values of $|\Delta\psi|$ (greater than 100 mV), mostlikely due to loss of MTPP $^+$ during separation on the Sephadex columns.

The inward and outward flux of Cl^- in these SPC systems was also characterized employing ^{36}Cl (see section 3.2.6). The permeability coefficients calculated from the observed influx and efflux of Cl^- are similar, P values of approximately 7.0×10^{-11} cm/sec, indicating that the transmembrane diffusion of Cl^- is electrically silent. It may be noted that the permeability coefficients for Cl^- are in close agreement with results obtained employing sonicated EPC vesicles (Toyoshima and Thompson, 1975) and EPC LUVs prepared by detergent dialysis employing octylglucoside (Mimms *et al.*, 1981), yet inconsistent with studies which have demonstrated rapid (P value of greater than 10^{-5}) transmembrane equilibration of Cl^- ions when the ion is present on both sides of the membrane (see section 1.8). Preliminary studies examining the permeability of H^+ in EPC LUVET systems indicate that this ion is not readily permeable across the vesicle bilayer, giving P values in the range of 10^{-11} to 10^{-14} cm/sec. Interpretation of these P values are complicated by the fact that these systems exhibit a H^+ diffusion potential (negative interior) which would be expected to decrease proton flux. This is indicated in Chapter 5 which demonstrates that a stable membrane potential can be established by a transmembrane H^+ ion gradient.

Fig. 22. Time course of the membrane potential as determined by [^3H]-MTPP $^+$ (■) and K^+ distribution (□) in soya PC LUVETs on application of a Na^+/K^+ transmembrane chemical gradient and subsequent introduction of valinomycin (see Fig. 20 legend and section 3.2.6 for details).

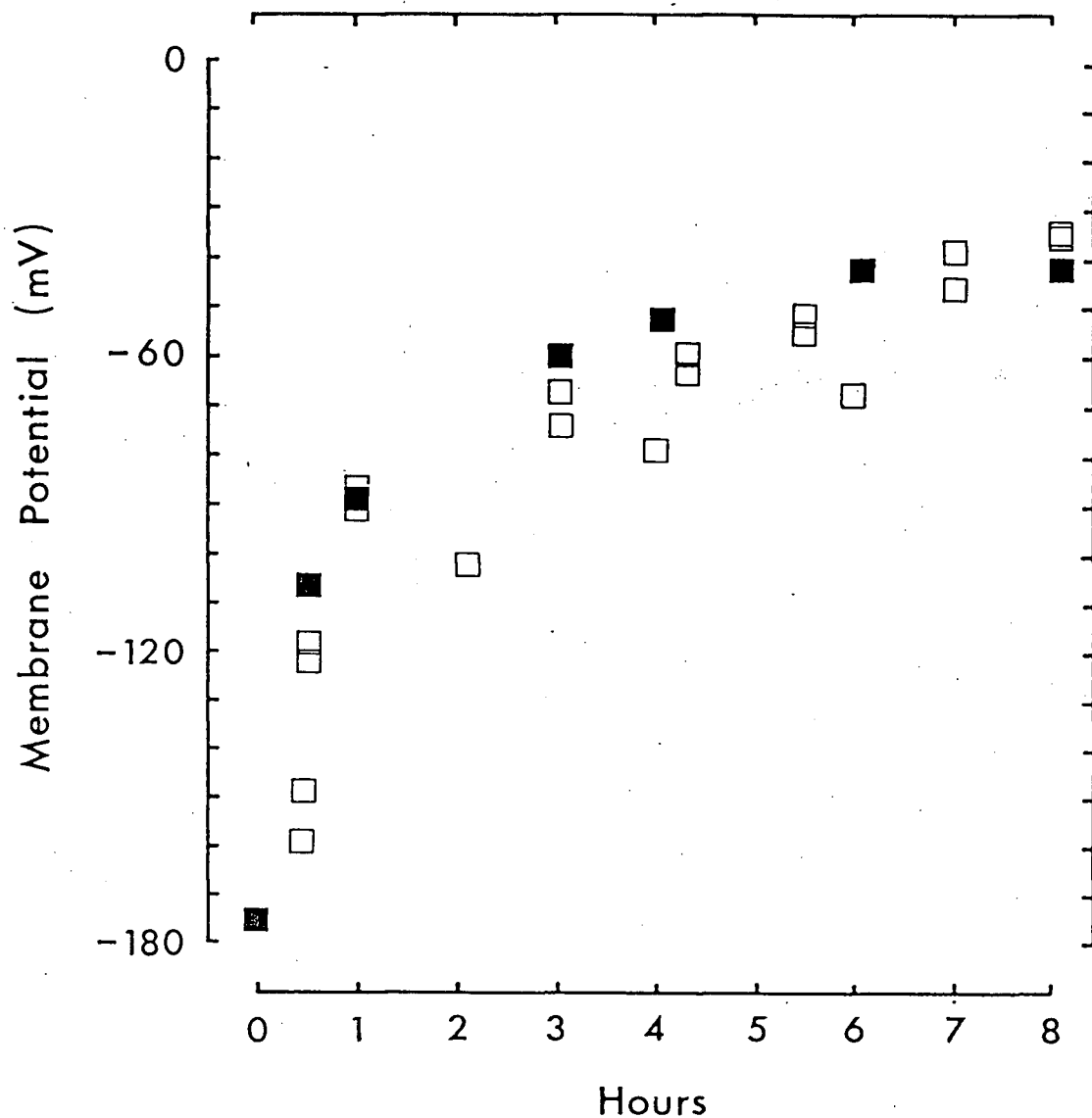
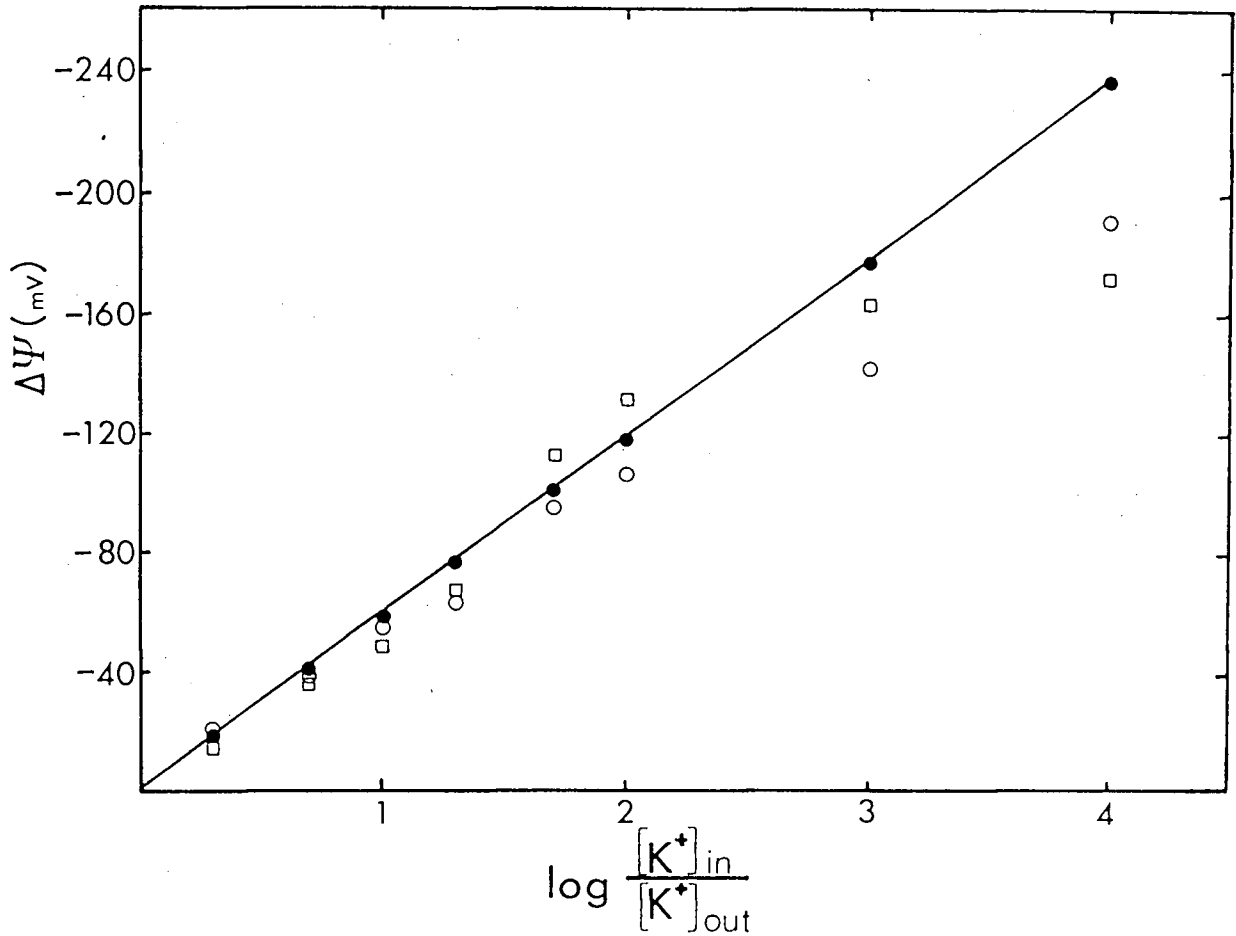


Fig. 23. Comparison between the membrane potentials obtained for various transmembrane K^+ chemical gradients as detected by $[^3H]$ -MTPP $^+$ for regular (\circ) and freeze-thawed (\square) LUVETs and the theoretical potentials (\bullet) predicted by the Nernst equation. EPC LUVETs were prepared in a K glutamate buffer (169 mM KGlu, 10 mM HEPES (pH = 7.5)), and the untrapped (exterior) buffer replaced by an isoosmotic NaCl buffer (150 mM NaCl, 10 mM HEPES (pH = 7.5)) containing various amounts of KGlu. The membrane potential $\Delta\psi$ was determined employing $[^3H]$ -MTPP $^+$ (see section 3.2.6) in the presence of valinomycin after a 6 hr incubation at 20°C to ensure an equilibrium transmembrane distribution of MTPP $^+$. The solid line indicates the theoretical potential given by the Nernst equation: $\Delta\psi$ (mV) = $-59 \log ([K]_i/[K]_o)$.



3.4 Discussion

This work presents a new procedure for generating large unilamellar vesicles which have been employed to develop a simple unilamellar system exhibiting a K^+ diffusion potential. The LUVET procedure per se will be discussed first and subsequently the utility of a model membrane exhibiting a well defined $\Delta\psi$ will be discussed.

The LUVET system obtained by extrusion of large multilamellar vesicles through polycarbonate filters of 100 nm pore size appear to possess significant advantages over LUV systems produced by other means. One of the most important is the absence of residual organic solvent or detergent. While it is arguable whether the low levels of such contaminants present after extensive dialysis significantly perturbs such properties as permeability and dynamic behaviour of component lipids, the situation is clearly less ambiguous when such agents are not present at all. In addition, in applications such as the generation of drug carrier systems, the total absence of these potentially toxic agents is obviously beneficial.

A second advantage of the LUVET procedure concerns the generality of the technique. All lipid systems thus far investigated, which give rise to large multilamellar vesicles on mechanical agitation (vortexing) in the presence of buffer, can subsequently be converted to LUVET form employing the extrusion procedure. Further, these systems exhibit a relatively constant size distribution and associated trapped volume, allowing direct comparisons of the properties of unilamellar systems with differing lipid compositions. These features, coupled with the ease and speed of preparation, the range of lipid concentrations that can be employed, the high trapping efficiencies that can be achieved and the relatively gentle nature of the procedure establish it as a most attractive protocol.

One drawback of the LUVET systems as detailed here, however, concerns the relatively low trapped volumes ($1-3 \mu l / \mu mol$ lipid) that can be achieved. Although high trapping efficiencies can be attained by increasing the lipid concentration, situations can be envisioned where it is desirable to employ unilamellar systems with increased trap to lipid ratios. In this regard preliminary studies on soya PC and egg PC systems show that a freeze-thaw of

LUVETs prepared by extrusion through the 0.1 μm pore size filters, followed by extrusion through filters with larger (0.2 μm) pore size results in larger systems with trapped volumes on the order of 10 $\mu\text{l}/\mu\text{mol}$ lipid.

The LUVET systems exhibiting a large membrane potential are an important step in achieving more sophisticated and accurate models of biological membranes and understanding the functional roles of individual components. Aside from obvious applications in examining possible roles of various lipid species (such as cholesterol) in the maintenance of $\Delta\psi$ as well as a simple test and calibration system for development of fast and accurate probes of membrane potential, this system exhibiting a $\Delta\psi$ should allow several aspects of membrane structure and function to be examined in a direct manner. Three examples include the influence of $\Delta\psi$ on transbilayer distribution of charged lipid and protein components, the role of membrane potential in protein insertion (Wickner, 1983; Zwizinski, 1983) as well as relationships between $\Delta\psi$ and certain membrane transport processes. With regard to the latter area, the massive uptake of safranin and other biologically relevant lipophilic cations (drugs and biogenic amines) into LUVET systems in the presence of a membrane potential has been demonstrated and is described in the following chapters. Finally, the application of a membrane potential or pH gradient to LUV systems reconstituted with specific membrane transport proteins could also provide simple assay procedures for transport mechanisms relying on K^+ or H^+ symport and antiport processes.

UPTAKE OF SAFRANINE AND OTHER LIPOPHILIC CATIONS INTO MODEL MEMBRANE SYSTEMS IN RESPONSE TO A MEMBRANE POTENTIAL†

4.1 Introduction

As shown in the previous chapter, membrane permeable lipophilic cations, such as $[^3\text{H}]\text{-MTPP}^+$, can be accumulated by cells or organelles exhibiting a membrane potential. Subsequent determination of the interior and exterior concentrations of these cations can allow estimates of $\Delta\psi$ to be made. In addition to MTPP, there are a variety of other probe molecules including those which exhibit optical and fluorescent responses (such as safranin O) when accumulated into the interior of the energized system. These agents have been utilized to determine $\Delta\psi$ in mitochondria and chloroplasts (Skulachev, 1971; Waggoner, 1979), vesicles derived from prokaryotic and eukaryotic membranes (Schuldiner and Kaback, 1975; Ramos *et al.*, 1979) as well as a variety of intact cells (Lichtshtein *et al.*, 1979; Young *et al.*, 1983).

An interest in this uptake of lipophilic cations was stimulated by two observations. First, the accumulation of these components by energized systems can result in substantial differences between the concentrations of the probes in the external and internal compartments. A membrane potential of -100 mV as detected by MTPP^+ , for example, reflects an interior probe concentration which is 50 times higher than in the external environment. As the redistributions of the probes across the membranes can occur within minutes, it is clear that accumulation of lipophilic cations in response to $\Delta\psi$ reflects a rather effective membrane transport process. Second, a large variety of biologically active agents such as certain biological amines and many drugs are essentially lipophilic cations. Thus processes involved in the uptake of lipophilic cations employed as membrane potential probes may well be of more general significance to metabolite and drug distributions *in vivo*.

† This chapter has been based on the references Bally *et al.* (1984), Mayer *et al.* (1984a), and Mayer *et al.* (1984b).

In this work the ability of LUVET systems to accumulate selected lipophilic cations in response to a membrane potential, is characterized with three objectives in mind. First, to show that the large changes in absorbance observed on accumulation of optical probes such as safranin in biological preparations can also be observed in model systems exhibiting a $\Delta\psi$, and to characterize the mechanisms involved. Second, as usually employed, probes of membrane potential are present at as low levels as possible to avoid perturbing the electrochemical gradient giving rise to $\Delta\psi$. From the transport point of view, it is of interest to determine whether higher exterior concentrations can lead to high absolute concentrations of probe accumulated in the vesicle interior. Finally, to determine whether representative drugs can also be accumulated by vesicles exhibiting a membrane potential, which may provide information regarding the non-specific uptake and distribution of these agents *in vivo*.

It is demonstrated that the safranin optical response can be observed for egg phosphatidylcholine (EPC) vesicle systems exhibiting a K^+ diffusion potential, and that the marked absorbance changes observed appear to correspond to precipitation of the dye in vesicle interior. Further, both safranin and $MTTP^+$ can be concentrated to high levels (greater than 75 mM) in the vesicle interior for initial exterior concentrations in the range 1–2 mM. Finally, it is shown that a variety of different classes of drugs, including the local anaesthetics chlorpromazine and dibucaine, the adrenergic blocking agent propranolol, and the anticancer drugs vinblastine and adriamycin, can also be accumulated into model membrane vesicle systems in response to $\Delta\psi$.

4.2 Materials and Methods

4.2.1 Materials

Egg phosphatidylcholine (EPC) and soya PC (SPC) were isolated from hen egg yolk and crude soya lecithin (Sigma) respectively employing procedures described in chapter 2. Egg phosphatidylserine (EPS) was obtained from EPC utilizing the headgroup exchange capacity of

phospholipase D (see section 2.2.1). Cholesterol, MTPPBr, chlorpromazine, dibucaine, propranolol, vinblastine, valinomycin and HEPES buffer were obtained from Sigma. Safranin O was obtained from MCB whereas methoxy [^{14}C]-inulin and [^3H]-methyltriphenylphosphonium iodide (^3H -MTPP $^+$) were obtained from NEN (Canada) and ^{42}KCl from Amersham. Adriamycin was the generous gift of Dr. A.C. Eaves. For ease of reference, the structures of safranin, MTPP $^+$, chlorpromazine, dibucaine, propranolol, adriamycin and vinblastine are given in Fig. 24. All lipids employed were more than 99% pure as determined by TLC, and all other reagents were employed without further purification.

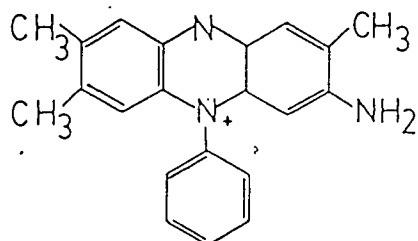
4.2.2 Vesicle preparation

Vesicles were prepared according to the LUVET procedure detailed in the preceding chapter which involved hydration of a dry lipid film to produce large multilamellar vesicles (50–100 μmol phospholipid/ml) which were subsequently extruded 10 times through two (stacked) polycarbonate filters with 100 nm pore size (Nucleopore). Lipids were hydrated in either the potassium glutamate (KGlu) and NaCl buffers contained 20 mM HEPES adjusted to pH 7.5 employing NaOH (final Na $^+$ concentration 10 mM) and were adjusted to a common osmolarity of 310 mOsm/kg (NaCl concentration 150 mM, KGlu concentration 169 mM).

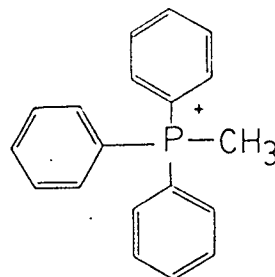
4.2.3 Generation of a membrane potential

Transmembrane Na $^+$ –K $^+$ chemical gradients (K $^+$ inside) were generated by forming LUVETs in the KGlu buffer and subsequently exchanging the untrapped KGlu for NaCl employing a Sephadex G–50 column. Defined K $^+$ gradients were generated by pre-equilibrating the G–50 columns with isoosmotic NaCl buffers containing the appropriate concentration of KGlu. Where employed, the K $^+$ ionophore valinomycin was added to achieve a concentration of 0.5 $\mu\text{g}/\mu\text{mol}$ lipid.

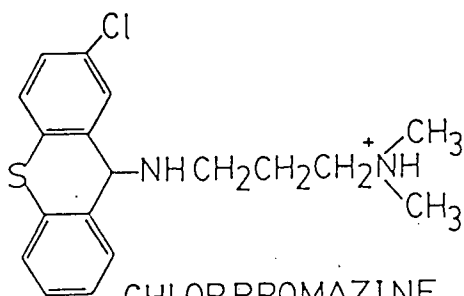
Fig. 24. Structures of safranine, methyltriphenylphosphonium (MTPP⁺), chlorpromazine, dibucaine, propranolol, vinblastine, and adriamycin.



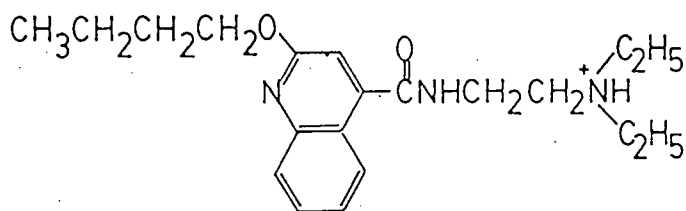
SAFRANINE



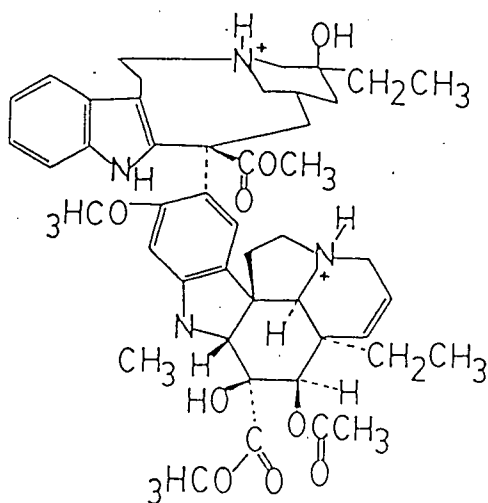
METHYLTRIPHENYLPHOS-
PHONIUM



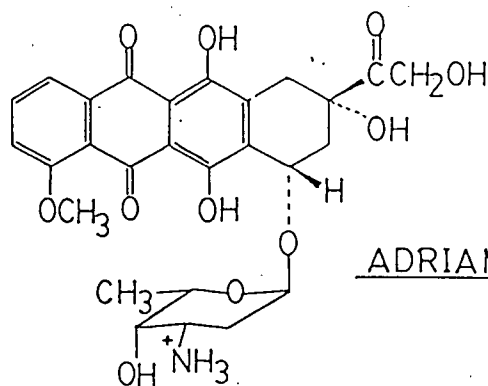
CHLORPROMAZINE



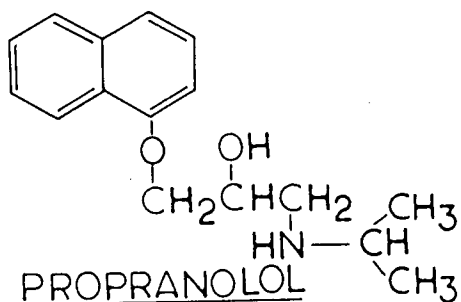
DIBUCAINE



VINBLASTINE



ADRIAMYCIN



PROPRANOLOL

4.2.4 Uptake of safranine

The uptake of safranine was (qualitatively) monitored spectrophotometrically over the interval 560–460 nm employing a Pye Unicam SP8–200 spectrophotometer (see Fig. 25 and related text). The actual amount of safranine accumulated was determined quantitatively by adding safranine from a saturated (96.8 mM at 20°C) stock solution to a LUVET dispersion (2–10 μmol lipid/ml) to achieve a 2 mM safranine concentration. Subsequently, at appropriate time intervals, the unsequestered dye was removed by passing aliquots of the vesicles through small (1 ml) Sephadex G–50 columns, and aliquots of the effluent were mixed with 0.5% (w/v) Triton X–100 to disrupt the vesicles and release sequestered safranine. Safranine concentrations were then determined from the absorbance at 516 nm, and the phospholipid phosphorus assayed by the technique described 3.2.3.

4.2.5 Determination of membrane potential and K^+ efflux

Membrane potentials were determined employing [^3H]-MTPP $^+$ (see section 3.2.6) and the efflux of K^+ measured employing ^{42}K in combination with the ultrafiltration technique described in the preceding chapter (see section 3.2.6).

4.2.6 Uptake of assorted drugs

Uptake of chlorpromazine, dibucaine, propranolol, vinblastine, and adriamycin was determined quantitatively employing similar procedures as for safranine. Accumulation of chlorpromazine was monitored in a system containing 200 μM chlorpromazine (containing 2 $\mu\text{Ci/ml}$ [^3H]-chlorpromazine) which was added to EPC LUVETs (1 μmol phospholipid/ml). After various incubation times, the vesicles were separated from unsequestered chlorpromazine (employing 1 ml Sephadex G–50 columns). The effluent was counted to assay for chlorpromazine and phospholipid was assayed as described previously (Ames and Dubin, 1960). Dibucaine uptake was measured in a system which contained 100 μM dibucaine and 1 mM phospholipid. The vesicle associated dibucaine was measured fluorometrically (excitation, 330nm;

emission, 416 nm) employing a Perkin-Elmer 650-10S fluorescent spectrophotometer after disruption of the vesicles in 0.5% Triton X-100. Accumulated propranolol was also assayed fluorometrically (excitation, 292 nm; emission, 337 nm) after the vesicles (1 mM) were incubated for various times with 200 μ M propranolol. In the case of vinblastine and adriamycin, vesicles (1 mM) were incubated with a 200 μ M solution of the respective drug, and the LUVET associated adriamycin and vinblastine were assayed (after disruption with 0.5% Triton X-100 or 93% (v/v) ethanol) spectrophotometrically at 480 nm and 265 nm, respectively.

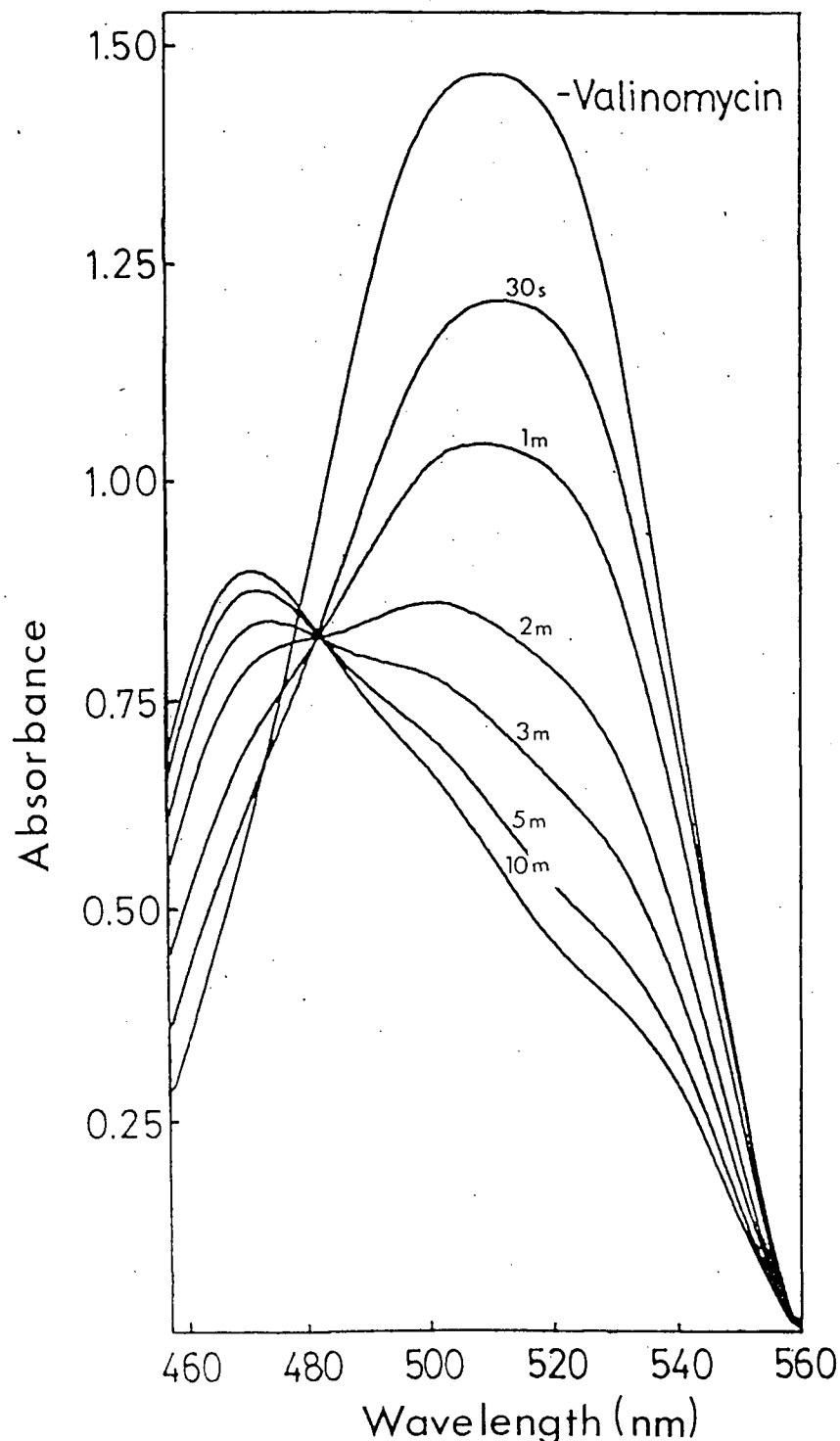
4.3 Results

4.3.1 Characterization of safranine accumulation by LUVETs

Large absorbance changes can occur when safranine is incubated in the presence of energized biological systems such as mitochondria (Colonna *et al.*, 1973) and vesicles derived from *E. coli* membranes (Schuldiner and Kaback, 1975). Such a "safranine response" has been correlated with the presence of a membrane potential $\Delta\psi$. This response can also be observed for EPC LUVET systems experiencing a K^+ diffusion potential induced by valinomycin as illustrated in Fig. 25. The addition of valinomycin to LUVETs prepared with asymmetric Na^+-K^+ transmembrane distributions (K^+ inside) and incubated in the presence of safranine results in a marked time dependent decrease in absorption in the region of 516 nm, which is combined with a shift in the absorbance maximum (λ_{max}) from 516 to 472 nm. The change in the absorbance at 516 nm (ΔA_{516}) is essentially complete after 20 min and the situation is then relatively stable as ΔA_{516} decreased by less than 20% over a 24 hr time course (results not shown).

As may be expected, the extent of the absorbance changes associated with the safranine response were found to be sensitive to the vesicle and safranine concentrations employed. In order to determine optimum conditions, the (normalized) absorbance changes were monitored as a function of safranine concentration for a fixed vesicle concentration corresponding to 0.5 mM phospholipid. As indicated in Fig. 26, the normalized optical

Fig. 25. Spectrophotometric response observed for safranin incubated at 20°C in the presence of EPC LUVETs exhibiting an electrochemical Na⁺/K⁺ gradient (K interior) in the presence of valinomycin. The LUVETs were prepared in the KGlu buffer, and the untrapped buffer exchanged for the NaCl buffer as described in section 4.2.2. Subsequently the vesicles were diluted to achieve a concentration of 0.5 mM phospholipid in 3 ml of NaCl buffer which contained 60 μM safranin. Spectra were taken before (upper trace) and at various times (in seconds(s) and minutes(m)) after the addition of valinomycin (0.5 μg/μmole phospholipid).



response then exhibits a maximum in the region of 60 μ M safranin. Other investigators (for review see Zanotti and Azzone, 1980) have suggested that the safranin response arises from active uptake of safranin followed by a membrane associated "stacking" phenomenon, which gives rise to the observed absorbance changes. This process (which, as indicated below, appears to correspond to precipitation of safranin in the vesicle interior) could explain the behaviour noted in Fig. 26. At low safranin concentrations the dye concentrations achieved in the vesicle interior may not be sufficient to result in precipitation or "stacking", whereas at higher exterior safranin levels, the spectral response for accumulated material will be swamped by the absorption from excess exterior safranin.

The results of Figs. 25 and 26 are consistent with an accumulation of safranin into the EPC LUVET system which is driven by a K^+ diffusion potential. It is of interest to quantify the extent of safranin uptake in response to a given $\Delta\psi$. Two situations were investigated; first, where the safranin was in excess so that the maximum levels of accumulated safranin could be characterized, and second, where the safranin was limiting, therefore allowing a determination of the efficiency of the trapping process. Briefly, LUVETs were prepared with varying transbilayer K^+ concentration gradients which give rise to corresponding variations in the $\Delta\psi$ obtained on addition of valinomycin (see 3.3.2, Fig. 23). These vesicles were incubated for 30 min in the presence of valinomycin and 0.05 μ mol safranin per μ mol phospholipid (safranin limiting) or 0.2 μ mol safranin per μ mol phospholipid (safranin in excess). The untrapped safranin was then removed by passing the vesicles over a Sephadex G-50 column (see section 4.2.4). Determination of the vesicle-associated safranin per μ mol phospholipid resulted in the data shown in Fig. 27, which leads to two conclusions. First, when the amount of safranin is limiting, vesicle-associated safranin reaches levels in excess of 0.04 μ mol safranin per μ mol phospholipid for $\Delta\psi$ greater than 80 mV (interior negative) indicating trapping efficiencies in excess of 80%, with a resulting transmembrane safranin gradient in excess of 500 fold. Second, when safranin is in excess, extremely high levels of accumulated safranin can be achieved (greater than 0.12 μ mol safranin per μ mol phospholipid). Given the measured

Fig. 26. Influence of increasing safranin concentrations on the (normalized) safranin response obtained in the presence of EPC LUVET systems (0.5 mM phospholipid). The LUVET systems were prepared with Na^+/K^+ electrochemical gradients as indicated in the legend to Fig. 25 (and section 4.2.4) and the normalized safranin response ($\Delta A_{516}^{\text{max}}/A_{516}^0$) is measured as the difference between the initial absorbance (A_{516}^0) at 516 nm (before the addition of valinomycin) and the absorbance observed 20 min after the addition of valinomycin divided by A_{516}^0 .

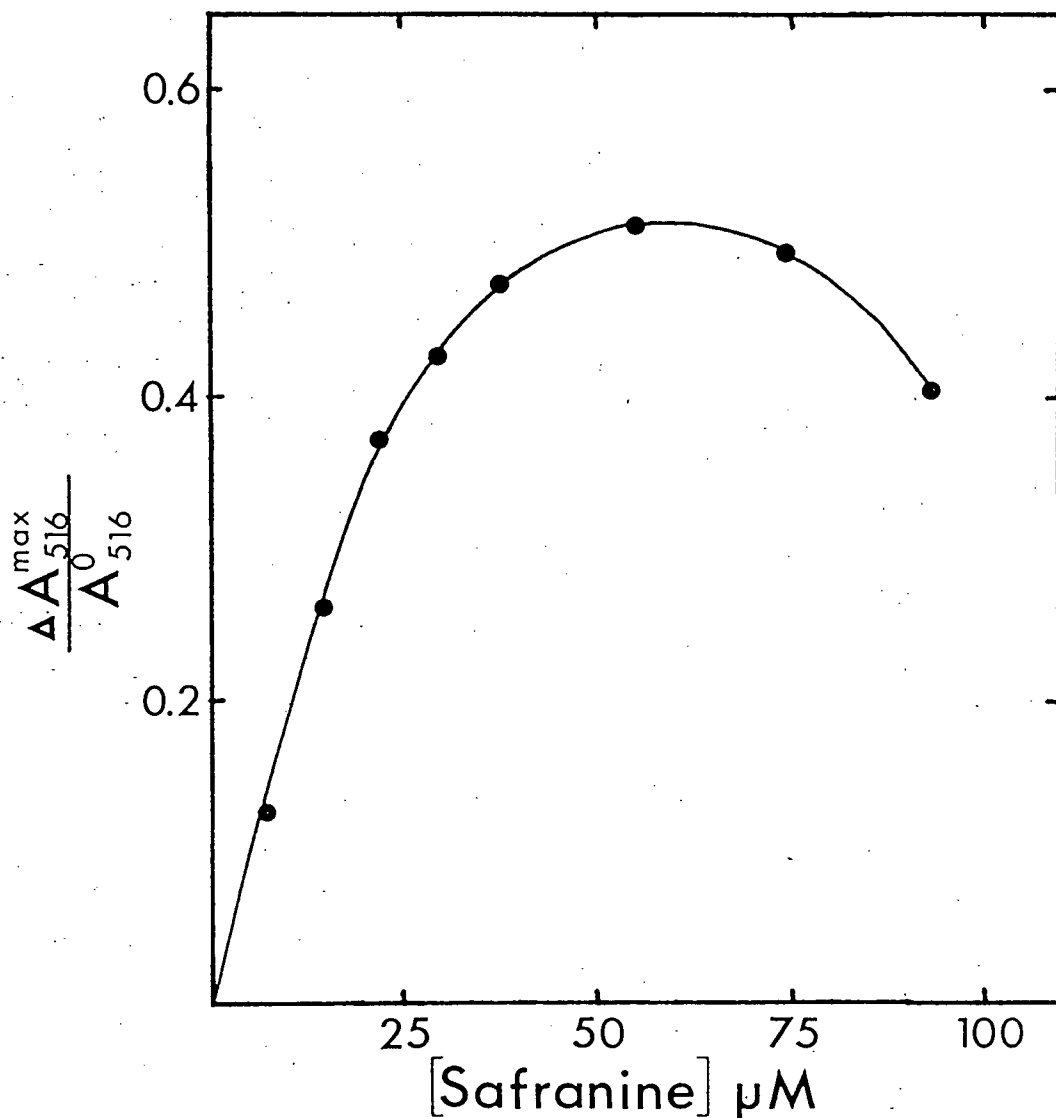
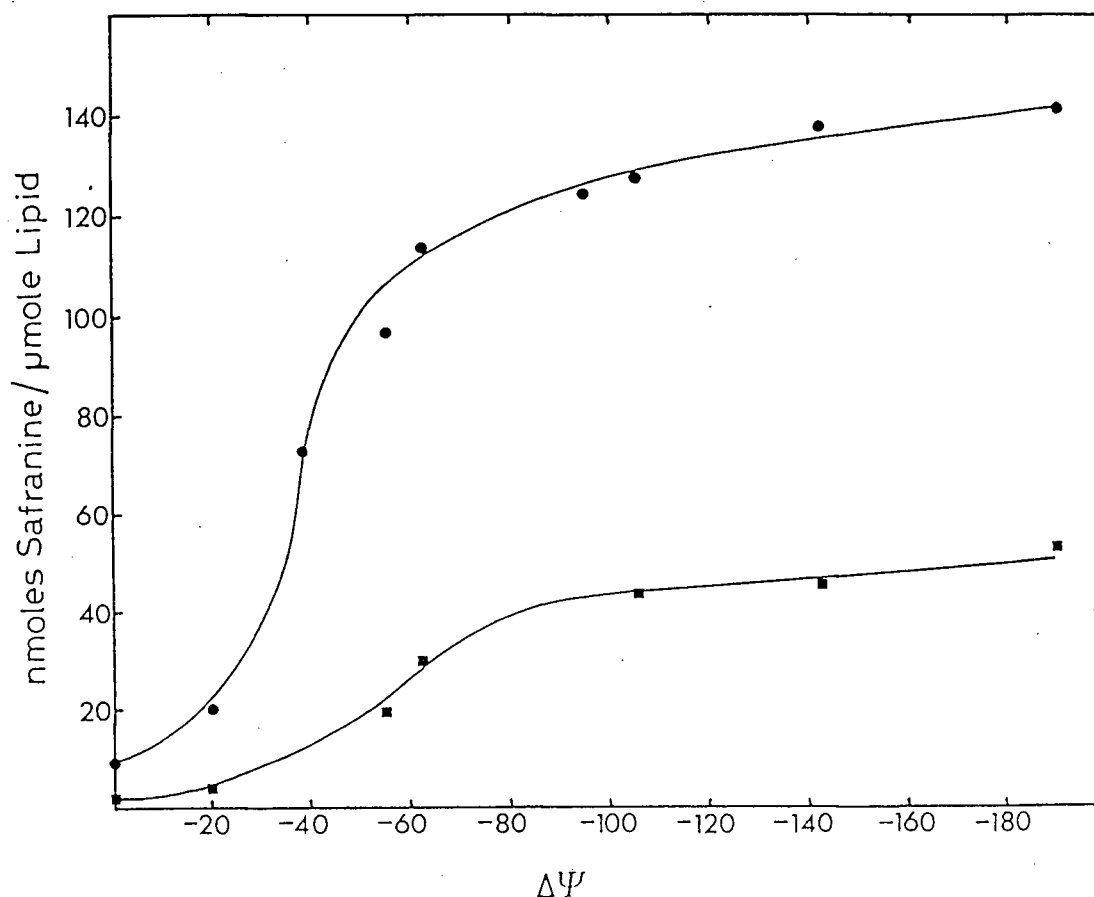


Fig. 27. Levels of LUVET associated safranin obtained as a function of (initial) transmembrane potential $\Delta\psi$. The vesicles were prepared from EPC dispersed in the KGlu buffer, and the external medium was replaced by a NaCl buffer containing various concentrations of KGlu (see legend of Fig. 23) to establish a range of K^+ gradients. The membrane potential $\Delta\psi$ developed in the presence of valinomycin was assayed employing $[^3H]$ -MTPP $^+$ (see section 3.2.6). Subsequently, the amount of safranin accumulated by the LUVETs 30 min after incubation in $0.2 \mu\text{mol safranin}/\mu\text{mol lipid}$ (●) and $0.05 \mu\text{mol safranin}/\mu\text{mol lipid}$ (■) in the presence of valinomycin was monitored as described in section 4.2.4. In the case of the system containing $0.2 \mu\text{mol safranin per } \mu\text{mol lipid}$ the safranin was in excess (not all of it could be accumulated by the LUVET systems) whereas at $0.05 \mu\text{mol safranin per } \mu\text{mol phospholipid}$ the amount of safranin available limited the uptake.



trapped volumes ($1.5 \mu\text{ l} / \mu\text{ mol}$ phospholipid) of these LUVET systems, this indicates interior safranin concentrations of 100 mM or more. As a saturated solution of safranin at 20°C is 96.2 mM , this suggests that the marked changes in safranin absorption result from precipitation of the dye in the vesicle interior. In order to determine whether this may be the case, the safranin response ($\Delta A_{516\text{max}}$) was measured for LUVETs with various transmembrane K^+ gradients (as for Fig. 27, $0.2 \mu\text{ mol safranin} / \mu\text{ mol phospholipid}$) allowing a correlation to be obtained between $\Delta A_{516\text{max}}$ and the amount of safranin accumulated. As indicated in Fig. 28(a), a dramatic increase in $\Delta A_{516\text{max}}$ occurs for amounts of vesicle-associated safranin corresponding to interior concentrations of 100 mM or more. This is clearly consistent with the proposal that the safranin response reflects a precipitation of safranin inside the vesicles, and results in a non-linear relation between ΔA_{516} and (Fig. 28(b)).

It is useful to characterize the stability of the vesicle systems containing high levels of safranin. A LUVET preparation (K^+ inside) was incubated in the presence of safranin ($0.2 \mu\text{ mol safranin} / \mu\text{ mol phospholipid}$) and valinomycin, and the amount of vesicle associated safranin determined at various time intervals. As shown in Fig. 29, the safranin accumulated in the presence of valinomycin reaches a plateau after 2 hr and remains constant at $0.14 \mu\text{ mol safranin per } \mu\text{ mol phospholipid}$ for 8 hr or more. It is interesting to note that significant safranin uptake is achieved, albeit at a much slower rate, in the absence of valinomycin. Accumulation of lipophilic cations such as safranin likely proceeds in exchange for an efflux of K^+ (Harris and Baum, 1980), and thus the slow valinomycin independent uptake may arise in response to passive efflux of K^+ .

To further characterize the relation between safranin uptake and K^+ efflux, the release of K^+ from vesicles on uptake of safranin was monitored employing the radioisotope ^{42}K . As illustrated in Fig. 30, limited release of K^+ is observed on addition of valinomycin which arises in response to valinomycin-facilitated influx of Na^+ (see Fig. 21 previous chapter). The subsequent addition of safranin results in a rapid release of the remaining entrapped K^+ , and the time course of this release is similar to that observed for safranin uptake (Fig. 29).

Fig. 28. Magnitude of the maximum safranin response (ΔA_{516}^{\max}) as: (A) a function of the internal concentration of safranin inside EPC LUVETs and (B) as a function of the membrane potential measured from a known K^+ diffusion potential (see Fig. 23 previous chapter). The system of Fig. 27 containing $0.2 \mu\text{mol}$ safranin per μmol phospholipid was employed in both cases and the ΔA_{516}^{\max} determined 30 min after addition of valinomycin. The safranin concentration inside the vesicles was calculated from the results of Fig. 27 employing a measured trapped volume of $1.15 \mu\text{l}/\mu\text{mol}$ phospholipid.

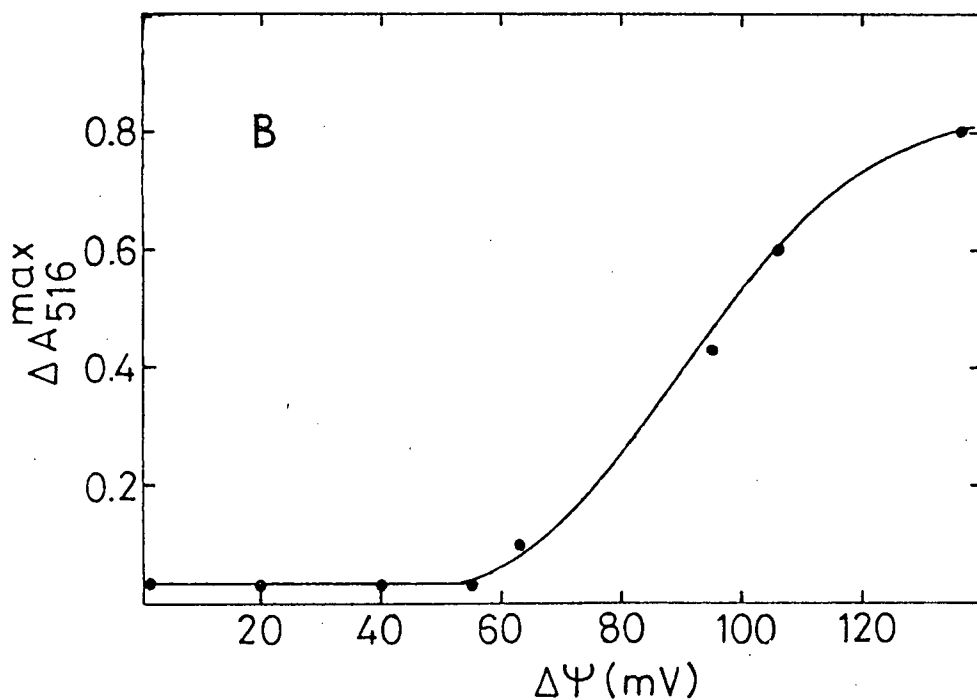
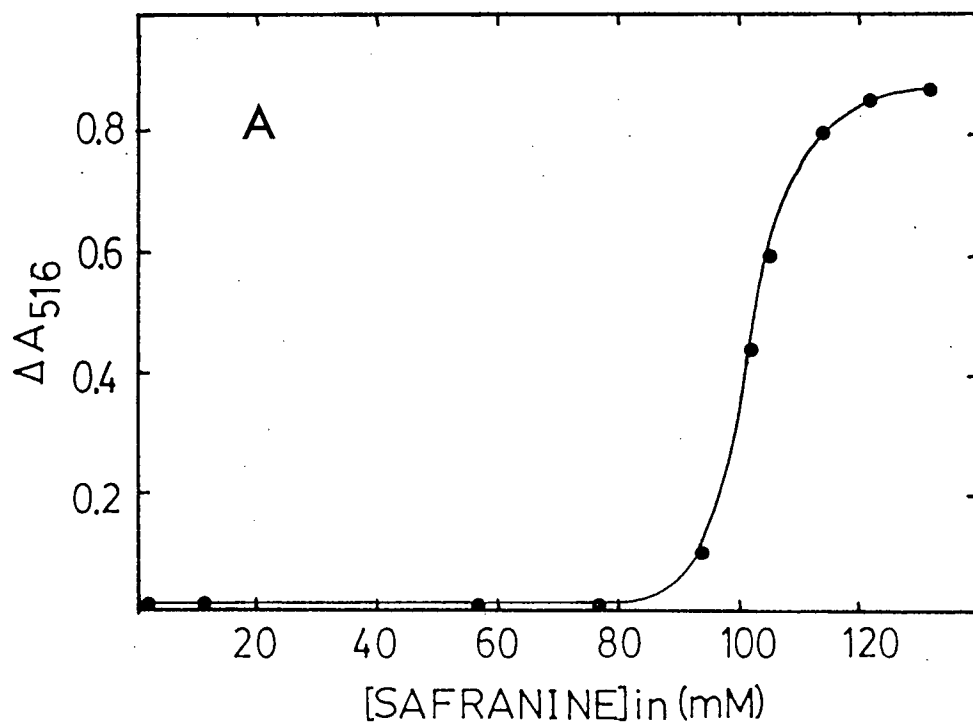


Fig. 29. Time course for accumulation of safranin by EPC LUVET systems experiencing a Na^+/K^+ transmembrane electrochemical gradient (prepared as described in the legend of Fig. 25) in the presence (●) and absence (■) of valinomycin ($0.5 \mu\text{g}/\mu\text{mol}$ phospholipid). The safranin taken up into the vesicles was determined by removing untrapped safranin on a gel filtration column (see section 4.2.4). The open symbols indicate background uptake in the absence of an electrochemical gradient (KGlu buffer on both sides of the membrane) and in the presence (○) and absence (□) of valinomycin.

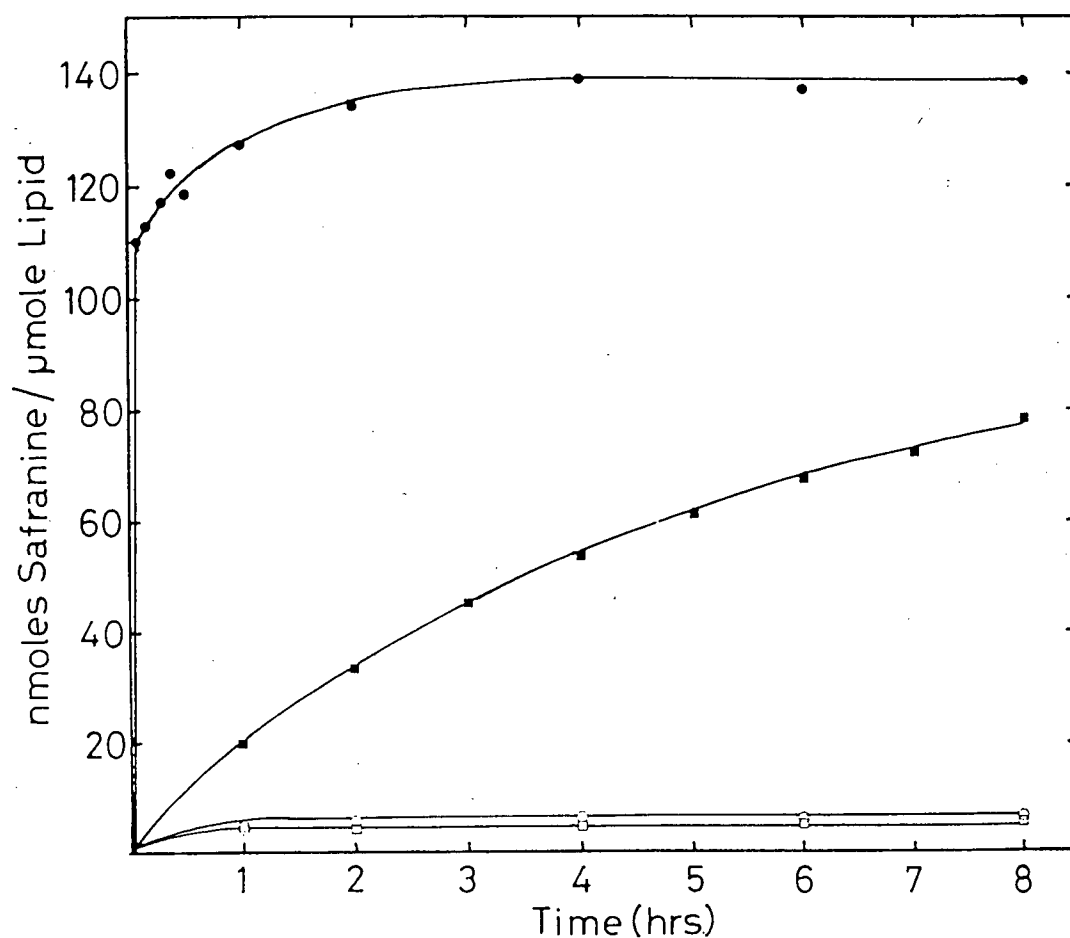
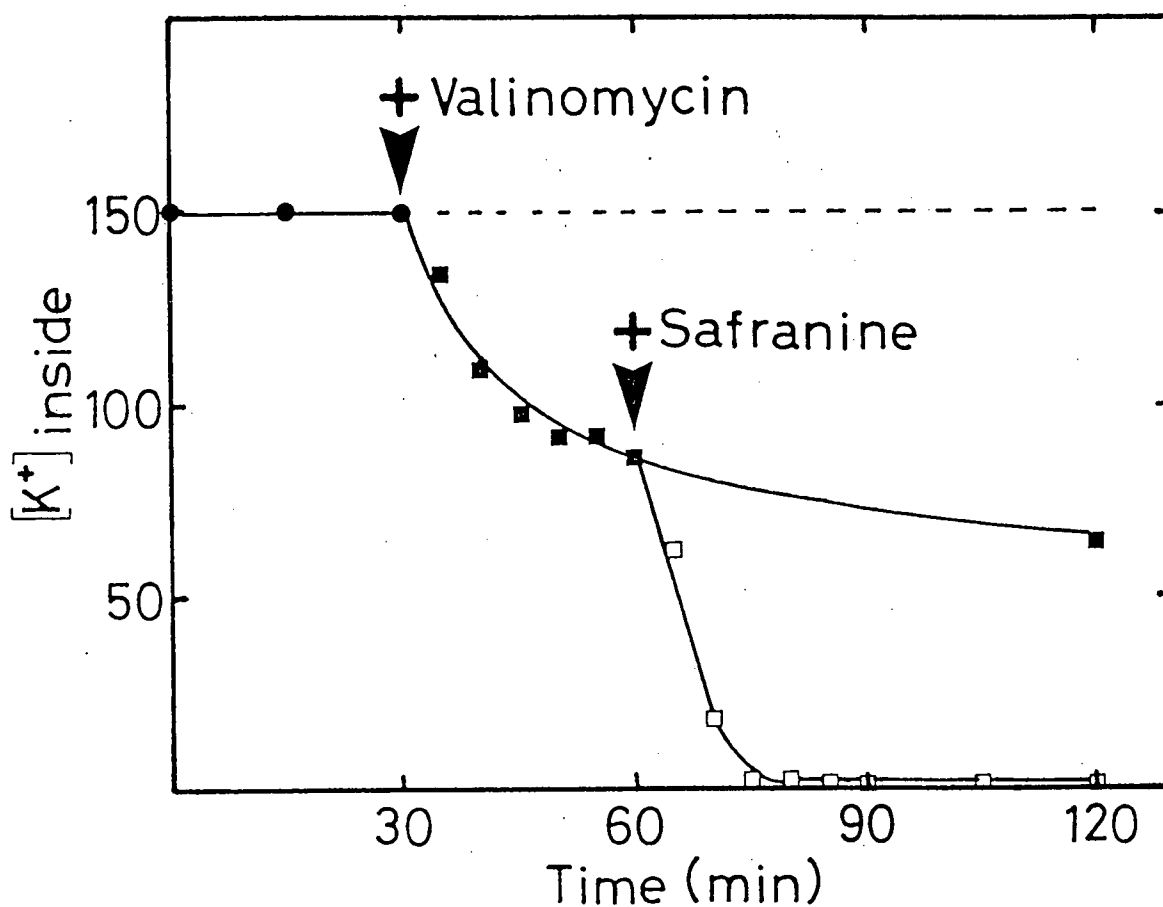


Fig. 30. Demonstration of K^+ release from EPC LUVETs on addition of safranin. The LUVETs were prepared in the presence of ^{42}KCl where the untrapped buffer was replaced by the NaCl buffer, and were subsequently incubated in an Amicon ultrafiltration cell in the presence of valinomycin as indicated in section 3.2.6. The $^{42}K^+$ released from the vesicles was determined in the filtered eluate from the ultrafiltration cell by scintillation counting. This eluate did not contain measurable levels of phospholipid.



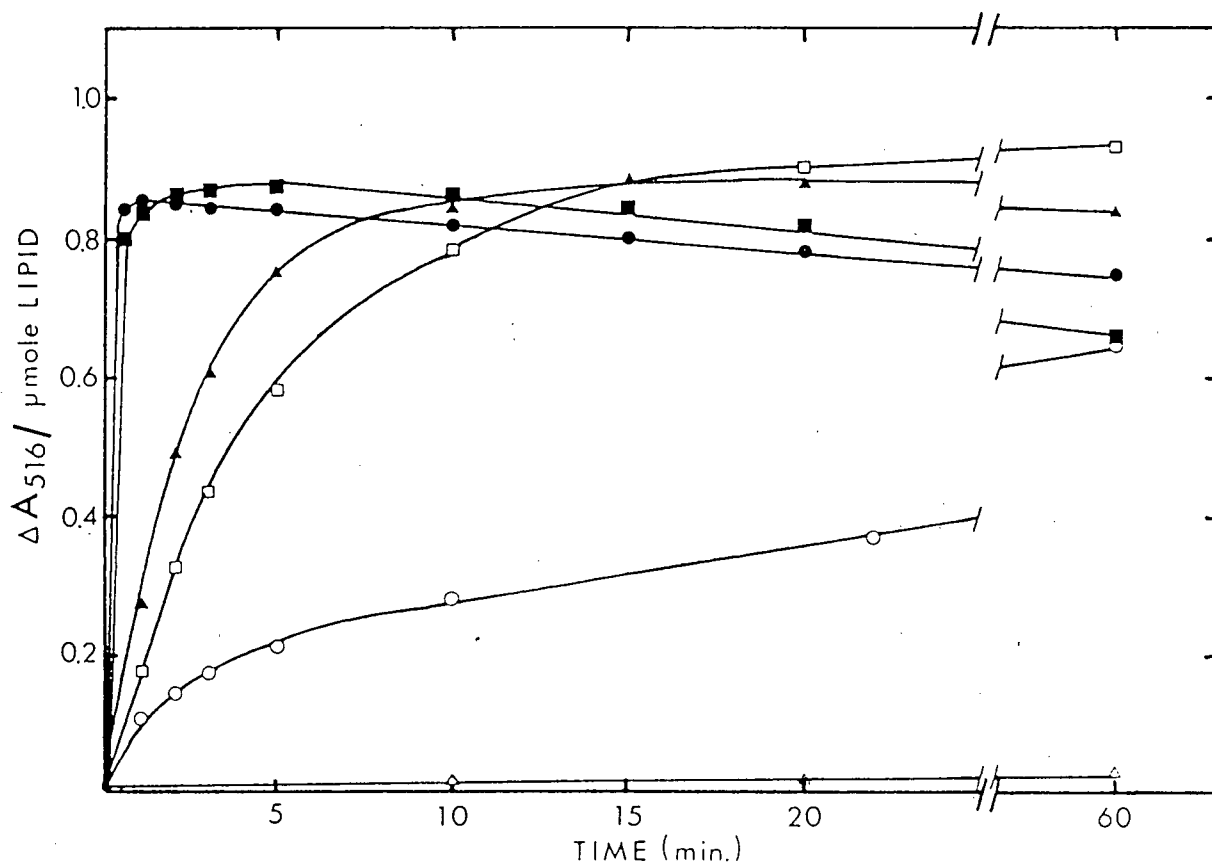
These observations are consistent with a safranin uptake mechanism which involves an electroneutral safranin- K^+ exchange process.

The results presented to this stage establish that EPC LUVETs exhibiting a K^+ diffusion potential accumulate the lipophilic cation safranin in a manner which is consistent with a safranin- K^+ transmembrane exchange mechanism. In order for this to occur the safranin and the K^+ -valinomycin complex must traverse the hydrocarbon region, suggesting that such transport should be sensitive to the acyl chain composition and "order" in the acyl chain region (see section 1.5). That this is the case is illustrated in Fig. 31 for LUVETs composed of SPC, EPC in the presence of varying amounts of cholesterol, and EPC/PS (1:1) mixtures. Uptake into the relatively unsaturated SPC system (soya PC is considerably more unsaturated than egg PC, due to the high content of linoleic acid in soya PC (Tilcock and Cullis, 1981)) is faster than for the more saturated EPC LUVET system and the additional presence of cholesterol results in a progressive inhibition of safranin accumulation. At equimolar cholesterol levels little or no uptake occurs within 1 hr at 20°C. This inhibition could result from a decreased permeability of safranin or a reduced effectiveness of the K^+ ionophore in less fluid membranes. Further, the presence of the (negatively charged) egg phosphatidylserine (PS) enhances the redistribution of safranin, possibly arising from an increased partitioning of the safranin into the lipid bilayer.

4.3.2 Uptake of methyltriphenylphosphonium (MTPP⁺)

The results obtained for safranin uptake into model membrane systems exhibiting a K^+ diffusion potential show that safranin can be efficiently accumulated to high levels into the vesicle interior. It is important to determine how general these findings are, and therefore the $\Delta\psi$ -dependent uptake of a variety of other lipophilic cations has been characterized. Initially MTPP⁺ was investigated because transmembrane redistributions of this agent in radiolabelled form ($[^3H]$ -MTPP⁺) can be detected for very low concentrations (2×10^{-8} M). This leads to minimal perturbations of the electrochemical gradients giving rise to $\Delta\psi$, and has therefore been utilized to obtain quantitative measures of $\Delta\psi$ in energized membrane

Fig. 31. Influence of lipid composition on the safranin response (ΔA_{516} max measured as the difference in absorbance at 516 nm between the spectrum obtained at zero time and the spectrum obtained at various times after addition of valinomycin. All vesicle systems were prepared and spectra recorded under conditions similar to those indicated for Fig. 25. The various LUVET systems employed were composed of EPC (\blacktriangle); SPC(\blacksquare); EPC/EPS (1:1; \bullet); EPC containing 10 mol% cholesterol (\square), 25 mol% cholesterol (\circ), and 50 mol% cholesterol (Δ).



systems (Schuldiner and Kaback, 1975; Lambardi *et al.*, 1974; also, see previous chapter).

The uptake of $[^3\text{H}]\text{-MTPP}^+$ into EPC LUVET systems in response to a valinomycin-induced K^+ diffusion potential, employing an (initial) exterior concentration of $2 \times 10^{-8} \text{ M}$ $[^3\text{H}]\text{-MTPP}^+$ is illustrated in Fig. 32. Equilibrium is achieved after 2 hr indicating a membrane potential of greater than 100 mV (negative interior). It is interesting to note that a slower valinomycin independent uptake of MTPP^+ also occurs, presumably by a mechanism involving passive K^+ efflux similar to the valinomycin-independent accumulation of safranine (Fig. 29). Again, the uptake process is markedly sensitive to lipid composition (for example the SPC systems illustrated in the previous chapter achieved probe equilibration in less than 15 min) and is inhibited by equimolar levels of cholesterol (results not shown).

These MTPP^+ uptake studies were extended to determine the levels of accumulated MTPP^+ obtained for higher (initial) external MTPP^+ concentrations to ascertain whether massive uptake (similar to that observed for safranine) could be achieved. As shown in Fig. 33, the presence of 2 mM external MTPP^+ results in valinomycin-induced accumulation of MTPP^+ to levels which correspond to concentrations in the vesicle interior which approach 75 mM.

4.3.3 Uptake of charged lipophilic drugs

It is of interest to extend these uptake studies to include lipophilic cations with acknowledged biological activities. A large proportion of commonly employed drugs are lipophilic cations. This is presumably because most drugs must traverse the plasma membrane of cells in order to exert their biological effects, and in the absence of a specific transport protein this will be facilitated if the drug has lipophilic and cationic characteristics. In particular, it is possible that the membrane potential could then encourage drug accumulation in a manner similar to that observed here for safranine and MTPP^+ .

Five representative drugs were studied, including chlorpromazine (a local anaesthetic with application in treatment of schizophrenia), dibucaine (a local anaesthetic), propranolol (a beta adrenergic blocking agent), and vinblastine and adriamycin (both of which are anticancer drugs). Structures of these agents are given in Fig. 24. All of these compounds could be

Fig. 32. Time course of the accumulation of ^3H labelled methyltriphenylphosphonium (^3H)-MTPP $^+$) by EPC LUVETs prepared as indicated in section 4.2.2 with KGlucose in and NaCl out. The ^3H -MTPP $^+$ (50 Ci/mmol) was added to achieve a concentration of $20 \times 10^{-8} \text{ M}$ ($1 \mu\text{Ci/ml}$) of MTPP $^+$ in a dispersion of EPC LUVETs ($10 \mu\text{mol}$ phospholipid/ml). The accumulation of labelled MTPP $^+$ was monitored in the presence (●) and absence (■) of valinomycin as described in section 4.2.4. The open symbols indicate the uptake in the absence of an electrochemical Na^+/K^+ gradient.

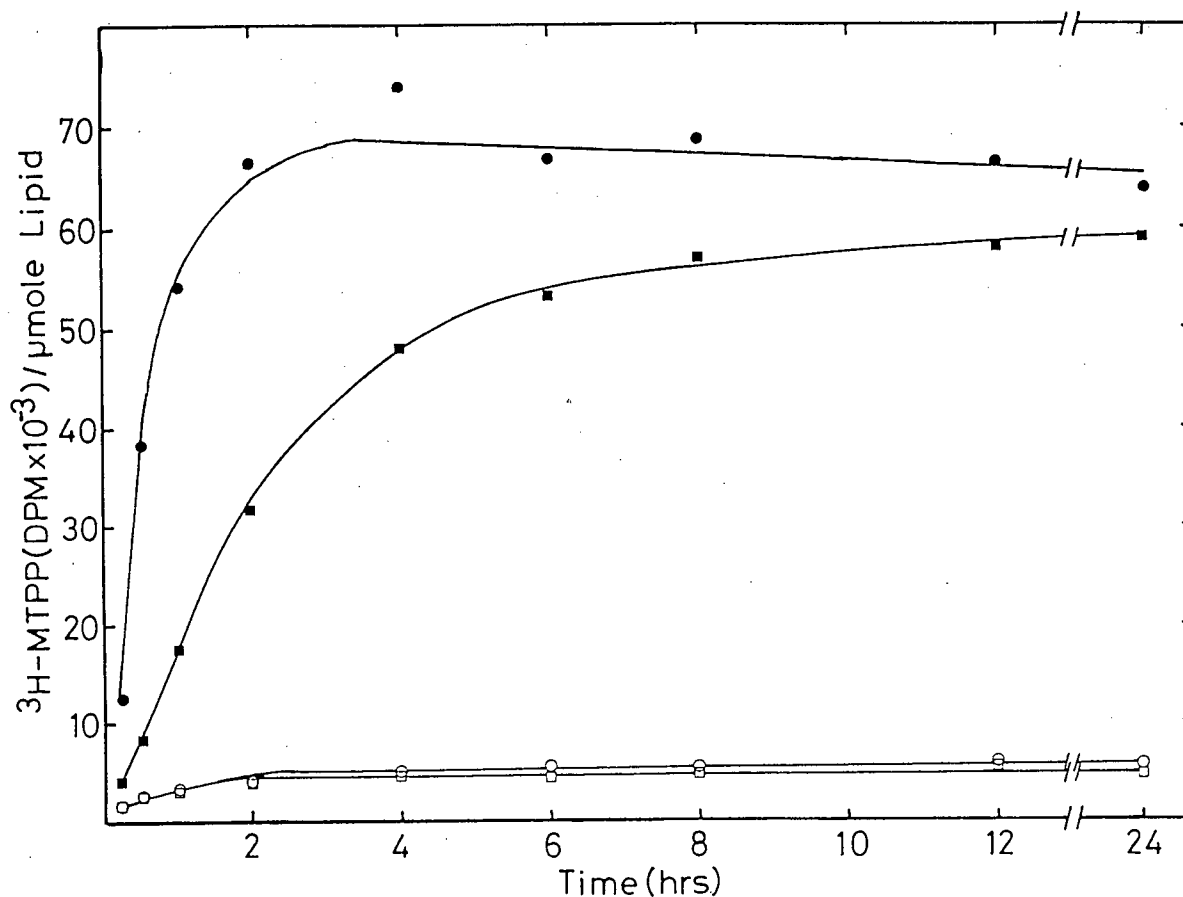
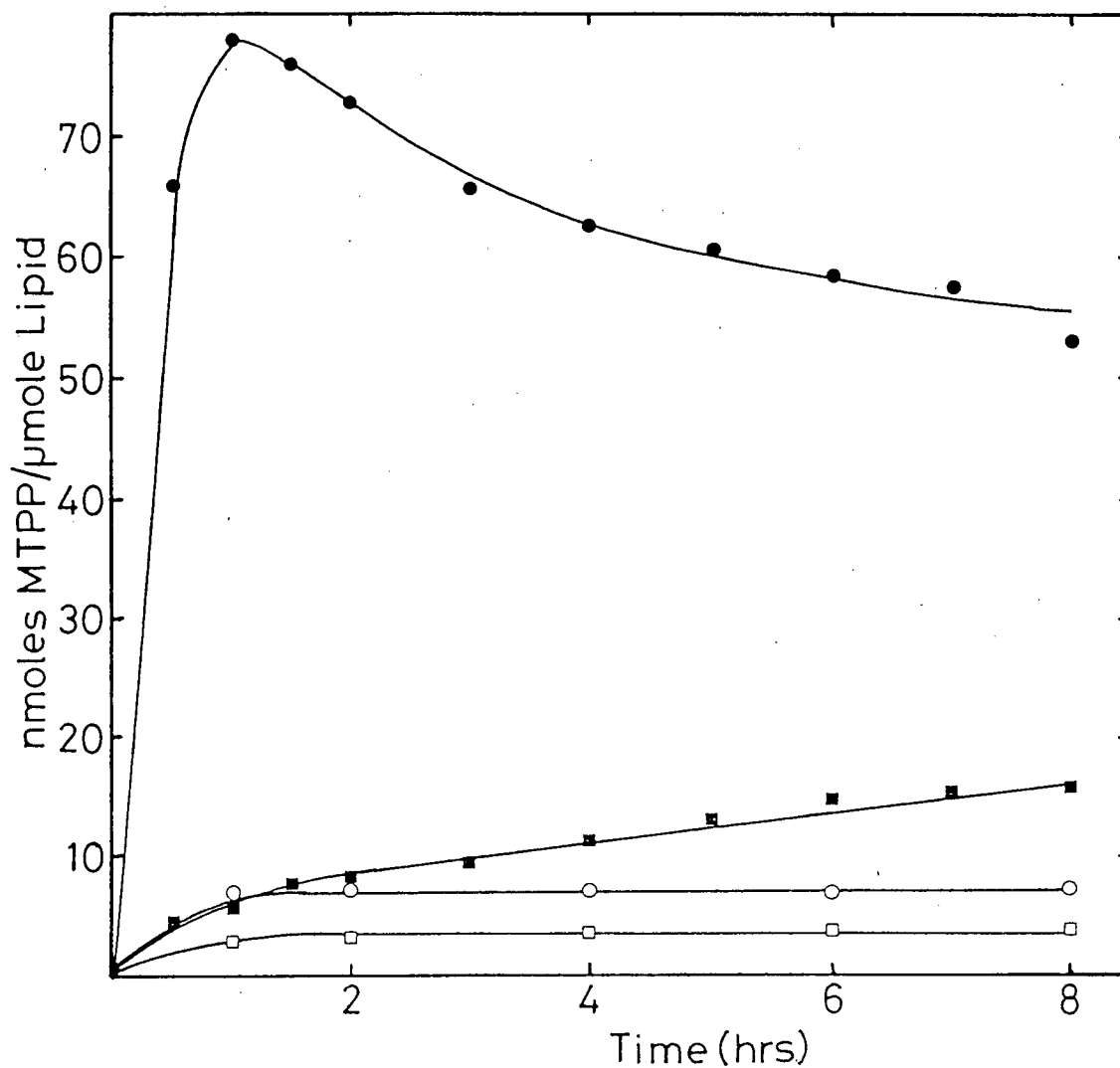


Fig. 33. Time course of the accumulation of methyltriphenylphosphonium (MTPP⁺) into EPC LUVETs under the conditions of Fig. 32 but where the initial exterior concentration of MTPP⁺ was 2 mM. The labelled [³H]-MTPP was diluted into cold MTPP⁺ to achieve radioisotope levels corresponding to 1 μ Ci/ml. The uptake was determined in the presence (●) and absence (■) of valinomycin. The open symbols indicate the uptake obtained in the absence of a Na⁺/K⁺ electrochemical gradient.



accumulated into LUVET systems displaying a K^+ diffusion potential as illustrated in Figs. 34, 35, and 36. In the case of the local anaesthetics dibucaine and chlorpromazine, LUVET systems experiencing Na^+/K^+ chemical gradients accumulated these agents to levels of 55 nmole/ μ mol lipid and 75 nmole/ μ mol lipid, respectively. Vesicles with the K^+ buffer inside and out exhibited much lower levels (less than 5 nmoles/ μ mol lipid) and these levels of uptake were unaffected by the presence of valinomycin. It is interesting to note that valinomycin was not essential for the uptake of the local anaesthetics. This behaviour would be consistent with the previous observations that a $\Delta\psi$ can be established by the passive efflux of K^+ (see previous chapters) as well as altered K^+ permeabilities due to the presence of the anaesthetic itself (McLaughlin, 1975). Similarly, the rate of propranolol and vinblastine uptake (to levels of 90 nmoles and 40 nmoles / μ mole phospholipid, respectively) was enhanced by the presence of valinomycin, however these agents were also accumulated in the absence of this ionophore. Adriamycin was accumulated most efficiently (to levels of greater than 180 nmoles/ μ mole lipid, representing a trapping efficiency of better than 90%), an uptake process that was observed to be markedly sensitive to the presence of valinomycin.

4.4 Discussion

The results presented here provide new information on the mechanisms of action of indicators of membrane potential such as safranin and have important implications for the transmembrane distributions of lipophilic cationic molecules in model and biological systems. These two areas will be discussed in turn.

The optical response of safranin has been employed to estimate $\Delta\psi$ in mitochondrial preparations (Colonna *et al.*, 1973; Zanotti and Azzone, 1980; Harris and Brown, 1980). These studies indicate that safranin is accumulated by an energy dependent mechanism and that the spectral changes occur as a result of a "stacking" of the dye on the inner surface of the membrane. This stacking was proposed to involve an association with negatively charged lipids in the inner monolayer. The results presented here are consistent with the optical response of safranin to $\Delta\psi$ arising from stacking or precipitation of the dye, which may occur at the

Fig. 34. Time course of the accumulation of (A) chlorpromazine and (B) dibucaine into EPC LUVETs experiencing a Na^+/K^+ electrochemical gradient. The chlorpromazine uptake was determined for LUVETs ($1 \mu\text{mol}$ phospholipid/ml) incubated in the presence of $200 \mu\text{M}$ chlorpromazine ($2 \mu\text{Ci/ml}$ [^3H]-chlorpromazine) and the vesicle-associated drug determined subsequently as indicated in section 4.2.6. Similarly, dibucaine uptake was determined for LUVETs ($1 \mu\text{mol}$ phospholipid/ml) incubated with $100 \mu\text{M}$ dibucaine. Dibucaine accumulation was quantitated as described in section 4.2.6. Both uptake experiments were conducted in the presence (●) and absence (■) of valinomycin ($0.5 \mu\text{g}/\mu\text{mol}$ phospholipid). The open symbols indicate uptake observed in the absence of a Na^+/K^+ chemical gradient. Data for the dibucaine figure was collected and reproduced with permission from L. D. Mayer.

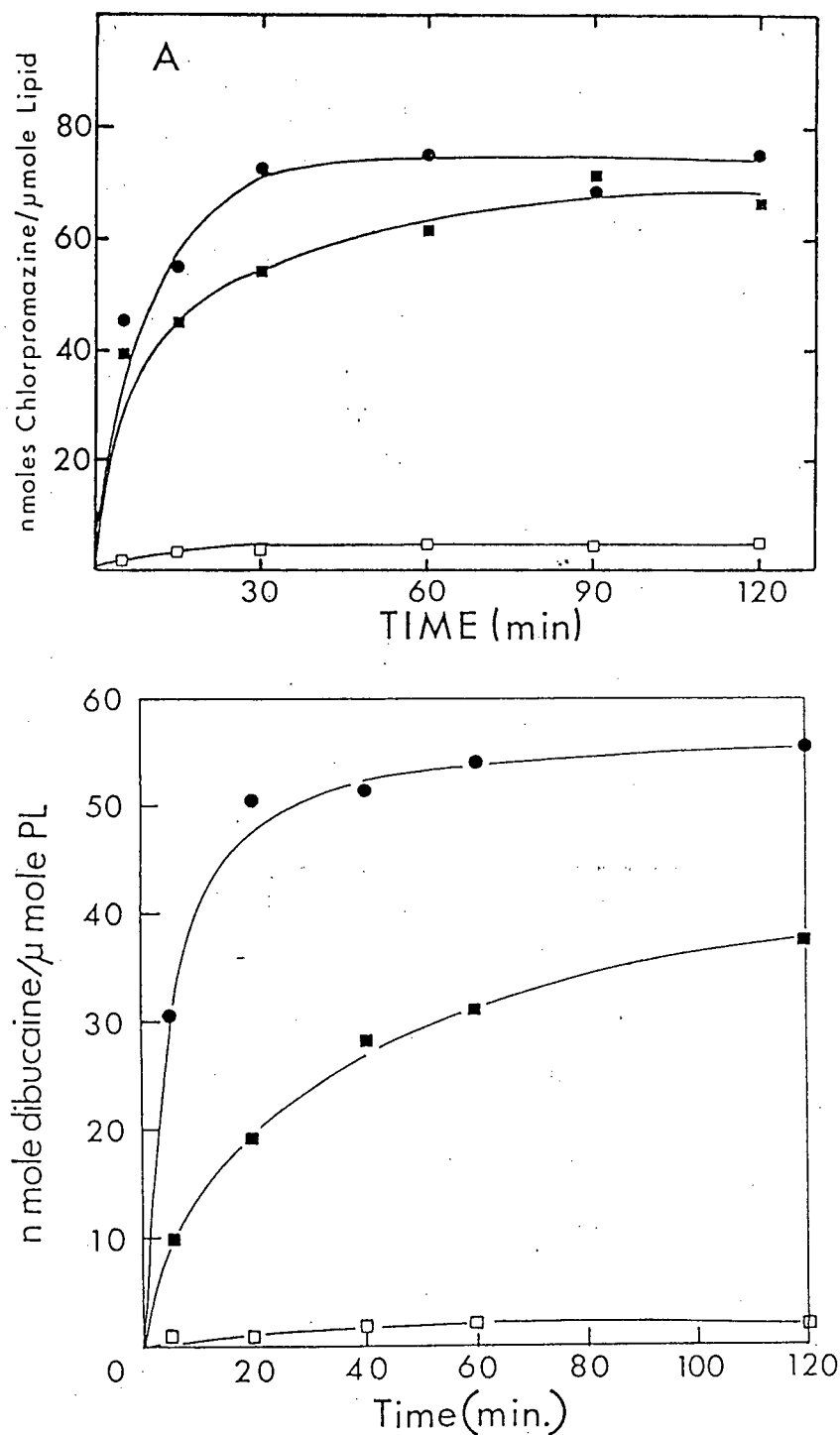


Fig. 35. Time course of propranolol uptake by LUVETs with a transmembrane Na^+/K^+ chemical gradient. Egg PC LUVETs ($1 \mu\text{mol}$ phospholipid/ml) were incubated in the presence of $200 \mu\text{M}$ propranolol. Vesicle preparation and quantitation of vesicle-associated propranolol was accomplished as described in section 4.2.6. Uptake was measured in the presence (●) and absence (■) of valinomycin. The open symbols represent accumulation in the absence of a electrochemical gradient. Data collected and reproduced with permission from T. Redelmeier.

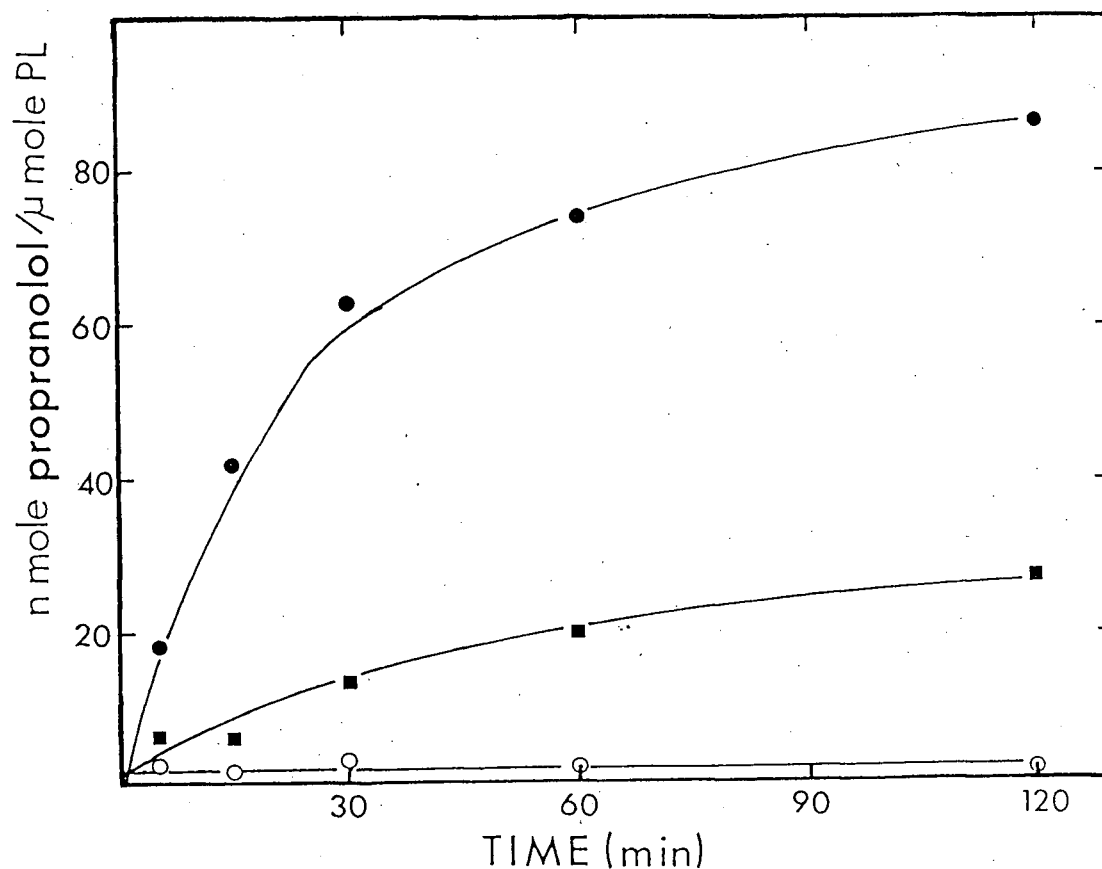
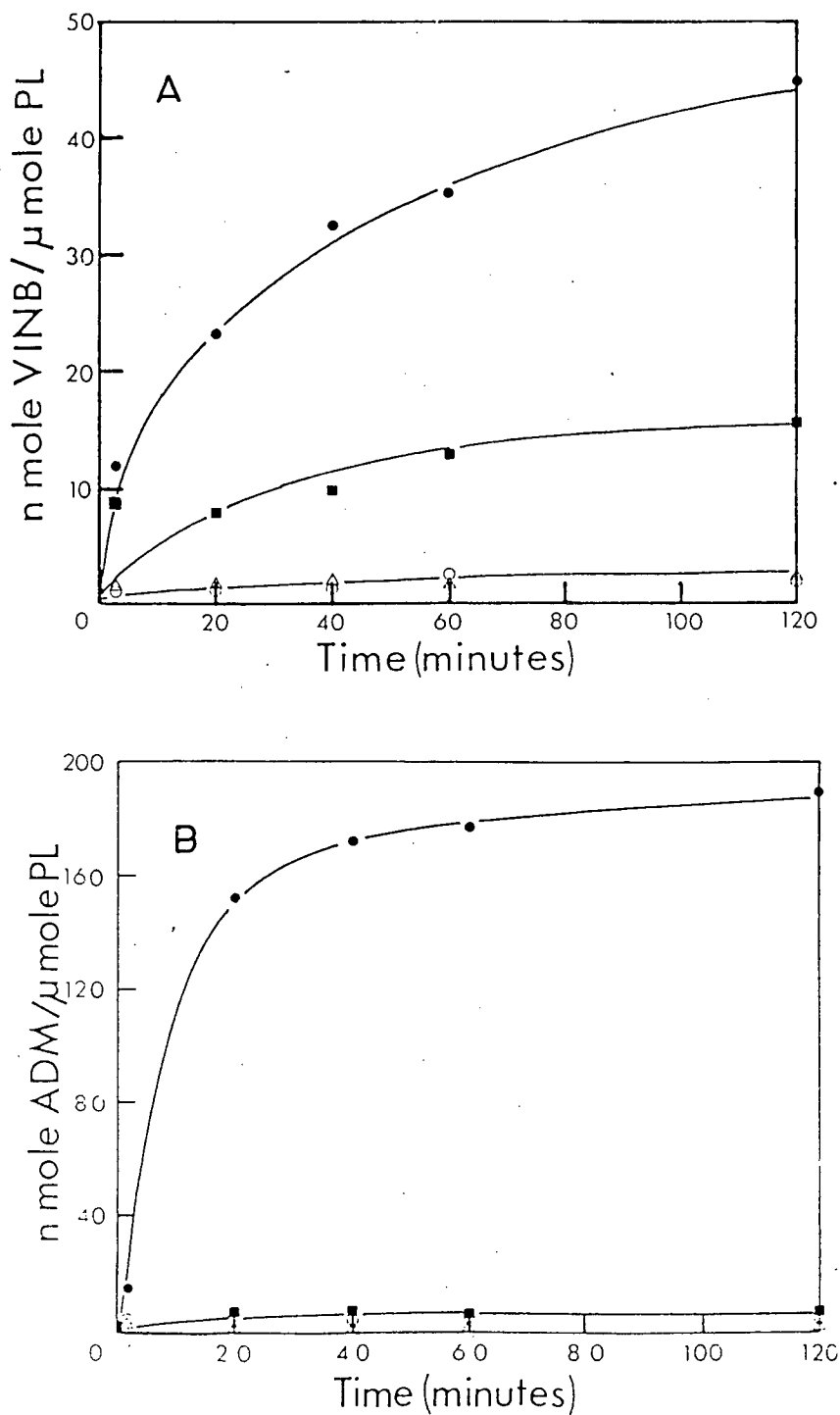


Fig. 36. Time course for the accumulation of (A) vinblastine and (B) adriamycin into EPC LUVETs experiencing a Na^+/K^+ electrochemical gradient. The vinblastine uptake was determined for LUVETs ($1 \mu\text{mol}$ phospholipid/ml) incubated with $200 \mu\text{M}$ vinblastine sulphate and the vesicle-associated vinblastine was determined by removal of untrapped material and subsequently assayed as described in section 4.2.6. The adriamycin uptake was measured in a similar fashion, as described in section 4.2.6. Both uptake experiments were conducted in the presence (●) and absence (■) of valinomycin ($0.5 \mu\text{g}/\mu\text{mol}$ phospholipid). The open symbols indicate uptake observed in the absence of a Na^+/K^+ chemical gradient.



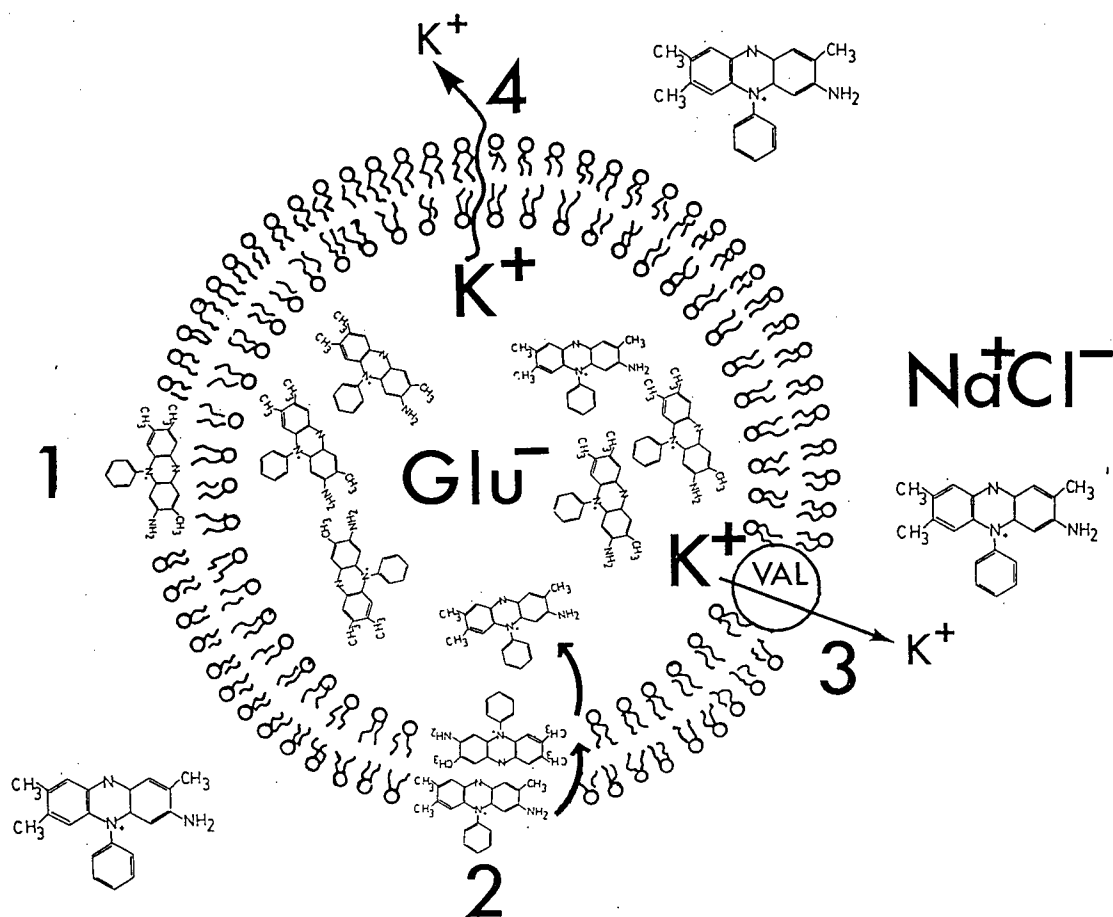
inner monolayer-water interface. However, it is clear that negatively charged lipids are not required. The limitations of the optical response of safranin as a quantitative indicator of the membrane potential are equally clear due to the inherent non-linearity of the stacking or precipitation events giving rise to this response, which give rise to non-linear absorbance changes as $\Delta\psi$ is increased.

The mechanism whereby safranin is accumulated by the LUV systems is of particular interest. The results presented here are consistent with an electroneutral "antiport" K^+ -safranin transmembrane exchange mechanism (modeled in Fig. 37), as indicated by release of entrapped K^+ on safranin accumulation as well as the fact that the maximum levels of safranin accumulated are comparable to the initial levels of trapped K^+ (greater than 100 mM as compared to 150 mM). Such a proposal is not new (Harris and Baum, 1980) - indeed, it is difficult to imagine any other process that could drive safranin uptake in the relatively simple model systems investigated here. The important points are that the lipophilic cation appears to "flip" across the bilayer in a charged form in response to the $\Delta\psi$ dependent electric field gradient, and that extremely high levels of internalized safranin can be achieved. This clearly reflects a rather efficient and effective transport process which, as indicated below, may be of general significance for the distributions of lipophilic cations *in vivo*.

In the case of MTPP⁺, the ability to employ low concentrations of the radiolabeled form allows reasonable correlations to be obtained between $\Delta\psi$ calculated on the basis of experimentally determined interior and exterior concentrations of [³H]-MTPP⁺ and the actual K^+ diffusion potential (see Figs. 22 and 23, preceding chapter). Alternatively, higher (2 mM) initial exterior levels of MTPP⁺ lead to accumulation of high (greater than 75mM) internal concentrations of MTPP⁺ (Fig. 33), behaviour which corresponds to that observed for safranin.

Before discussing the similar uptake characteristics of the biologically active lipophilic cations investigated here, it is of interest to note problems that may be involved in obtaining accurate measures of $\Delta\psi$ derived from equilibrium transmembrane redistributions of lipophilic cationic probe molecules such as MTPP⁺ or safranin. A particular difficulty concerns the length of time required for equilibrium redistributions to occur, which may be on the order

Fig. 37. Model of safranin uptake. It is suggested that the uptake process would involve (1) partitioning of safranin into the lipid bilayer, subsequently the molecule would "flip" across the bilayer in the charged form in response to the $\Delta\psi$ dependent electric field gradient (2). The transport step would be associated with an electroneutral "anti-port" K^+ -safranin transmembrane exchange that would be facilitated by the presence of the K^+ -ionophore valinomycin (3), but could also occur in response to the passive efflux of K^+ through the bilayer (4).



of hours. Further, in less fluid membranes, such as those containing cholesterol, these redistributions may be sufficiently slow as to preclude achievement of equilibrium in a reasonable time frame (see Fig. 31). This may reflect reduced partitioning of the probe molecule into the membrane or inhibition of the transmembrane "flip" process in response to the electrochemical gradient. In any event, a requirement for an extended time course to determine whether probe uptake has achieved equilibrium is apparent, particularly for systems such as plasma membranes containing high levels of cholesterol. Gross underestimates of $\Delta\psi$ may otherwise result.

The observation that lipophilic cationic drugs such as chlorpromazine, dibucaine, propranolol, adriamycin, and vinblastine can be accumulated to high levels within LUV systems exhibiting a membrane potential has far reaching implications in four areas. First, chlorpromazine and dibucaine are local anaesthetics. A fundamental problem in understanding the mechanism whereby local anaesthetics induce their effects has been that clinical concentrations of anaesthetics have little influence on the physical properties of lipid systems, even though available evidence suggests that these agents exert their effects via the lipid component of membranes (Seeman, 1972). The results presented here suggest that the presence of a membrane potential could lead to local anaesthetic concentrations on the interior of a nerve membrane, for example, which are more than two orders of magnitude higher than plasma concentrations. Additional studies (Mayer *et al.*, 1984) characterizing the uptake of dibucaine in response to a $\Delta\psi$ suggest that this is the case. This investigation indicated that the protonated form of the anaesthetic is transported in response to the Na^+/K^+ chemical gradient, leading to inner monolayer anaesthetic concentration an order of magnitude larger than predicted on the basis of anaesthetic lipid-water partition coefficient.

It is of interest to determine whether similar considerations apply to the accumulation of naturally occurring lipophilic cations, such as biological amines. The chromaffin granule of the adrenal medulla, for example, concentrates dopamine to high levels. Since dopamine has lipophilic and cationic characteristics, the possibility exists that dopamine uptake could proceed in association with cation efflux, without a requirement for a specific transport protein.

Previous studies (Nichols and Deamer, 1976) have demonstrated the accumulation of biogenic amines in LUVs with a transmembrane pH gradient, a process that is characterized in greater detail in the following chapter.

The third and fourth areas concern drug design and efficient loading of liposomal drug carrier systems. Model systems such as those employed here (and described in detail in the previous chapter) clearly provide convenient systems for evaluating the possible influence of a given structural alteration on non-specific uptake into cells in response to a membrane potential. Alternatively, LUV systems containing high levels of lipophilic cationic drugs concentrated in response to $\Delta\psi$ may well have application as vehicles for drug delivery (see Poste, 1983). Reasons for this include the high drug trapping efficiencies that are possible for many anticancer agents, such as the costly antitumor alkaloids. Further studies employing vinblastine and adriamycin show that trapping efficiencies in excess of 95% can easily be achieved (Mayer *et al.*, 1984).

In summary, the studies presented in this chapter reveal a remarkable ability of LUV systems to accumulate safranin and other lipophilic cations in response to a K^+ diffusion potential. This ability may have important and general implications for the equilibrium transmembrane distributions of biologically active cations *in vivo*.

UPTAKE OF DOPAMINE AND OTHER BIOGENIC AMINES INTO LARGE
UNILAMELLAR VESICLES IN RESPONSE TO A MEMBRANE POTENTIAL:
ACTIVE TRANSPORT IN THE ABSENCE OF A CARRIER PROTEIN†

5.1 Introduction

In a variety of biological systems biogenic amines are stored in high concentrations within specialized organelles. Examples include catecholamines (ie. dopamine, epinephrine, norepinephrine) which are stored at high concentrations (0.6 M) in the chromaffin granules of the adrenal medulla (Winkler, 1976; Smith, 1968), serotonin which is stored in serotonin granules of blood platelets (Wilkins *et al.*, 1978; Fukami *et al.*, 1978), and neurotransmitters which are stored in neural synaptic vesicles (Martin, 1973). The mechanism by which these amines are accumulated in these organelles has been the subject of intense investigation (for reviews see Njus *et al.*, 1981; Kanner, 1983).

Previous investigations have indicated that catecholamine accumulation in the chromaffin granule occurs by a reserpine sensitive carrier-mediated process which is directly coupled to ATP hydrolysis (Kanner *et al.*, 1979; Schuldiner *et al.*, 1978). A variety of data, indicating that the uptake of amines was dependent on the formation of ion gradients (Holz, 1979) and was sensitive to the presence of proton ionophores (Johnson *et al.*, 1981), supported a chemiosmotic mechanism of biogenic amine transport whereby accumulation is driven by an ion gradient. Briefly, it was proposed that the carrier mediated transport process involves an inwardly directed proton-translocating ATPase which is responsible for maintaining a transmembrane electrochemical proton gradient (acid interior) that provides the driving force for the uptake of catecholamines (Schuldiner *et al.*, 1978; Maron *et al.*, 1983; Knoth *et al.*, 1980; Johnson *et al.*, 1978). Further, it was suggested that the inward flux of amines was coupled to H⁺ efflux providing a H⁺/amine antiport type of mechanism that is coupled through the

†This chapter has been based on the reference Bally *et al.* (1984).

carrier protein (Njus *et al.*, 1981; Johnson *et al.*, 1981). A similar mechanism has been proposed for the transport of serotonin, where it has been shown that vesicles accumulate this amine in exchange for K^+ (Kanner, 1983) and for the uptake of neurotransmitter by synaptosomes, which appear to employ a Na^+ -coupled transport system (Fukami *et al.*, 1981).

The role of the various components (pH gradient, ATPase, carrier protein) which are involved in catecholamine transport are still not understood at the molecular level. It has been suggested that the characteristics of biological amines as weak bases, allow the molecules to accumulate across the membrane according to the transmembrane pH gradient (Schuldiner *et al.*, 1978), where the neutral form of the amine permeates across the lipid bilayer. This theory was supported by data that demonstrated a variety of catecholamines could be accumulated in egg PC vesicles in response to a pH gradient (interior acid; Nichols and Deamer, 1976). The difficulty with this proposal lies in the fact that the pKa values of the biological amines are significantly higher than physiological pH. For example the pKa of the amino group of dopamine is approximately 9.9, and the catechol hydroxyls demonstrate a pKa of about 8.8. Therefore at the pH values examined in many of the reports which demonstrate the transport of biogenic amines, the amine exists predominately in the protonated form. In addition, if amine transport occurs by the proposed H^+ /amine antiport mechanism, ATP independent uptake of the amine by chromaffin granule ghosts would result in alkalinization of the vesicle. This does not appear to be the case (Knoth *et al.*, 1983), suggesting that the amine may be transported in a charged (protonated) form.

In the previous chapter it was suggested that the lipophilic cation safranin, a quaternary amine which exists exclusively in a positively charged form, is accumulated by LUVs exhibiting a membrane potential (interior negative). Since at physiological pH the biological amines have both lipophilic and cationic characteristics it may be possible that these molecules could be accumulated by a similar, membrane potential driven, uptake process. In this investigation the uptake of dopamine in model large unilamellar vesicles (LUVETs) composed of egg phosphatidylcholine (EPC) which have a transmembrane electrochemical potential (interior negative) in the presence and absence of a pH gradient (interior acid) has

been characterized. The results clearly demonstrate that a membrane potential can provide the driving force for biological amine transport by a process that is sensitive to the presence of CCCP (a H^+ ionophore) and valinomycin (a K^+ ionophore). The results are consistent with the proposal that dopamine crosses the lipid bilayer in a charged form and that in the presence of an aqueous trap for dopamine, such as ATP, this uptake results in the accumulation of dopamine to levels in excess of 120 mM against an exterior concentration of 20 μM .

5.2 Materials and Methods

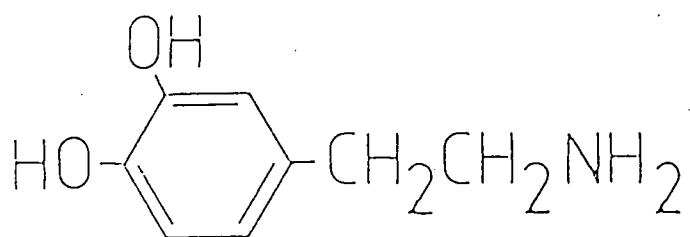
5.2.1 Materials

Egg phosphatidylcholine (EPC) was isolated from hen egg yolk as described in section 2.2.2. Dopamine, 5-hydroxytryptamine (serotonin), and epinephrine were all obtained from Sigma (St. Louis, MO). $[^3H]$ -inulin, $[^{14}C]$ -cholesterol oleate, $[^3H]$ -methyl triphenylphosphonium iodide (MTPP⁺), $[^3H]$ -dopamine HCL and $[^3H]$ -epinephrine were obtained from NEN (Canada). For ease of reference the structures of the various biogenic amines are shown in Fig. 38.

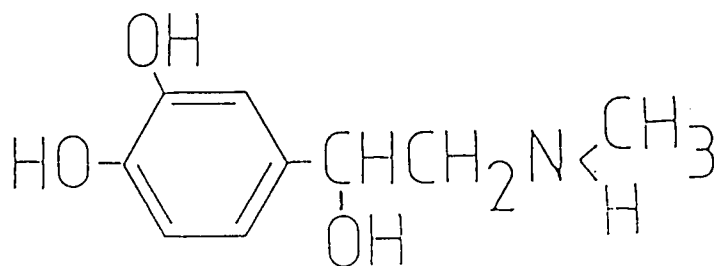
5.2.2 Preparation of vesicles

Vesicles were prepared utilizing the LUVET (large unilamellar vesicles by extrusion techniques) procedure described in section 3.2.2. Briefly a dry lipid film was hydrated with an appropriate buffer to produce multilamellar vesicles (25–100 μ moles lipid/ml) which were extruded 10 times through two (stacked) polycarbonate filters with a defined pore size of 100 nm (Nucleopore). Subsequently the vesicle preparation was freeze-thawed twice and resized through the 100 nm filters 5 times. The resulting vesicle suspension was largely unilamellar with an average diameter of 90 nm as determined by freeze fracture and negative stain microscopy (see section 3.3.1). The vesicles exhibited an average trapped volume of 1.5 $\mu l/\mu$ mole phospholipid as determined by $[^3H]$ -inulin.

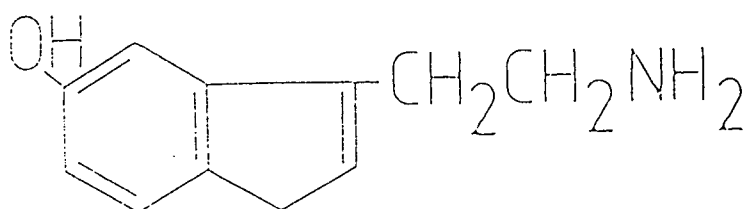
Fig. 38. Structures of Dopamine, Epinephrine, and Serotonin.



DOPAMINE



EPINEPHRINE



SEROTONIN

Transmembrane Na^+ - K^+ chemical gradients (interior K^+) were formed by trapping a K^+ buffer (169 mM K glutamate, 20 mM HEPES adjusted to pH 7.5 with 1M NaOH; 310 mOsm/kg) and subsequently exchanging the untrapped K^+ buffer for an iso-osmotic Na^+ buffer (150 mM NaCl, 20 mM HEPES adjusted to pH 7.5 with 1M NaOH; 310 mOsm/kg) utilizing a Sephadex G-50 desalting column (as described in section 4.2.2). Similarly, transmembrane pH gradients (interior acid) were formed using a trap buffer with low pH (150mM KOH, 175 mM glutamic acid pH 4.65; 290 mOsm/kg) which was then exchanged with a high pH buffer (150 mM KOH, 125 mM glutamic acid, 30 mM NaCl pH 7.5; 290 mOsm/kg) on a Sephadex G-50 column. Defined pH gradients were generated by trapping the low pH buffer and subsequently passing the vesicles down Sephadex G-50 columns pre-equilibrated with buffers containing 150 mM KOH, 10 mM MES ($\text{pK}_a = 6.15$), 10 mM EPPS ($\text{pK}_a = 8.0$), 10 mM CAPS ($\text{pK}_a = 10.4$) and varying concentrations of glutamic acid ($\text{pK}_a = 4.2$) and NaCl to give iso-osmotic buffers of the desired pH. A similar buffering mixture (glutamic acid, MES, EPPS) was utilized when the pH was varied under conditions of a constant Na^+/K^+ ion gradient (interior K^+). Where ATP was utilized as a trap, the internal buffer consisted of 150 mM KOH, 175 mM glutamic acid and 125 mM Na_2ATP giving a pH of 4.3 (470 mOsm/kg). This was exchanged against either a buffer containing 150 mM KCl, 20 mM glutamic acid, and 80 mM NaCl (adjusted to pH 4.3 with 1 M NaOH; 470 mOsm/kg) for control samples or 220 mM NaCl and 20 mM Hepes (adjusted to pH 7.5 with 1 M NaOH; 450 mOsm/kg) for experimental samples. All biogenic amine uptake studies were preformed with buffers containing 5 mM sodium ascorbate as an antioxidant. Where employed the K^+ ionophore valinomycin was added to give a final concentration of 0.5 $\mu\text{g}/\mu\text{mole}$ lipid and the H^+ ionophore CCCP was added to give a final concentration of 20 μM . The same concentrations of each were used in samples that contained both ionophores.

5.2.3 Determination of membrane potential

The membrane potential was measured by determining the distribution of the lipophilic cation $[^3\text{H}]\text{-MTPP}^+$ as described in section 3.2.6. Briefly, 1 μCi of $[^3\text{H}]\text{-MTPP}^+$ (50

Ci/mmol) was added to a 1 ml LUVET dispersion which was subsequently incubated at room temperature for 1 hr before an aliquot was withdrawn and the untrapped [^3H]-MTPP $^+$ was removed by passing over a small (1 ml) Sepadex G-50 column. The trapped [^3H]-MTPP $^+$ was determined by liquid scintillation counting employing a Phillips PW-4700 liquid scintillation counter and the phospholipid was determined by a phosphate assay (see section 3.2.2). Utilizing the trapped volume, as determined with [^3H]-inulin (see section 3.2.2), the internal and external concentration of MTPP $^+$ was calculated and the membrane potential was estimated employing the Nernst equation (see section 3.2.6).

5.2.4 Uptake assays

The amount of dopamine accumulated was determined by adding dopamine from a 2 mM stock solution which contained [^3H]-dopamine (45.4 Ci/ mmol) to a LUVET dispersion to achieve a 200 μM dopamine concentration with 1 $\mu\text{Ci/ ml}$ labeled amine and a 1 mM lipid concentration. Subsequently, at appropriate time intervals, the unsequestered amine was removed by passing aliquots of the vesicles through 1 ml Sephadex G-50 columns as described in the preceding chapter (section 4.2.6). Aliquots of the effluent were counted to assay for dopamine and phospholipid phosphorous was assayed by standard techniques. Where ATP was used as a trap, [^{14}C]-cholesterol oleate (56.6 mCi/mmol) was used (1 $\mu\text{Ci/20}$ $\mu\text{moles lipid}$) as a probe to assay for lipid .

The uptake of epinephrine and serotonin was determined employing similar procedures as for dopamine. Accumulation of epinephrine was monitored using [^3H]-epinephrine in systems containing 200 μM amine and 1 mM EPC LUVETs. In the case of serotonin, similar concentrations of amine and lipid were utilized and the LUVET associated serotonin was assayed fluorometrically (excitation, 309 nm; emission, 340 nm) employing a Perkin-Elmer 650-10S fluorescent spectrophotometer after disruption of the vesicles with 0.5% Triton X-100.

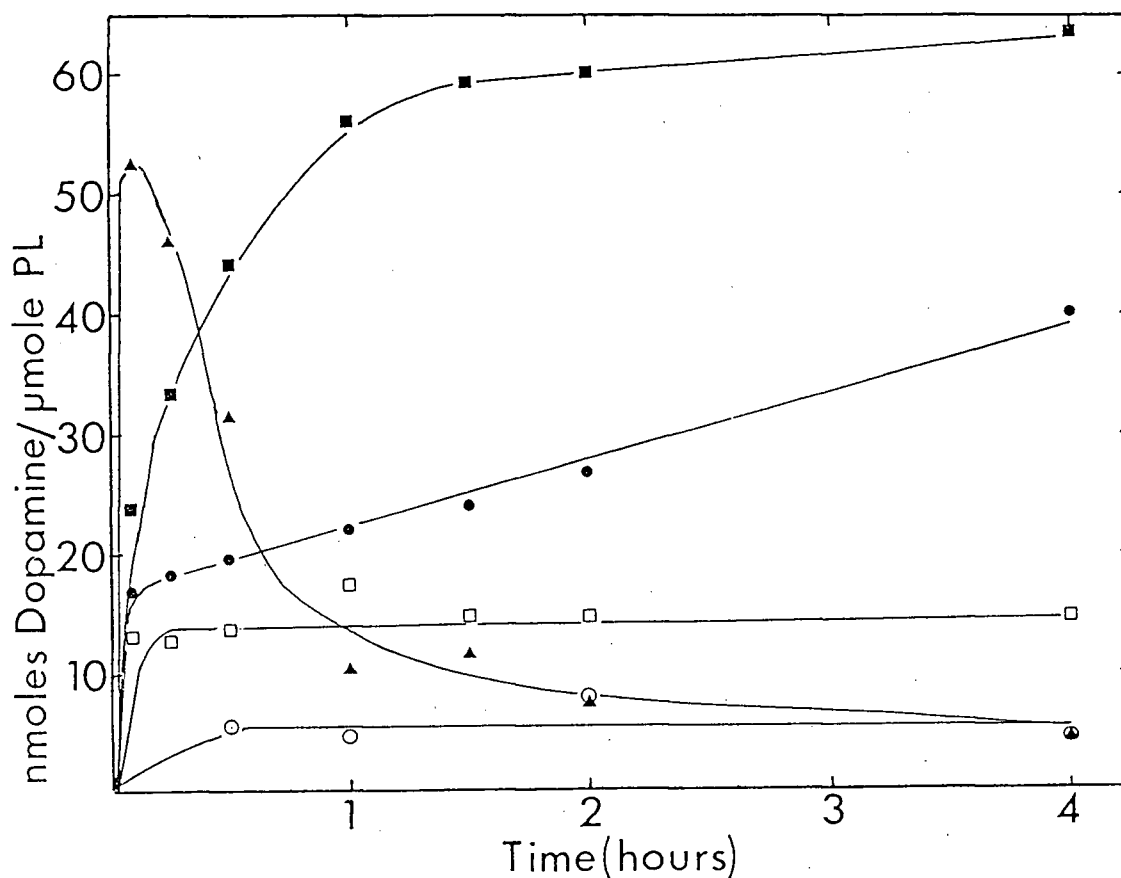
5.3 Results

5.3.1 Accumulation of dopamine in response to a transmembrane electrochemical potential

The previous chapter demonstrated that a variety of molecules with lipophilic and cationic characteristics can be accumulated in a vesicle (LUVET) preparation in response to a transmembrane membrane potential (interior negative) generated by a Na^+/K^+ ion gradient (K^+ inside) across the lipid bilayer. The mechanism of uptake appeared to occur by an electroneutral $\text{K}^+/\text{lipophilic cation}$ exchange process that was facilitated by the K^+ ionophore valinomycin. It is of interest to determine whether the uptake of biological amines, which have lipophilic and cationic characteristics at neutral pH, could also be accumulated by a similar mechanism. This is shown to be the case in Fig. 39 where it is shown that the accumulation of dopamine by EPC LUVETs can be driven by a transmembrane K^+ ion diffusion potential. The uptake is dependent on the presence of the K^+ ionophore valinomycin, and levels of greater than 50 nmoles dopamine/ μmole lipid are achieved within a 1 hr incubation. This level remains constant for periods greater than 8 hr (data not shown). In the absence of valinomycin the uptake is reduced 5 fold to 12 nmoles dopamine/ μmole lipid. Uptake levels of only 3 nmoles dopamine/ μmole lipid are obtained for samples which lack a Na^+/K^+ electrochemical gradient (equal concentration of K^+ inside and outside). Assays employing the membrane potential probe $[\text{}^3\text{H}]\text{-MTPP}^+$ revealed a potential of greater than 100 mV (interior negative) for these vesicles in the presence of valinomycin, while in the absence of the ionophore a potential of -40 to -60 mV was detected (for example, see preceding chapter). These data indicate that the accumulation process is dependent on both the transmembrane electrochemical potential and the efflux of K^+ which is facilitated by valinomycin, and are qualitatively similar to previous results demonstrating that K^+ efflux is coupled to uptake of the lipophilic cation safranine.

Dopamine uptake in the presence of valinomycin resulted in a 200 fold or larger concentration gradient of the amine across the membrane (based on an trapped volume of 1.5

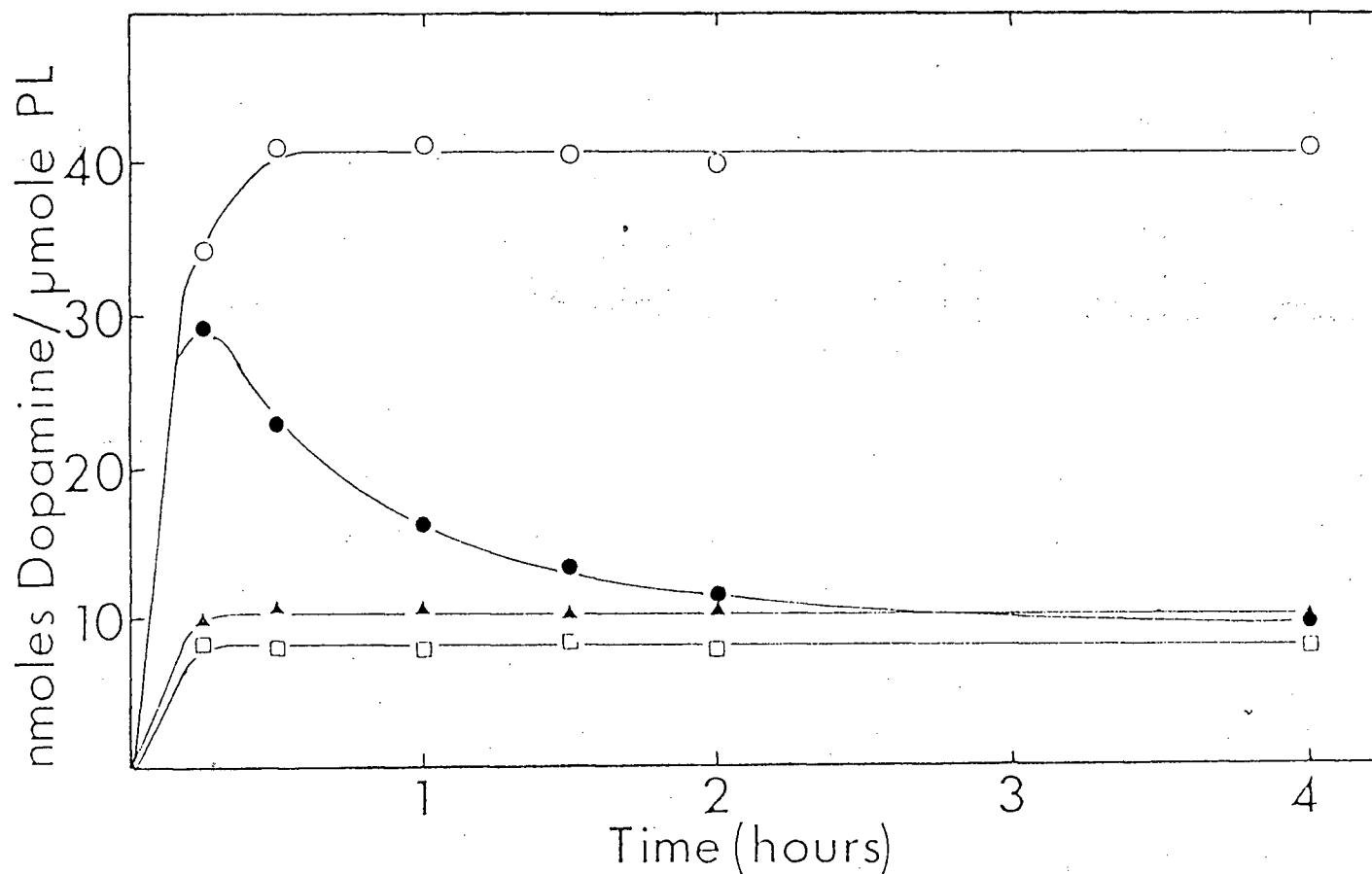
Fig. 39. Time course for accumulation of dopamine by EPC LUVET systems experiencing a Na^+/K^+ electrochemical gradient. The LUVETs were prepared in a K glutamate buffer, and the untrapped buffer was exchanged for a NaCl buffer as described in section 5.2. Subsequently the vesicles were diluted to achieve a concentration of 1 mM phospholipid in a NaCl buffer containing 200 μM dopamine (1 $\mu\text{Ci}/\text{ml}$ [^3H]-dopamine). The dopamine taken up into the vesicles was determined using liquid scintillation counting after the untrapped dopamine was removed by gel filtration. The open circles represent uptake in control samples which have equal concentrations of K^+ on both sides of the membrane. The other symbols represent uptake in the absence of added ionophores (\square), and in the presence of valinomycin (0.5 $\mu\text{g}/\mu\text{mole}$ lipid; \blacksquare), or CCCP (20 μM ; \bullet), or both ionophores (\blacktriangle).



μ l/ μ mole lipid). The gradient formed is sensitive to the initial external dopamine concentration, as similar levels of uptake were obtained when external dopamine concentrations were as high as 1 mM. Fig. 39 also indicates that the uptake process can be uncoupled by the presence of both valinomycin and CCCP. The presence of these ionophores initially results in a more rapid accumulation of dopamine to levels of greater than 50 nmole/ μ mole lipid. Subsequently there is a rapid efflux of the entrapped amine to control levels within 1 hr. A similar time course is observed for the transmembrane membrane potential assayed by MTPP⁺, where a maximum of -60 mV is obtained at 15 min decreasing to less than 5 mV (negative interior) at 4 hours. Addition of CCCP alone to vesicles with a Na⁺/K⁺ ion gradient also facilitated transport of dopamine, albeit at a much reduced rate.

Since chromaffin granules maintain a transmembrane pH gradient (Johnson *et al.*, 1978) and it has been demonstrated that this pH gradient can drive the uptake of dopamine and other biogenic amines in these membrane preparations and in model vesicle systems (Schuldiner *et al.*, 1978; Johnson *et al.*, 1981; Nichols and Deamer, 1976), it was of interest to determine whether dopamine uptake in LUVETs could also be driven by a pH gradient (interior acid) in the absence of a K⁺ ion gradient. This is demonstrated to be the case in Fig. 40, where levels of 40 nmoles dopamine/ μ mole lipid are obtained (representing a 150 fold gradient across the membrane) within 30 min after addition of the amine to vesicles with a transmembrane pH gradient of 3 units. This level of uptake is stable for periods exceeding 8 hours and appears to be unaffected by the exterior concentration of dopamine. The H⁺ diffusion potential generated by vesicles with this transmembrane pH gradient was determined to be greater than 100 mV (interior negative) and was stable for periods in excess of 8 hr. The presence of the H⁺ ionophore CCCP results in a rapid accumulation followed by efflux of the amine to control levels by 2 hr. It is interesting that the membrane potential exhibited by these CCCP containing vesicles is stable, maintaining a potential of greater than 100 mV (interior negative) for periods in excess of 8 hr. As was shown for vesicles with a transmembrane K⁺ diffusion potential, the presence of both a K⁺ and a H⁺ ionophore uncouples the uptake process indicating that K⁺/H⁺ exchange eliminates the driving

Fig. 40. Time course for accumulation of dopamine by EPC LUVET systems experiencing a pH gradient (interior acid). The LUVETs were prepared in a low pH buffer (pH 4.65), and the untrapped buffer was exchanged for a high pH buffer (pH 7.5) as described in section 5.2. The conditions for uptake were as described in Fig. 39. The open square symbols represent control samples with a low pH buffer inside and outside the vesicle. The other symbols represent uptake in the presence of no added ionophore (\circ), CCCP (\bullet), and CCCP and valinomycin (Δ). Ionophores were used at the concentrations specified in Fig. 39.

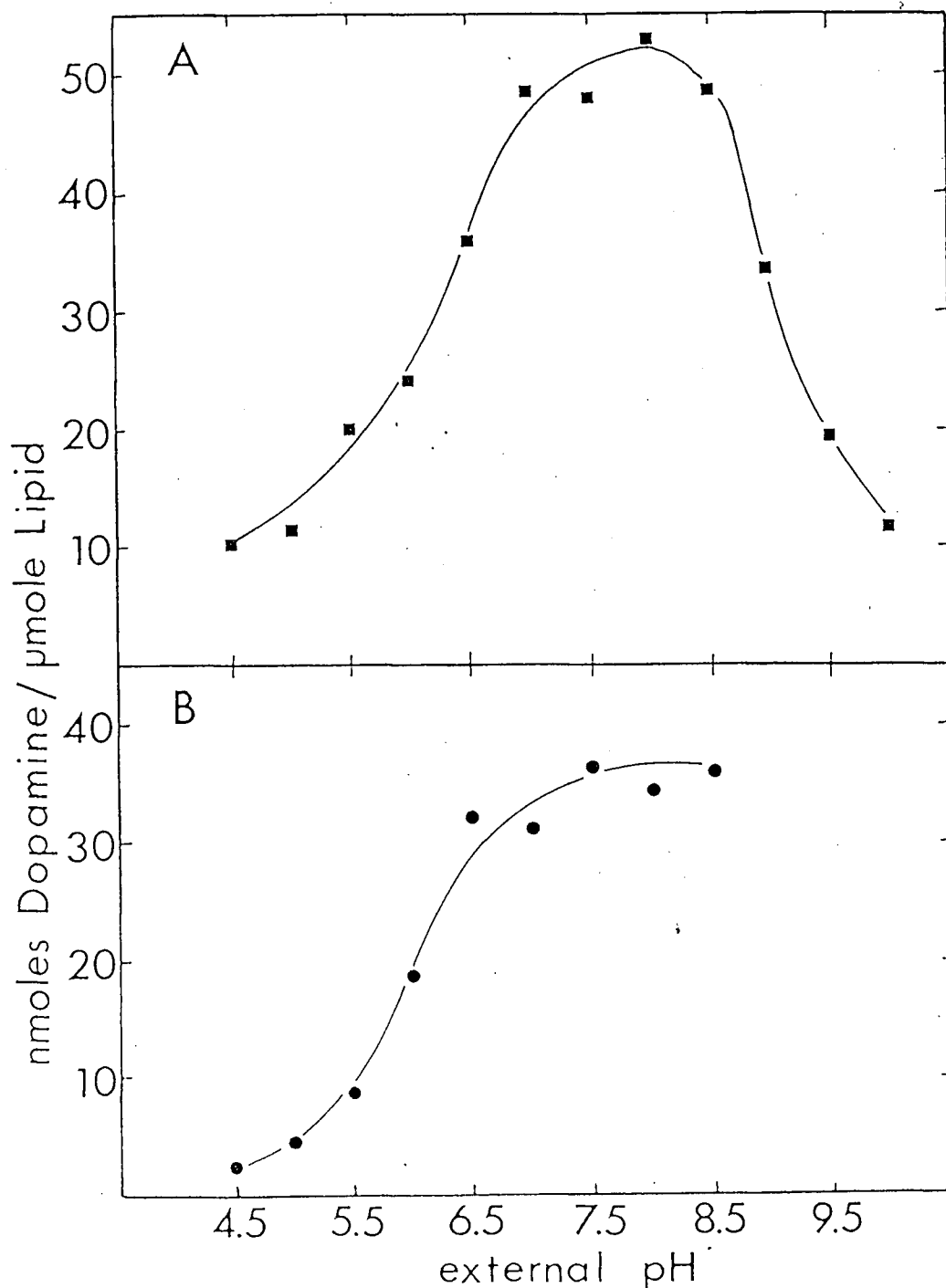


force for dopamine uptake in these model systems. Similar results have been obtained for chromaffin granule preparations which discharge entrapped catecholamines in systems where the pH gradient is uncoupled by the presence of both these ionophores (Bangham *et al.*, 1980).

5.3.2 Influence of external pH on the uptake of dopamine

It has been suggested that weak bases, such as dopamine, cross the lipid bilayer in a neutral rather than charged form (Johnson *et al.*, 1978; Johnson *et al.*, 1981) which implies that these molecules distribute across a membrane according to the transmembrane pH gradient. However, if dopamine is accumulated in LUVETs by a similar mechanism described in the previous chapter for the positively charged safranin, then it may be expected that it is the charged form of dopamine which is translocated across the membrane. If this is the case the accumulation should be sensitive to the pH of the surrounding medium. To investigate this aspect of transport further, dopamine uptake in LUVETs was examined under two situations: a) where the transmembrane electrochemical potential was held constant utilizing a defined Na^+/K^+ ion gradient in the presence of valinomycin while the external and internal pH was varied (no pH gradient was present; Fig. 41A); b) where the electrochemical potential was varied by creating different transmembrane pH gradients (in the absence of a K^+ ion gradient), maintaining an internal pH of 4.5 and varying the external pH (Fig. 41B). The first situation clearly demonstrates a pH optimum for uptake of dopamine by LUVETs. The distribution of $[^3\text{H}]\text{-MTPP}^+$ in these systems indicated that a constant membrane potential (-120mV) was established by the K^+ ion gradient in the presence of valinomycin at all pH values examined. The maximum level of dopamine uptake occurs in the range of pH 7.5–8.5, which is similar to the pH optimum (pH 8.3) demonstrated for biological amine transport by granule membranes (Maron *et al.*, 1979). Above pH 8.5 the levels of uptake decrease markedly, presumably due a decrease in the availability of the protonated form of the amine. This is supported by data which indicate that at pH 9.5 the rate of dopamine uptake is reduced, therefore longer incubations would be required to obtain levels of uptake demonstrated at pH 8.0. Lowering the pH below 6.5 results in a decrease in the level of

Fig. 41. Influence of external pH on dopamine uptake. (A) Dopamine uptake by egg PC LUVETs with a constant membrane potential established by a valinomycin induced K^+ ion diffusion potential and no pH gradient (initially external pH = internal pH). The buffer system utilized is described in section 5.2. The symbols represent uptake in the presence of valinomycin. (B) Dopamine uptake by vesicles with varying membrane potential established by trapping a low pH (pH 4.65), and exchanging the untrapped buffer with buffers of varying pH (see section 5.2). The symbols represent uptake in the absence of added ionophores. Uptake was evaluated in both experiments after a 2 hr incubation at room temperature.



amine uptake where at pH 4.5 control (systems which lack a Na^+/K^+ ion gradient) levels of uptake are obtained. This is also reflected in Fig. 41B, however in this situation the magnitude of the membrane potential is varying according to the pH gradient present. This is indicated in the data presented in Fig. 42, which demonstrate the relationship between the membrane potential measured by the distribution of $[\text{}^3\text{H}]\text{-MTPP}^+$ and the value calculated based on the initial transmembrane H^+ gradient. Deviations from the ideal potential probably result from dissipation of the pH gradient due to H^+ permeability such that the initial pH gradient is not an accurate measure of the pH gradient at the time the potential was assessed with MTPP $^+$. This pH dependency of dopamine uptake may reflect the reduced permeability of dopamine at the lower pH values, arguing that the protonated form of the amine can not permeate across the lipid bilayer and thus cannot be transported. Evaluation of the passive permeability of entrapped dopamine (at a concentration of 40 mM) indicate, however, that at pH 4.5 and 7.5 (where greater than 99% of the dopamine is present in a protonated form), 80% of the entrapped amine is released within 1 hr.

5.3.3 Influence of trapped ATP on dopamine accumulation

It has been proposed by several investigators that the large (125 mM) concentration of ATP within the chromaffin granule may effectively trap internalized catecholamines in the form of mixed amine-nucleotide aggregates allowing for accumulation of amines as they diffuse across the membrane against an effective "downhill" concentration gradient (Berneis *et al.*, 1969; Berneis *et al.*; 1974). The influence of trapped ATP on the electrochemical driven transport of dopamine by LUVET's is shown in Fig. 43. The presence of trapped ATP increased the level of dopamine accumulation five fold compared to the similar situation in the absence of ATP, obtaining levels of 180 nmoles dopamine/ μmole lipid in vesicles with a transmembrane pH gradient (interior acid) and a trap of 125 mM ATP. This accumulation appears to be dependent on the transmembrane electrochemical gradient since control samples with trapped ATP and no pH gradient, either 4.5 or 7.5 inside and outside, showed no accumulation of dopamine indicating that ATP is not capable of acting as a passive trapping

Fig. 42. Comparison between the membrane potentials obtained for various pH gradients as detected by [^3H]-MTPP $^+$ and the theoretical potentials based on the H^+ ion gradient as predicted by the Nernst equation. LUVETs were prepared as described in Fig. 41B and section 5.2. The membrane potential was determined employing [^3H]-MTPP $^+$ (see section 3.2.6) in the presence (■) and absence (□) of CCCP after a 2 hr incubation at room temperature to ensure equilibration of the probe. The dashed line indicates the theoretical potential given by the Nernst equation: $\Delta\psi \text{ (mV)} = -59 \log ([\text{H}^+]_i/[\text{H}^+]_p)$

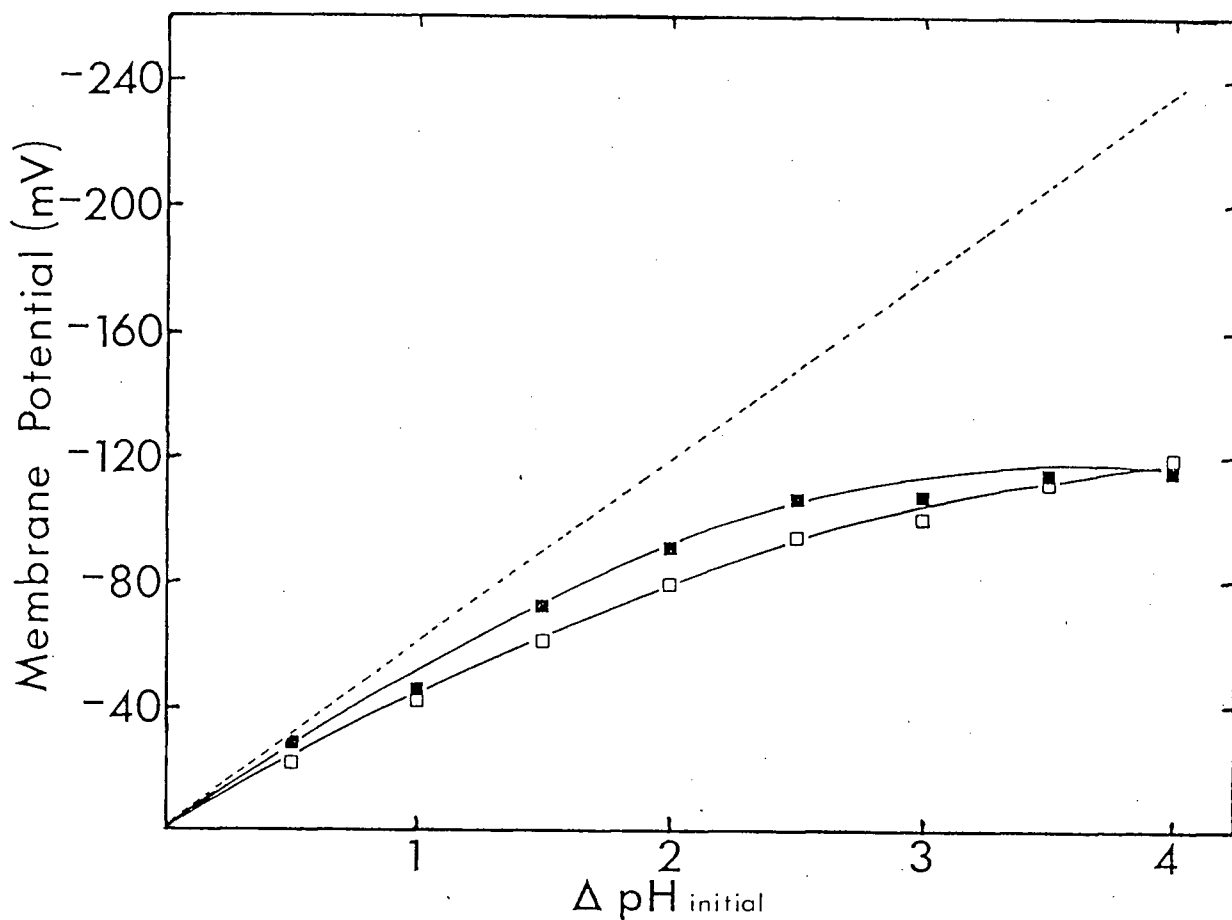
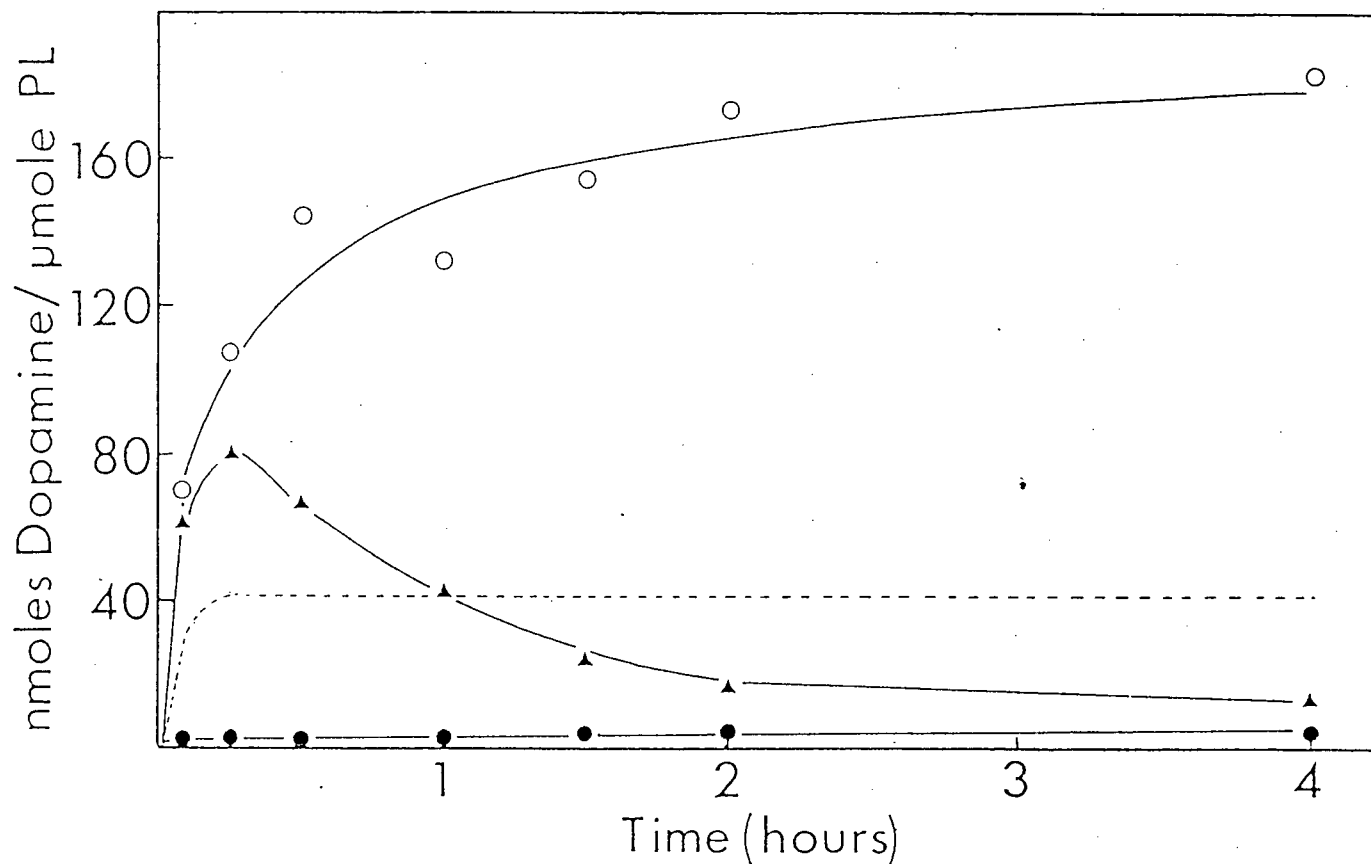


Fig. 43. Effect of trapped ATP on dopamine accumulation by LUVETs composed of EPC. LUVETs were prepared as described in section 5.2, such that 125 mM ATP was trapped within the vesicles. The conditions for dopamine uptake were as described in Fig. 39. The closed circles represent uptake by control samples, which had trapped ATP with no pH gradient (pH interior = pH exterior). The other symbols represent uptake in the absence of added ionophores (○), or in the presence of both CCCP and valinomycin (▲) at concentrations described in Fig. 39. The dashed line represents uptake by vesicles with a transmembrane pH gradient and no trapped ATP (see Fig. 40).

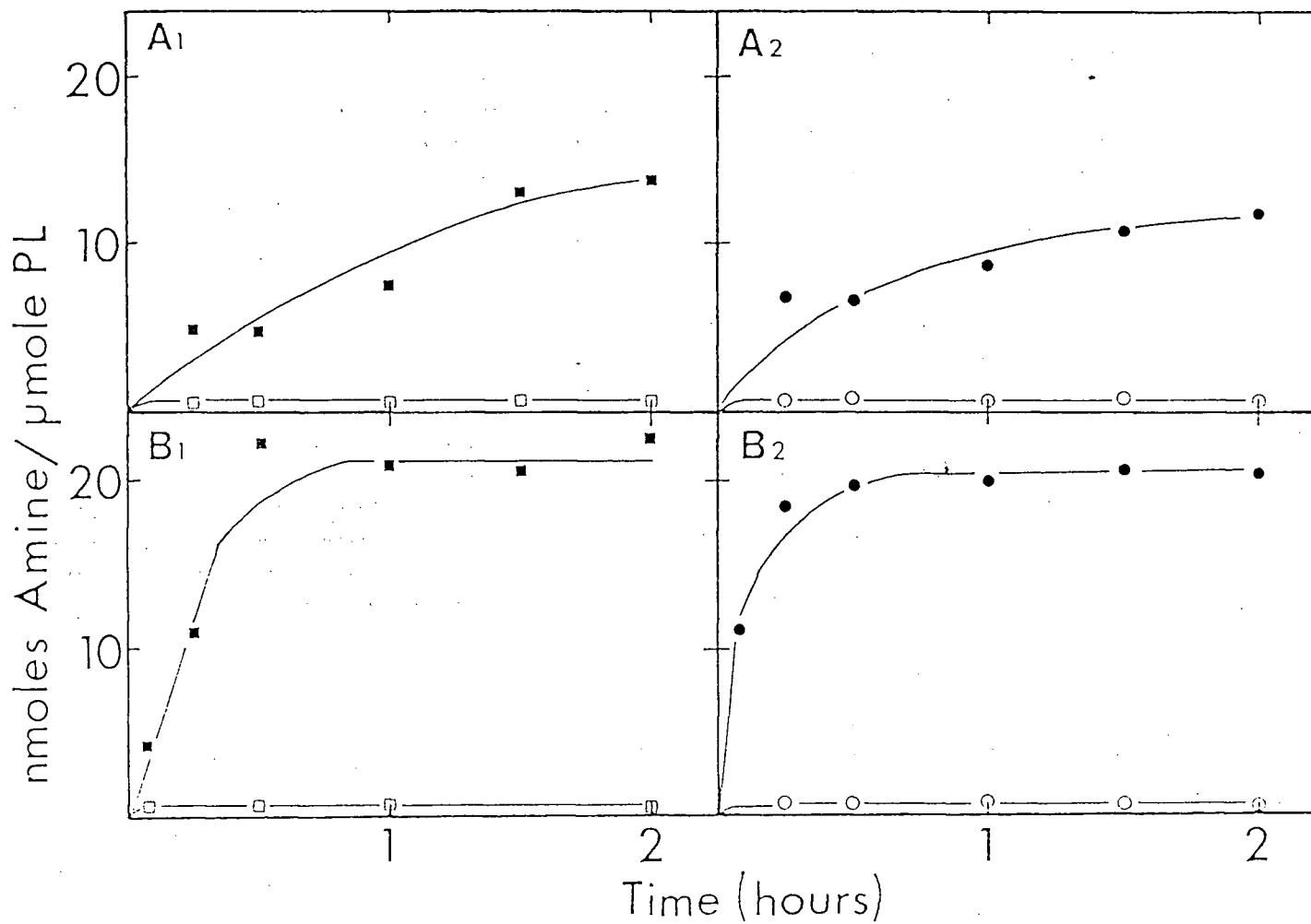


agent. Under the conditions of the uptake assay greater than 80% of the available dopamine was associated with the vesicles, resulting in the formation of a concentration gradient in excess of 500 fold. As before the concentration gradient formed appears to be dependent on the external concentration of amine utilized since similar levels of uptake were obtained when the outside dopamine concentration was 500 μM . Fig. 43 also shows that the presence of both valinomycin and CCCP can uncouple this ATP enhanced accumulation of dopamine, suggesting that if an ATP-dopamine aggregate is formed, the resulting complex can dissociate under conditions where the pH gradient is dissipated.

5.3.4 Electrochemical driven uptake of other biogenic amines

It is of interest to determine whether the accumulation process shown to occur for dopamine is general and could result in the accumulation of other biogenic amines. In particular, it has been demonstrated that a K^+ ion gradient (Kanner, 1983) and transmembrane pH gradient (interior acid; Bangham *et al.*, 1980; Carty *et al.*, 1981) play a role in the transport of serotonin by granule membranes. In addition, both uptake processes appear to be sensitive to a variety of similar inhibitors, such as reserpine. Fig. 44 shows the uptake of epinephrine (Fig. 44A) and serotonin (Fig. 44B) by EPC LUVETs with either a transmembrane Na^+/K^+ ion gradient (K^+ interior; Fig. 44 A1 and B1) or pH gradient (interior acid; Fig. 44 A2 and B2). The uptake of these amines show similar sensitivity to the presence of ionophores as was demonstrated for dopamine uptake. Valinomycin facilitated transport of both epinephrine and serotonin, indicating that a similar mechanism of transport may be responsible for the uptake of these amines. Differences in the level and rate of accumulation may be a reflection of the hydrophilicity of the amine. For example, epinephrine, which contains a hydroxyl on the methylene group adjacent to the catechol ring (see Fig. 38) is accumulated at a slower rate and saturates at lower levels than does dopamine, which lacks this group.

Fig. 44. Time course for the accumulation of epinephrine (A) and serotonin (B) by EPC LUVET systems with either a Na^+/K^+ ion gradient (1) or a transmembrane pH gradient (2). Gradients were formed as described in Figs. 39 and 40. Open symbols represent uptake in control samples which lacked a transmembrane ion gradient. The other symbols represent uptake in the presence of valinomycin (■) and in the absence of added ionophores (●).



Discussion

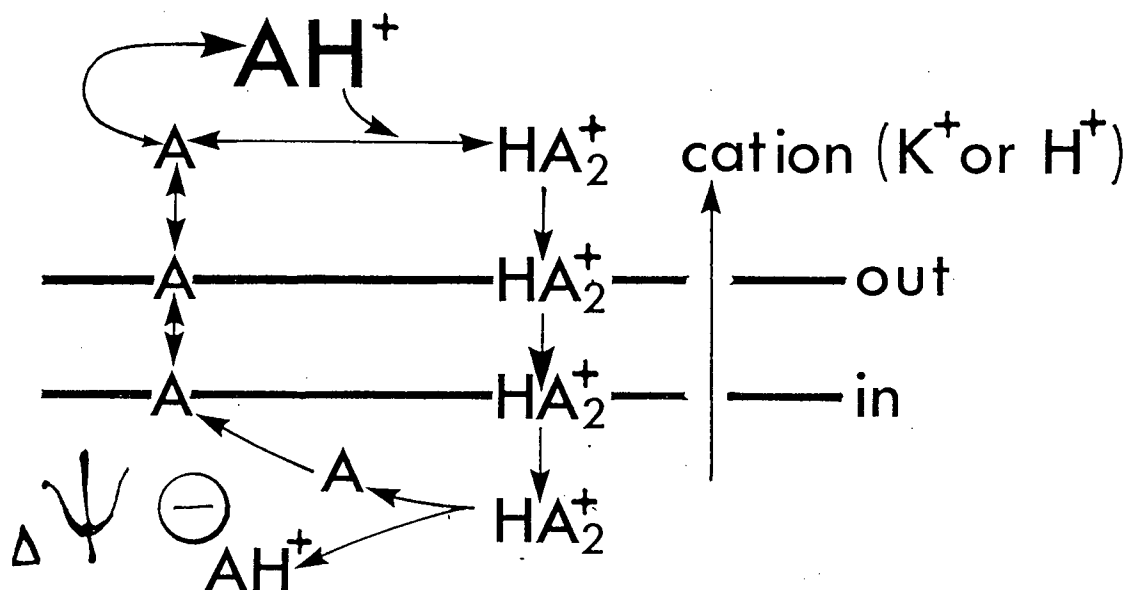
This investigation clearly demonstrates that biogenic amines can be accumulated into large unilamellar vesicles systems in the absence of a specific carrier protein. This transport appears to be driven by an electrochemical potential gradient established by either a transmembrane Na^+/K^+ ion gradient (K^+ interior) or a pH gradient (acid interior). There are two areas of interest generated by the data presented here. The first concerns the mechanism whereby biological amines are accumulated in LUVETs and the second has to do with the physiological relevance of this accumulation process with regard to the transport, and inhibition of transport, of biological amines *in vivo*. Each of these areas will be discussed in turn.

Previous investigators (Schuldiner *et al.*, 1978; Johnson *et al.*, 1978; Johnson *et al.*, 1981; Maron *et al.*, 1983) suggested that the mechanism of dopamine uptake was dependent on the amine distributing across the vesicle membrane according to the transmembrane pH gradient, resulting in accumulation of the amine inside an acidic vesicle. This mechanism implied that the neutral form of the weakly basic amine permeates the membrane and was supported by investigations demonstrating that liposomes composed of soyabean lipids were impermeable to the protonated form of biological amines. Others (Knoth *et al.*, 1980; Maron *et al.*, 1979) have argued that amines are transported in the protonated form rather than the neutral form, a hypothesis which is supported by data that showed chromaffin granule ghosts are not permeable to the neutral species of the amine and that ATP dependent uptake of biological amines by chromaffin granule ghosts did not result in alkalinization of the vesicle (Knoth *et al.*, 1983). In addition, since the pK_a of the amine group of these molecules is relatively high (for dopamine the pK_a is approximately 9.9), the predominant species present at physiological pH is the protonated form and hence the neutral form would not be as available for transport. For numerous reasons the results presented here are consistent with the concept that dopamine is transported in a charged form. First, dopamine uptake can be driven by a K^+ ion diffusion potential (negative interior), which is initially established in the absence of a pH gradient (see Fig. 39). This accumulation is facilitated under conditions where K^+

efflux occurs, *ie.* in the presence of valinomycin, suggesting an electroneutral K^+ /dopamine exchange process similar to that postulated in the previous chapter for safranin. It should be noted, however, that it is possible that the charge gradient established by addition of valinomycin may engender a H^+ gradient by a H^+/K^+ exchange mechanism. Second, if dopamine uptake relies on the movement of the neutral species and the resulting distribution is dependent on the pH gradient, then one would expect that larger exterior concentrations of dopamine would result in increased accumulation. This does not appear to be the case as saturation levels of 40 nmoles dopamine/ μ mole lipid were obtained utilizing exterior dopamine concentrations from 200 μM to 1 mM. Third, since other biological amines are also weak bases, the uptake of these amines should be similar under conditions where the amine accumulates in accordance to the pH gradient. The data in Fig. 44 suggest that this does not occur, epinephrine and serotonin are accumulated at different rates and to a lesser extent than dopamine in response to LUVETs with similar transmembrane pH gradients. Finally, it was demonstrated that dopamine is permeable at a pH where the amine exists primarily in a protonated form (pH 4.5 and 7.5), indicating that this species is capable of crossing the egg PC bilayer. This data would also suggest that an additional factor, other than a low internal pH, is required for maintaining the level of dopamine which has been accumulated.

In order to investigate the role of charge on the transport of dopamine, uptake was investigated under conditions where there was a constant membrane potential (established by a K^+ ion gradient in the presence of valinomycin) and no pH gradient (Fig. 41A) or a variable electrochemical potential (Fig. 41B) as established by changes in the transmembrane pH gradient. These data indicate that at pH 4.5, where the amine is present in the protonated form, there is no transport of the molecule, even under conditions where a substantial (greater than 100 mV) negative potential is present. This result is clearly inconsistent with the model of uptake based on the protonated form of the amine being transported across the vesicle membrane. However, it can be suggested (Fig. 45) that the charged permeant species is a HA_2^+ complex formed between a protonated amine and a neutral amine. Therefore at pH 4.5 uptake of the amine would be limited due to the reduced presence of the neutral species.

Fig. 45. Postulated mechanism for the uptake of dopamine by large unilamellar vesicles.



Further, optimal uptake would occur at a pH close to the pKa of the amine examined, as indicated in Fig. 41A. Formation of a HA_2^+ complex has been postulated previously as a mechanism for the permeation of local anesthetics through bilayer membranes (McLaughlin, 1975). This model of uptake still suggests that biological amine transport in LUVETs occurs by an electroneutral cation (H^+ or K^+)/ cation (HA_2^+) antiport mechanism that is driven by the membrane potential (interior negative). In addition, the presence of the membrane potential (negative interior) would inhibit the efflux of the positively charged amine, therefore dissociation of the HA_2^+ complex in the vesicle interior would "trap" the protonated form of the amine resulting in net accumulation. The neutral amine would be free to shuttle across the membrane.

It is difficult to differentiate between the mechanism suggested here, and the previous mechanisms based on the equilibration of the amine according to the pH gradient. In all the uptake experiments presented in this chapter the presence of a negative membrane potential was maintained, whether the result of a H^+ or a K^+ ion diffusion potential. Similarly, in membrane systems which have demonstrated ATP independent uptake of biogenic amines in response to a pH gradient (Schuldiner *et al.*, 1978; Johnson *et al.*, 1978; Knoth *et al.*, 1980; Johnson *et al.*, 1981; Maron *et al.*, 1983; Nichols and Deamer, 1976; Carty *et al.*, 1981; Maron *et al.*, 1979), the pH gradient present would also result in formation of a negative potential. It has been demonstrated that in the absence of ATP the membrane potential present across the chromaffin granule membrane approximates the H^+ equilibrium potential of -70 mV (Holz, 1979). Further, the results present here do not preclude the possibility that dopamine may be translocated in a protonated form in association with a counterion such as Cl^- .

Although the accumulation of dopamine by LUVET systems shows similarities to the uptake of biological amines *in vivo*, it is difficult to relate the two situations. It has been demonstrated, for example, that the chromaffin granule membrane supports a positive (interior) membrane potential in the presence of ATP and Mg^{2+} (Holz, 1979) yet can still transport amines. The model suggested here clearly depends on the presence of a transmembrane

potential that is negative interior. In addition, the uptake of dopamine could not be demonstrated in vesicles which had a transmembrane pH gradient (interior acid) and a positive (interior) membrane potential (40 mV; established by a Cl^- ion diffusion potential, *ie.* a $\text{glutamate}^-/\text{Cl}^-$ gradient (Cl^- interior); unpublished observation). It is not clear from these experiments whether the pH gradient is maintained under conditions where a positive (interior) membrane potential exists. Further, the rate of uptake by vesicles composed of EPC is substantially slower than that demonstrated for amine uptake in chromaffin granules. This rate, however, would be markedly sensitive to the lipid composition and temperature as indicated in the previous chapter (see section 4.3.1), and may be enhanced if a lipid composition similar to that of the chromaffin granule membrane is utilized at 37°C.

The role of ATP as a trapping agent responsible for the storage of catecholamines in chromaffin granules is supported by data presented in this report. This data (see Fig. 43) suggests that formation of the ATP-dopamine complex increases the vesicle's capacity for accumulating biogenic amines. The mechanism of uptake, however, would still be dependent on an electrochemical potential (interior negative) driven cation/cation exchange mechanism postulated previously. This is indicated by data which demonstrated that dissipation of the electrochemical gradient by addition of both a H^+ and a K^+ ionophore inhibited uptake of dopamine in these ATP containing vesicles. This would also suggest that the ATP-amine complex allows for rapid exchange with the free amine pool and could not act as a passive trapping agent as suggested by Berneis *et al.* (1974).

The general mechanism of lipophilic cation transport presented here and in the previous chapter, based on an electrochemically driven uptake process suggests that the presence of a transmembrane potential could have an important role in regulating the uptake of biological amines *in vivo*. It is demonstrated that both epinephrine and serotonin can be accumulated in vesicles in response to a membrane potential (Fig. 44), suggesting that the uptake process is relatively non-specific. In addition, it is interesting to note that a variety of inhibitors of biogenic amine transport in biological systems, such as reserpine and imipramine, are lipophilic cations. Due to the greater hydrophobicity of these cations, they may be able

to compete with or block amine uptake and/or release. Generally, a single inhibitor shows a broad specificity for a number of different amine transport systems. Reserpine, for example, inhibits catecholamine uptake in chromaffin granules (Kanner *et al.*, 1979) as well as serotonin uptake in serotonin granules of blood platelets (Maron *et al.*, 1979). Further, it has been shown that the putative transporter molecule for biogenic amines also has a broad specificity for a variety of substrates, such as hydroxyindolamines, hydroxyquinolines, tetrabeozine and reserpine like alkaloids (Maron *et al.*, 1983), which all have lipophilic and cationic characteristics. Finally, the influence of local anesthetics, which are accumulated in a similar manner as described for dopamine (Mayer *et al.*, 1984), on the uptake and release of these biologically active neurotransmitters and hormones is of obvious interest.

SUMMARIZING DISCUSSION

The studies presented in this thesis illustrate the utility of model membrane systems to investigate the structural and functional properties of lipids in biological membranes. The simplest model system which can be generated involves hydrating a dry lipid film. The resulting multilamellar vesicles (MLVs) are useful for characterizing the structural properties of lipids in membranes. This is demonstrated by the investigations of Chapter 2 which examine the influence of cholesterol on the polymorphic phase properties of lipids. These studies support the surprising conclusion that cholesterol engenders formation of non-bilayer H_{11} phase structures and hence serves to destabilize the bilayer structure of membranes. This property is illustrated by model systems containing PS and PE where the presence of cholesterol, in conjunction with physiological concentrations of Mg^{2+} (2 mM), can reduce the level of Ca^{2+} required to trigger H_{11} -phase structure in these systems from 4 to 0.25 mM, a concentration which more closely approximates that observed in vivo. These results suggest that a role of cholesterol in membranes may be to facilitate processes that require the formation of non-lamellar structures, as may be the case in Ca^{2+} induced membrane fusion events.

With regard to the ability of phospholipids to assume formation of non-bilayer structures in membranes the results of Chapter 2 also demonstrate that in complex multicomponent systems individual phospholipids have no tendency to associate with any one particular phase in samples where bilayer, hexagonal and "isotropic" phases coexist. This suggests that in complex lipid systems, such as the biological membrane, that different, functionally significant, structural phases could be assumed without the segregation of individual lipid species into distinct domains.

The next area of investigation concerns the barrier properties of lipid membranes and the influence of a membrane potential on certain transport processes. For studies such as these MLVs are of limited value, thus a more sophisticated large unilamellar vesicle (LUV) model system was developed and utilized. The procedure, described in Chapter 3, required the

repeated extrusion of multilamellar vesicles under moderate pressures (less than 500 psi) through polycarbonate filters with a defined pore size of 100 nm. The resulting LUVETs (large unilamellar vesicles by extrusion techniques) are shown to be unilamellar with diameters in the range of 60–100 nm and trapped volumes in the region of 1–3 $\mu\text{l}/\mu\text{mole}$. Particular advantages of this procedure are that lipid solubilizing agents (such as organic solvents and detergents) are not required and vesicles can be prepared reproducibly from a variety of different lipid species and mixtures. This model large unilamellar vesicle system, therefore, provides a very attractive model system.

This vesicle preparation was used to model a basic feature of biological membranes, namely the presence of a transmembrane potential. Vesicles exhibiting a membrane potential were obtained by imposing a Na^+/K^+ ion gradient (K^+ inside) across the vesicle membrane. This ion gradient resulted in the formation of a $\Delta\psi$ (as detected by the lipophilic cation MTPP $^+$), the magnitude of which correlated well with the transmembrane concentration gradient and showed a time dependent decay which reflected the flux of Na^+ into the vesicles.

This model system exhibiting a transmembrane potential was employed to investigate the role of $\Delta\psi$ in certain transport functions of membranes. In particular an ability to accumulate a variety of molecules which have lipophilic and cationic characteristics is demonstrated. In Chapter 4 this accumulation process was characterized using the dye safranine O. It is concluded that accumulation of this molecule proceeds by a antiport $\text{K}^+/\text{safranine}$ exchange process that is driven by the transmembrane potential. The transport resulted in the rapid formation of a large (greater than 100 fold) transmembrane concentration gradient of safranine and clearly reflected a very efficient transport mechanism.

The generality of this transport process is shown in chapters 4 and 5, where it is demonstrated that a variety of biologically active lipophilic cations can be accumulated by vesicles to achieve interior cation concentrations which are more than two orders of magnitude higher than exterior concentrations. These cations include the drugs chlorpromazine, dibucaine, propranolol, vinblastine and adriamycin; and the biogenic amines dopamine, serotonin and epinephrine. Biogenic amine accumulation occurred in response to vesicles exhibiting either

transmembrane H^+ or K^+ diffusion potentials, a result which indicates that the uptake of these molecules in vivo could proceed without a requirement for a specific transport protein.

The observations made in this thesis define several areas of research that warrant further investigation. In particular, the model membrane system described here exhibiting a $\Delta\psi$ can be utilized to examine other $\Delta\psi$ dependent transport processes, such as those involved in metabolite and protein transport, as well as protein insertion and transbilayer distribution of charged lipid components. Research within the immediate future, however, should concentrate on evaluating the relationship between the physical and structural properties of lipids and the permeability of membranes to small ions. As indicated in the introduction present studies do not clearly define the basic permeability properties of lipids in membranes. Difficulties are due to the variety of different model systems utilized, the presence of impurities which complicate the interpretation of results, and the complexities involved in determining ion flow under conditions where a membrane potential exists, all aspects which have been considered at various points in this thesis. Clearly by utilizing the model system described here, in the presence of appropriate ion gradients and ionophores, definitive information regarding the roles of different lipid species in mediating permeability properties should be obtainable.

BIBLIOGRAPHY

- Ames, B. and Dubin, C. (1960) *J. Biol. Chem.* **235**, 769-775.
- Arnold, K., Lösche, A., and Gawrish, K. (1981) *Biochim. Biophys. Acta* **645**, 143-148.
- Bally, M.B., Tilcock, C.P.S., Hope, M.J., and Cullis, P.R. (1983) *Can. J. Biochem.* **61**, 346-352.
- Bally, M.B., Hope, M.J., van Echteld, C.J.A., and Cullis, P.R. (1984) *Biochim. Biophys. Acta*, in press.
- Bally, M.B., Mayer, L.D., Loughrey, H., Hope, M.J., and Cullis, P.R. (1984) *J. Biol. Chem.*, submitted.
- Bangham, A.D., Standish, M.M., and Watkins, J.D. (1965) *J. Mol. Biol.* **13**, 238-244.
- Bangham, A.D., Hill, M.W., and Miller, N.G.A. (1974) *Meth. Membrane Biol.* **1**, 1-68.
- Bangham, A.D., Hill, M.W., and Mason, W.T. (1980) in *Molecular Mechanisms of Anesthesia*, Vol. 2 (Fink, B.R. ed.), Raven Press, N.Y., pp. 69-77.
- Benz, R., Frohlich, O., Lauger, P., and Mandol, M. (1975) *Biochim. Biophys. Acta* **394**, 323-334.
- Benz, R., Frohlich, O., and Lauger, P. (1977) *Biochim. Biophys. Acta* **464**, 465-481.
- Berneis, K.H., Pletscher, A., and da Prada, M. (1969) *Nature* **224**, 281.
- Berneis, K.H., da Prada, M., and Pletscher, A. (1974) *Nature* **248**, 604-606.
- Blaurock, A.E. (1982) *Biochim. Biophys. Acta* **650**, 167-207.
- Bligh, E.G. and Dyer, W.J. (1959) *Can. J. Biochem. Physiol.* **37**, 911-918.
- Bloch, K.E. (1981) *CRC Crit. Rev. Biochem.* **14**, 47-92.
- Blok, M.C., van Deenen, L.L.M., and de Gier, J. (1976) *Biochim. Biophys. Acta* **433**, 1-12.
- Blok, M.C. (1977) Ph.D. Thesis, 22-27.
- Blume, A. and Ackerman, T. (1974) *FEBS Letters* **43**, 71-74.
- Boggs, J.M. (1980) *Can. J. Biochem.* **58**, 755-770.
- Böttcher, C.J.F., van Gent, C.M., and Pries, C. (1961) *Anal. Chim. Acta* **24**, 203-204.
- Bretscher, M.S. (1973) *Science* **181**, 622-629.
- Brockerhoff, H. and Yurkowski, M. (1965) *Can. J. Biochem.* **43**, 1777-1785.
- Broekhuysse, R.M. (1969) *Clin. Chim. Acta* **23**, 457-461.
- Bunldt, G., Gally, H.U., Seelig, J., and Zaccari, G. (1979) *J. Mol. Biol.* **134**, 673-691.
- Cameron, D.G., Gudgin, E.F., and Mantsch, H.H. (1981) *Biochemistry* **20**, 4496-4500.

- Carty, S.E., Johnson, R.G., and Scarpa, A. (1981) *J. Biol. Chem.* **256**, 11244-11250.
- Chapman, D. (1966) *Ann. N. Y. Acad. Sci.* **137**, 745-762.
- Chapman, D., Urbino, J., and Keough, K.M. (1974) *J. Biol. Chem.* **249**, 2512-2516.
- Chapman, D. (1968) in *Biological Membranes Vol. 1* (Chapman, D. ed.), Academic Press, N.Y., pp. 125-153.
- Chapman, D. (1975) *Quart. Rev. Biophys.* **8**, 185-235.
- Chapman, D. and Correll, B.A. (1977) in *Structure of Biological Membranes* (Abrahamsson, S. and Poscher, I. eds.), Plenum Press, N.Y., pp. 85-94.
- Chapman, D. (1980) in *Membrane Structure and Function, Vol. 1* (Bittar, E.E. ed.), Wiley & Sons, N.Y., pp. 103-152.
- Collard, J.G., de Wildt, A., Oomen-Meulemons, E.P.M., Smeekens, J., and Emmelot, P. (1977) *FEBS Letters* **77**, 173.
- Colonna, R., Massari, S., and Azzone, G.F. (1973) *Eur. J. Biochem.* **34**, 577-585.
- Comfurius, P. and Zwaal, R.F.A. (1977) *Biochim. Biophys. Acta* **488**, 36-42.
- Cornell, B.A., Sacre, M.M., Peel, W.E., and Chapman, D. (1978) *FEBS Letters* **90**, 29-35.
- Creutz, C.E., Pazoles, C.J., and Pollard, H.B. (1978) *J. Biol. Chem.* **253**, 2858-2866.
- Cullis, P.R. and de Kruijff, B. (1978a) *Biochim. Biophys. Acta* **507**, 207-218.
- Cullis, P.R. and de Kruijff, B. (1978b) *Biochim. Biophys. Acta* **513**, 31-42.
- Cullis, P.R., van Dijck, P.W.M., de Kruijff, B., and de Gier, J. (1978a) *Biochim. Biophys. Acta* **513**, 21-30.
- Cullis, P.R., Verkleij, A.J., and Ververgaert, P.H.J.Th. (1978b) *Biochim. Biophys. Acta* **513**, 11-20.
- Cullis, P.R. and de Kruijff, B. (1979) *Biochim. Biophys. Acta* **559**, 399-420.
- Cullis, P.R., de Kruijff, B., Hope, M.J., Nayar, R., and Schimd, S. (1980) *Can. J. Biochem.* **58**, 1091-1100.
- Cullis, P.R., de Kruijff, B., Hope, M.J., Verkleij, A.J., Nayar, R., Farren, S.B., Tilcock, C.P.S., Madden, T.D., and Bally, M.B. (1983) in *Membrane Fluidity in Biology, Vol. 1* (Aloia, R.C. ed.), Academic Press, N.Y., pp. 40-83.
- Danielli, J.F. and Davson, H. (1935) *J. Cell Comp. Physiol.* **5**, 495-502.
- Davis, J.H. (1983) *Biochim. Biophys. Acta* **737**, 117-171.
- Dean, W.L. and Tanford, C. (1977) *J. Biol. Chem.* **252**, 3351-3356.
- de Kruijff, B., Verkleij, A.J., van Echteld, C.J.A., Gerritsen, W.J., Mombers, C., Noordam, P.C., and Gier, J. (1979) *Biochim. Biophys. Acta* **555**, 200-209.

- de Kruijff, B. and Cullis, P.R. (1980) *Biochim. Biophys. Acta* **602**, 477-490.
- de Kruijff, B., Cullis, P.R., Verkleij, A.J., Hope, M.J., van Echteld, C.J.A., and Taraschi, T.F. (1984) in *Enzymes of Biological Membranes* (Martinosi, A. ed.), Plenum Press, N.Y., pp. 131-204.
- Demel, R.A., Geurts van Kessel, W.S.M., and van Deenen, L.L.M. (1972) *Biochim. Biophys. Acta* **266**, 26-37.
- Demel, R.A. and de Kruijff, B. (1976) *Biochim. Biophys. Acta* **457**, 109-132.
- Demel, R.A., Jansen, J.W.C.M., van Dijck, P.W.M., and van Deenen, L.L.M. (1977) *Biochim. Biophys. Acta* **465**, 1-10.
- Dervichian, D.G. (1964) *Prog. Biophys. and Mol. Biol.* **14**, 263.
- Devaux, P.F. and Seigneuret, M. (1984) *Biochim. Biophys. Acta*, in press.
- Dluhy, D.G., Cameron, D.G., Mantsch, H.H., and Mendelson, R. (1983) *Biochemistry* **22**, 6312-6325.
- Edholm, O. (1981) *Chem. Phys. Lipids* **29**, 213-224.
- Eytan, G.D. (1982) *Biochim. Biophys. Acta* **694**, 185-202.
- Etemadi, A.H. (1980a) *Biochim. Biophys. Acta* **604**, 347-422.
- Etemadi, A.H. (1980b) *Biochim. Biophys. Acta* **604**, 423-475.
- Farren, S.B. and Cullis, P.R. (1980) *Biochem. Biophys. Res. Commun.* **97**, 182-191.
- Farren, S.B., Sommerman, E., and Cullis, P.R. (1984) *Chem. Phys. Lipids*, in press.
- Fettiplace, R., Gordon, L.G.M., Hladky, S.R., Reequene, J., Zingshen, H.B., and Haydon, D.A. (1974) in *Methods in Membrane Biology*, Vol. 4 (Korn, E.D. ed.), Plenum Press, N.Y., pp. 1-75.
- Finean, J.B. and Robertson, J.D. (1958) *Br. Med. Bull.* **14**, 267.
- Frye, C.D. and Edidum, M. (1970) *J. Cell Sci.* **7**, 313-321.
- Fujimura, T., Yamoto, I., and Anraku, Y. (1983) *Biochemistry* **22**, 1959-1967.
- Fukami, M.H., Bauer, J.S., Steward, G.J., and Salganicoff, L. (1978) *J. Cell Biol.* **77**, 389-399.
- Gennis, R.B. and Strominger, J.L. (1976) *J. Biol. Chem.* **251**, 1264-1271.
- Gorter, E. and Grendel, F. (1925) *J. Exp. Med.* **41**, 439-443.
- Grant, C.W.M. and McConnel, H.M. (1974) *Proc. Natl. Acad. Sci. USA* **71**, 4653-4657.
- Harlos, K., Stumpel, J., and Eibl, H. (1979) *Biochim. Biophys. Acta* **555**, 409-416.
- Harris, E.J. and Baum, H. (1980) *Biochem. J.* **192**, 551-557.

- Hauser, H., Oldami, D., and Phillips, M.C. (1973) *Biochemistry* **12**, 4507-4513.
- Hendler, R.W. (1971) *Physiol. Rev.* **51**, 66-97.
- Hilder, S. and Hakin, L. (1976) *Biochem. Biophys. Res. Commun.* **69**, 521-526.
- Holz, R.W. (1979) *J. Biol. Chem.* **254**, 6703-6709.
- Hong, K., Duzgunes, N., and Papahadjopoulos, D. (1981) *J. Biol. Chem.* **256**, 3641-3643.
- Hope, M.J. and Cullis, P.R. (1979) *FEBS Letters* **107**, 323-326.
- Hope, M.J. and Cullis, P.R. (1980) *Biochem. Biophys. Res. Commun.* **92**, 846-852.
- Hope, M.J. and Cullis, P.R. (1981) *Biochim. Biophys. Acta* **640**, 82-90.
- Hope, M.J., Walker, D.C., and Cullis, P.R. (1983) *Biochem. Biophys. Res. Commun.* **110**, 15-22.
- Hope, M.J., Bally, M.B., Webb, G., and Cullis, P.R. (1984) *Biochim. Biophys. Acta*, in press.
- Huang, C.H. (1977) *Lipids* **12**, 348-356.
- Hubbel, W.L. and McConnell, H.M. (1971) *J. Am. Chem. Soc.* **93**, 314.
- Israelachvili, J.N., Mitchell, D.J., and Ninham, B.W. (1977) *Biochim. Biophys. Acta* **470**, 185-201.
- Jacobs, S. and Cuatrecasas, P. (1977) *Proc. Natl. Acad. Sci. USA* **73**, 4410-4416.
- Jain, M.K. and Wagner, R.C. (1980) in *Introduction to Biological Membranes*, p. 134. Published by John Wiley and Sons, N.Y.
- Johnson, M. and Edidin, M. (1978) *Nature* **272**, 448.
- Johnson, R.G., Carlson, N.J., and Scarpa, A. (1978) *J. Biol. Chem.* **253**, 1512-1521.
- Johnson, R.G., Carty, S.E., and Scarpa, A. (1981) *J. Biol. Chem.* **256**, 5773-5780.
- Kachar, B. and Reese, T.S. (1982) *Nature* **296**, 464-466.
- Kanner, B.I. (1983) *Biochim. Biophys. Acta* **726**, 293-316.
- Kanner, B.I., Fishkes, H., Maron, R., Sharon, I., and Schuldiner, S. (1979) *FEBS Letters* **100**, 175-178.
- Kates, M. and Sastry, P.S. (1969) *Meth. Enzym.* **14**, 197-211.
- Kawasaki, Y., Wakayanon, N., Kaike, T., Kawai, M., and Amano, T. (1978) *Biochim. Biophys. Acta* **509**, 440-451.
- Kawato, S., Kinoshita, K., and Ikegami, A. (1978) *Biochemistry* **14**, 3927-3933.
- Kimelberg, H.K. (1977) in *Dynamic Aspects of Cell Surface Organization* (Poste, G. and Nicolson, G.L. eds), North-Holland Publishing Co., Amsterdam, pp. 205-293.

- Kirby, C.J. and Green, C. (1977) *Biochem. J.* **168**, 575-577.
- Kleeman, W. and McConnel, H.M. (1976) *Biochim. Biophys. Acta* **419**, 206-222.
- Knoth, R., Stern, Y., Kanner, B.I., and Schuldiner, S. (1981) *Biochemistry* **19**, 2938-2942.
- Korn, E.D. (1966) *Science* **153**, 1491-1498.
- Ladbroke, B.D., Williams, R.M. and Chapman, D. (1968) *Biochim. Biophys. Acta* **156**, 333-340.
- Lee, A.G. (1975) *Prog. Biophys. Molec. Biol.* **29**, 3-56.
- Lichtshstein, D., Kaback, R.H., and Blume, A.J. (1979) *Proc. Natl. Acad. Sci. USA* **76**, 650-654.
- Lombardi, F.J., Reeves, J.P., Short, S.A., and Kaback, H.R. (1974) *Ann. N.Y. Acad. Sci.* **227**, 312-323.
- Luzzatti, V. and Husson, F. (1962) *J. Cell. Biol.* **12**, 207-219.
- Luzzatti, V. (1968) in *Biological Membranes* (Chapman D. ed.), Academic Press, N.Y., pp. 71-123.
- Luzzatti, V., Gulik-Krzywicki, T., and Tardieu, A. (1968) *Nature* **218**, 1031-1034.
- Luzzatti, V. and Tardieu, A. (1974) *Ann. Rev. Phys. Chem.* **25**, 79-94.
- Madden, T.D., Chapman, D., and Quinn, P.J. (1979) *Nature* **279**, 538.
- Madden, T.D. and Cullis, P.R. (1981) *Biochim. Biophys. Acta* **684**, 149-153.
- Madden, T.D. and Cullis, P.R. (1984) *J. Biol. Chem.*, in press.
- Maron, R., Kanner, B.I., and Schuldiner, S. (1979) *FEBS Letters* **98**, 237-240.
- Maron, R., Stern, Y., Kanner, B.I., and Schuldiner, S. (1983) *J. Biol. Chem.* **258**, 11476-11481.
- Martin, D.L. (1973) *J. Neurochem.* **21**, 345-356.
- Marsh, D., Watts, A., Maschke, W., and Knowles, P.F. (1978) *Biochem. Biophys. Res. Commun.* **81**, 397-400.
- Marsh, D. and Seddon, J.M. (1982) *Biochim. Biophys. Acta* **690**, 117-123.
- Mayer, L.D., Bally, M.B., Hope, M.J., and Cullis, P.R. (1984a) *J. Biol. Chem.*, submitted.
- Mayer, L.D., Bally, M.B., Hope, M.J., and Cullis, P.R. (1984b) *Exp. Clin. Pharmac.*, submitted.
- McLaughlin, S. (1975) in *Progress in Anesthesiology* (Fink, R.B. ed.), Raven Press, N.Y., pp. 193-221.
- McNamee, M.G. and McConnell, H.M. (1973) *Biochemistry* **12**, 2951-2960.
- Melchoir, D.L., Morowitz, H.J., Sturtevant, J.M., and Tsang, T.Y. (1970) *Biochim. Biophys. Acta* **219**, 114-123.

- Mimms, L.T., Zampighi, G., Nozaki, Y., Tanford, C., and Reynolds, J.A. (1981) *Biochemistry* **20**, 833-840.
- Nayar, R., Schmid, S., Hope, M.J., and Cullis, P.R. (1982a) *Biochim. Biophys. Acta* **688**, 169-176.
- Nayer, R., Hope, M.J., and Cullis, P.R. (1982b) *Biochemistry* **21**, 4583-4589.
- Njus, D., Knoth, J., and Zallakain, M. (1981) *Curr. Top. Bioenerg.* **11**, 107-147.
- Nicholls, P. and Miller, N. (1974) *Biochim. Biophys. Acta* **356**, 184-191.
- Nichols, J.W. and Deamer, D.W. (1976) *Biochim. Biophys. Acta* **455**, 269-271.
- Nichols, J.W. and Deamer, D.W. (1981) *Proc. Natl. Acad. Sci. USA* **77**, 2038-2042.
- Noordam, P.C., van Echteld, C.J.A., de Kruijff, B. and de Gier, J. (1981) *Biochim. Biophys. Acta* **646**, 483-489.
- Ohki, S. (1972) *Biochim. Biophys. Acta* **282**, 55-71.
- Ohki, S. (1981) *Physiol. Chem. Phys.* **13**, 195-210.
- Ohnishi, S. and Ito, T. (1974) *Biochemistry* **13**, 881-887.
- Oldfield, E. and Chapman, D. (1972) *FEBS Letters* **23**, 285-295.
- Oldfield, E., Gilmore, R., Glaser, M., Gutawski, H.S., Hshung, J.C., Kang, S., Meadows, M., and Rice, D. (1978) *Proc. Natl. Acad. Sci. USA* **75**, 4657-4660.
- Oldfield, E., Gomez-Fernandez, J.C., Goni, F.M., and Chapman, D. (1979) *FEBS Letters* **98**, 224-227.
- Olson, F., Hunt, C.A., Szoka, F.C., Vail, W.J., and Papahadjopoulos, D. (1979) *Biochim. Biophys. Acta* **557**, 9-23.
- Ovchinnikov, Y.A. and Ivanov, V.T. (1977) in *Biochemistry of Membrane Transport* (Semenza, G. and Carafoli, E. eds.), Springer, N.Y., pp. 123-146.
- Pagano, R.E. and Weinstein, J.N. (1978) *Ann Rev. Biophys. Bioeng.* **7**, 435-461.
- Pai, V.S. and Mayment, E.W. (1972) *Molec. Pharmac.* **8**, 82-90.
- Papahadjopoulos, D. and Bangham, A.D. (1966) *Biochim. Biophys. Acta* **126**, 185-188.
- Papahadjopoulos, D., Jacobson, K., Nir, S., and Isac, T. (1973) *Biochim. Biophys. Acta* **311**, 330-339.
- Papahadjopoulos, D., Vail, W.J., Jacobson, K., and Poste, G. (1975a) *Biocim. Biophys. Acta* **394**, 483-491.
- Papahadjopoulos, D., Moscorello, M., Eylar, E.H., and Isac, T. (1975b) *Biochim. Biophys. Acta* **401**, 317-335.

- Papahadjopoulos, D. (1978) in *Membrane Fusion* (Poste, G. and Nicolson, G.L. eds.), North-Holland, Amsterdam, pp. 77-90.
- Parsegian, A. (1969) *Nature* **221**, 844-846.
- Patel, K.M. and Sparrow, J.T. (1978) *J. Chromat.* **150**, 542-547.
- Phillips, M.C. and Chapman, D. (1968) *Biochim. Biophys. Acta* **163**, 301-313.
- Phillips, M.C., Ladbroke, B.D., and Chapman, D. (1970) *Biochim. Biophys. Acta* **196**, 35-44.
- Pick, U. (1981) *Arch. Biochem. Biophys.* **212**, 186-194.
- Pinto da Silva, P. and Branton, D. (1970) *J. Cell Biol.* **457**, 598-605.
- Pontus, M. and Delmelle, M. (1975) *Biochim. Biophys. Acta* **401**, 221-234.
- Poste, G. (1983) *J. Cell Biol.* **47**, 19-39.
- Pressman, P.C. and de Guzman, N.T. (1975) *Ann. N.Y. Acad. Sci.* **264**, 373-386.
- Racker, E. (1979) *Meth. Enzymol.* **55**, 699-711.
- Ramos, S., Grollman, E.F., Lazo, P.S., Ayer, S.A., Habig, W.H., Hardgree, M.C., Kaback, H.R., and Kahn, L.D. (1979) *Proc. Natl. Acad. Sci. USA* **76**, 4783-4787.
- Rance, M., Jeffrey, K.R., Tullock, A.P., Butler, K.W., and Smith, I.C.P. (1982) *Biochim. Biophys. Acta* **688**, 191-200.
- Reed, P.W. (1979) *Meth. Enzymol.* **55**, 435-454.
- Robertson, J.D. (1957) *J. Biophys. Biochem. Cytol.* **3**, 1043-1047.
- Saris, N.E. and Akerman, K.E. (1980) *Curr. Top. Bioenerg.* **10**, 103-117.
- Schieren, H., Rudolph, S., Finkelstein, M., Coleman, P., and Weissmann, G. (1978) *Biochim. Biophys. Acta* **542**, 137-153.
- Schuh, J.R., Banerjee, U., Müller, L., and Chan, S.I. (1982) *Biochim. Biophys. Acta* **687**, 219-225.
- Schuldiner, S. and Kaback, H.R. (1975) *Biochemistry* **14**, 5451-5458.
- Schuldiner, S., Fishkes, H., and Kanner, B.I. (1978) *Proc. Natl. Acad. Sci. USA* **75**, 3713-3716.
- Seddon, J.M., Kaye, R.D., and Marsh, D. (1983) *Biochim. Biophys. Acta* **734**, 347-352.
- Seelig, J. (1977) *Quart. Rev. Biophys.* **10**, 353-418.
- Seelig, J. (1978) *Biochim. Biophys.* **515**, 105-140.
- Seeman, P. (1972) *Pharmacol. Rev.* **24**, 583-654.
- Seligman, B.E. and Gallin, J.I. (1983) *J. Cell Physiol.* **115**, 105-114.

- Sheltawy, A. and Dawson, R.M.C. (1969) in *Chromatographic and Electrophoretic Techniques* (Smith, J. ed.), Heineman, London.
- Silvius, J.R. (1982) in *Lipid-Protein Interactions, Vol. 2* (Jost, P.C. and Griffith, O.H. eds.), John Wiley and Sons, N.Y., pp. 239-280.
- Singer, S.J. and Nicolson, G.L. (1972) *Science* **175**, 720-731.
- Singer, S.J. (1977) in *Structure of Biological Membranes* (Abrahamsson, S. and Pascher, I. eds), Plenum Press, N.Y., pp. 443-461.
- Skulachev, V.P. (1971) *Curr. Top. Bioenerg.* **4**, 127-152.
- Smith, A.D. (1968) in *The Interaction of Drugs and Subcellular Components of Animal Cells* (Campbell, P.N. ed.), Churchill, London, pp. 239-292.
- Steim, J.M., Tourtellote, M.E., Reinert, J.C., McElhaney, R.N., and Rader, R.L. (1969) *Proc. Natl. Acad. Sci. USA* **63**, 104-109.
- Stoeckenius, W. and Engelman, D.M. (1969) *J. Cell Biol.* **42**, 613-646.
- Szoka, F. and Papahadjopoulos, D. (1980) *Ann. Rev. Bioeng.* **9**, 467-508.
- Tanford, C. (1980) in *The Hydrophobic Effect: Formation of Micelles and Biological Membranes*, Wiley and Sons, N.Y.
- Tilcock, C.P.S. and Cullis, P.R. (1981) *Biochim. Biophys. Acta* **641**, 189-201.
- Tilcock, C.P.S. and Cullis, P.R. (1982) *Biochim. Biophys. Acta* **684**, 212-218.
- Tilcock, C.P.S., Bally, M.B., Farren, S.B., and Cullis, P.R. (1982) *Biochemistry* **21**, 4596-4601.
- Tilcock, C.P.S., Bally, M.B., Farren, S.B., Cullis, P.R., and Gruner, S.M. (1984) *Biochemistry* **23**, 2696-2703.
- Tucker, W.P., Tove, S.B., and Kepler, C.R. (1971) *J. Labelled Compd.* **2**, 136-151.
- van Deenen, L.L.M. (1981) *FEBS Letters* **123**, 3-15.
- Vanderkooi, G. and Green, D.E. (1970) *Proc. Natl. Acad. Sci. USA* **66**, 615.
- van der Stein, A.T.M., de Kruijff, B., and de Gier, J. (1982) *Biochim. Biophys. Acta* **691**, 13-23.
- van Dijck, P.W.M., de Kruijff, B., van Deenen, L.L.M., de Gier, J., and Demel, R.A. (1976a) *Biochim. Biophys. Acta* **455**, 576-587.
- van Dijck, P.W.M., van Zoelen, E.J.I., Seldenryck, R., van Deenen, L.L.M., and de Gier, J. (1976b) *Chem. Phys. Lipids* **17**, 336-343.
- van Dijck, P.W.M., de Kruijff, B., Verkleij, A.J., van Deened, L.L.M., and de Gier, J. (1978) *Biochim. Biophys. Acta* **512**, 84-96.

- van Hoogevest, P., du Maine, A.P.M., de Kruijff, B., and de Gier, J. (1984a) *Biochim. Biophys. Acta*, in press.
- van Hoogevest, P., du Maine, A.P.M., de Kruijff, B., and de Gier, J. (1984b) *Biochim. Biophys. Acta*, in press.
- van Venetië, R., Leunissen-Bijvelt, J., Verkleij, A.J., and Ververgaert, P.H.J.Th. (1980) *J. Micros.* **118**, 401-408.
- Verkleij, A.J., van Echteld, C.J.A., Gerritsen, W.J., Cullis, P.R., and de Kruijff, B. (1980) *Biochim. Biophys. Acta* **600**, 620-624.
- Verkleij, A.J. (1984) *Biochim. Biophys. Acta* **779**, 43-63.
- Vik, S.B. and Capaldi, R.A. (1977) *Biochemistry* **16**, 5755-5762.
- Waggoner, A.S. (1979) *Meth. Enzymol.* **55**, 689-695.
- Warner, J.G. and Benson, A.A. (1977) *J. Lipid Res.* **18**, 545-552.
- Warren, G.B., Toon, P.A., Birdsall, N.J.M., Lee, A.G., and Metcalfe, J.C. (1974a) *Biochemistry* **13**, 5501-5509.
- Warren, G.B., Toon, P.A., Birdsall, N.J.M., Lee, A.G., and Metcalfe, J.C. (1974b) *Proc. Natl. Acad. Sci. USA* **71**, 622-627.
- Weber, A., Westhead, E.D., and Winkler, H. (1983) *Biochem. J.* **210**, 789-794.
- Wilkins, J.A., Greenwalt, J.W., and Huang, L. (1978) *J. Biol. Chem.* **253**, 6260-6265.
- Winkler, H. (1976) *Neuroscience* **1**, 65-80.
- Young, T.D., Unkeless, J.C., Kaback, H.R., and Cohn, Z.A. (1983) *Proc. Natl. Acad. Sci. USA* **80**, 1357-1361.
- Zaccai, G., Buldt, G., Seelig, A., and Seelig, J. (1979) *J. Mol. Biol.* **134**, 693-706.
- Zanotti, A. and Azzone, G.F. (1980) *Arch. Biochem. Biophys.* **201**, 255-265.
- Zubay, G., ed. (1983) *Biochemistry*, Addison-Wesley Pub. Co., Reading, MA.
- Zwizinski, C., Schleyer, M., and Neupert, W. (1983) *J. Biol. Chem.* **258**, 4071-4081.

Publications:

- Bally, M.B., Opheim, D.J., Shertzer, H.G.(1980). Di-(2-ethylhexyl) Phthalate Enhances the Release of Lysosomal Enzymes from Alveolar Macrophages During Phagocytosis. *Toxicology* 18,49-60.
- Thomas, P., Bally, M.B., and Neff, J.M.(1982). Ascorbic Acid Status of Mullet Exposed to Cadmium. *J. Fish Biology* 20,183-196.
- Cullis, P.R., de Kruiff, B., Hope, M.J., Verkleij, A.J., Nayar, R., Farren, S.B., Tilcock, C.P.S., Madden, T.D., and Bally, M.B.(1982). Structural Properties of Lipids and Their Functional Roles in Biological Membranes in Membrane Fluidity, Vol.2(Aloia, R.C., ed.) pp.39-81. Academic Press, New York.
- Tilcock, C.P.S., Bally, M.B., Farren, S.B., and Cullis, P.R.(1982). Influence of Cholesterol on the Structural Preferences of Dioleoylphosphatidylethanolamine - Dioleoylphosphatidylcholine systems: A ^{31}P and ^2H NMR Study. *Biochemistry* 21,4596-4601.
- Carr, R.S., Bally, M.B., Thomas, P., and Neff, J.M.(1983). Comparison of Methods for Determination of Ascorbic Acid in Animal Tissues. *Anal. Chem.* 55,1229-1232.
- Bally, M.B., Tilcock, C.P.S., Hope, M.J., and Cullis, P.R.(1983). Polymorphism of Phosphatidylethanolamine-Phosphatidylserine Model Systems: Influence of Cholesterol and Mg^{2+} on the Ca^{2+} -triggered Bilayer to Hexagonal(H_{II}) Transition. *Can. J. Biochem.* 61,346-352.
- Tilcock, C.P.S., Bally, M.B., Farren, S.B., Cullis, P.R., and Gruner, S.M. (1983). Cation Dependent Segregation Phenomena and Phase Behaviour in Model Membrane Systems Containing Phosphatidylserine: Influence of Cholesterol and Acyl Chain Composition. *Biochemistry*, 23, 2696-2703.
- Hope, M.J., Bally, M.B., and Cullis, P.R.(1984). Production of Large Unilamellar Vesicles by a Rapid Extrusion Procedure: Characterization of Size, Trapped Volume and Ability to Maintain a Membrane Potential. *Biochim. Biophys. ACTA*, in press.

Bally, M.B., Hope, M.J., van Echteld, C.J.A., and Cullis, P.R.(1984).

Uptake of Safranin and Other Lipophilic Cations into Vesicles in Response to a Membrane Potential. Biochim. Biophys. ACTA, in press.

Mayer, L.D., Bally, M.B., Hope, M.J., and Cullis, P.R.(1984). Uptake of Dibucaine into Large Unilamellar Vesicles in Response to a Membrane Potential, J. Biol. Chem., submitted.

Mayer, L.D., Bally, M.B., Hope, M.J., and Cullis, P.R.(1984). Uptake of Antineoplastic Agents into Large Unilamellar Vesicles in Response to a Membrane Potential, Biochim. Biophys. ACTA, submitted.

Thomas, P., Bally, M.B., and Neff, J.M. (1984) Influence of Some Environmental Variables on the Ascorbic Acid Status of Mullet (Mugil cephalus Linn.) Tissues II. Seasonal Fluctuations and Biosynthetic Ability, J. Fish Biol., submitted.

Bally, M.B., Opheim, D.J., Shertzer, H.G. (1984) Inhibition of Bacterial Killing by Alveolar Macrophages Exposed to Di-(2-ethylhexyl) phthalate, J. Clin. Immun., submitted.